Aus der Chirurgischen Klinik
der Medizinischen Fakultät Mannheim
(Direktor: Prof. Dr. med. Christoph Reißfelder)
und
Deutsches Krebsforschungszentrum
Nachwuchs-Klinische Kooperationseinheit Translationale Chirurgische Onkologie
(Leiter: Apl. Prof. Dr. med. Sebastian Schölch)

ARID1A mutations in colorectal cancer: Biological and therapeutic implications

Inauguraldissertation
zur Erlangung des medizinischen Doktorgrades
der
Medizinischen Fakultät Mannheim
der Ruprecht-Karls-Universität
zu
Heidelberg

vorgelegt von
Fukang Jin

Aus
Henan
2023

Dekan: Prof. Dr. med. Sergij Goerdt
Referent: Apl. Prof. Dr. med. Sebastian Schölch

TABLE OF CONTENTS

Page

ABBREVIATIONS

ACTB	Actin beta
ACTL6A	Actin like 6A
AKT	Protein kinase B
AP1	Activator protein 1
Apc	Adenomatous polyposis coli
ARID1A/B	AT-rich interaction domain 1A/B
ATR	Ataxia telangiectasia and Rad3-related protein
ATPase	Adenosine triphosphatase
ATRi	ATR inhibitors
BAF	BRG1/BRM-associated factor
BCL7A-C	B-cell CLL/lymphoma 7A-C
BRD4	Bromodomain-containing protein 4
CCK8	Cell Counting Kit-8
CDH1	Cadherin 1
CDK8	Cyclin-dependent kinase 8
cfDNA	Circulating cell-free DNA
ChIP-qPCR	Chromatin immunoprecipitation-quantitative real-time PCR
ChIP-seq	ChIP-sequencing
CRC	Colorectal cancer
CRISPR-Cas9	CRISPR-associated protein 9
ctDNA	Circulating tumor DNA
DMEM	Dulbecco´s modified Eagle medium
DNA	Deoxyribonucleic acid
DPF1-3	Double PHD fingers 1-3
EGFR	Epidermal growth factor receptor
EGFR-TKI	EGFR tyrosine kinase inhibitor
EMT	Epithelial-to-mesenchymal transition
ERK	Extracellular signal-regulated kinase

ERV	Endogenous retrovirus
EZH2	Enhancer of the polycomb repressive complex 2 subunit
FBS	Fetal Bovine Serum
FIT	Fecal immunochemical test
gFOBT	Guaiac-based fecal occult blood test
H3K27ac	Histone H3 lysine 27 acetylation
HERVH	Human endogenous retrovirus H
ICIs	Immune checkpoint inhibitors
MEK	Mitogen-activated protein kinase kinase
MLH1	mutL homolog 1
MMR	Mismatch repair
mTOR	Mammalian target of rapamycin kinase
OS	Overall Survival
PD-1	Programmed cell death protein 1
PI3K	Phosphatidylinositol 3-kinase;
PIK3CA	Phosphatidylinositol-4,5-bisphosphate 3-kinase catalytic subunit alpha
RNAi	RNA interference
siRNA	Small interfering RNA
SMG1/8/9	SMG1/8/9 nonsense-mediated mRNA decay factor
SP1	Sp1 transcription factor
STAT3	Signal transducer and activator of transcription 3
SWI/SNF	Structure of Switch/Sucrose Nonfermentable
TaTME	Transanal total mesorectal excision
TCGA	The Cancer Genome Atlas
TOP2A	Topoisomerase DNA topoisomerase II alpha
TP53	Tumor protein p53
TF	Transcription factor
VIM	Vimentin

1 INTRODUCTION

1.1 Colorectal cancer

1.1.1 Trends in CRC incidence and mortality

Recent data indicates that colorectal cancer (CRC) incidence patterns do not significantly differ by sex but exhibit age-related distinctions. From 2014 to 2018, the incidence rate among individuals aged 50 and above decreased by approximately 2% annually in the United States, contrasting with a 1.5% yearly increase in those under 50 (Siegel et al. 2022). Similar trends are evident in Canada, Australia, and numerous European countries (Araghi et al. 2019; Siegel et al. 2019; Vuik et al. 2019). The upsurge in CRC incidence among younger individuals since the mid-1990s in high-income countries is not entirely elucidated but is hypothesized to be linked to risk factor exposure, particularly related to lifestyles initiated by individuals born around 1950 (Siegel et al. 2017; Siegel et al. 2019).

The overall decline in CRC incidence in high-prevalence nations primarily stems from increased adoption of healthier lifestyles, such as smoking reduction, and enhanced early screening (Arnold et al. 2020; Edwards et al. 2010). While factors like dietary habits, overweight, and unhealthy lifestyles may contribute to the rise in young-onset CRC, the specific causal aspects necessitate further research, given that these adverse factors are also present in the elderly (Hyuna S n.d.).

Although CRC remains the second most prevalent cause of cancer-related deaths in both genders, mortality rates are decreasing. In the United States, CRC death rates have declined by 55% among men since 1980 and 60% among women since 1969 (Siegel et al. 2023). Overall CRC mortality has reduced by approximately 2% annually in the recent decade (2011-2020) (Siegel et al. 2023). However, a concealed trend of escalating mortality among relatively younger patients is apparent; from 2005 to 2020, CRC mortality increased by 1.2% yearly in those under 50 and 0.6% in individuals aged 50-54 (Siegel et al. 2023).

Since 1991, cancer mortality rates have consistently diminished due to diverse factors, including lifestyle modifications, screening accessibility, and advancements in treatment options (Siegel et al. 2023). Continuous progress in existing cancer management strategies and treatments is imperative for expediting advancements in the battle against cancer (Siegel et al. 2023).

1.1.2 Prevention and treatment

The current global scenario is characterized by a substantial epidemic burden of colorectal cancer (CRC). Strategies for addressing this challenge encompass primary, secondary, and tertiary prevention approaches (Figure 1).

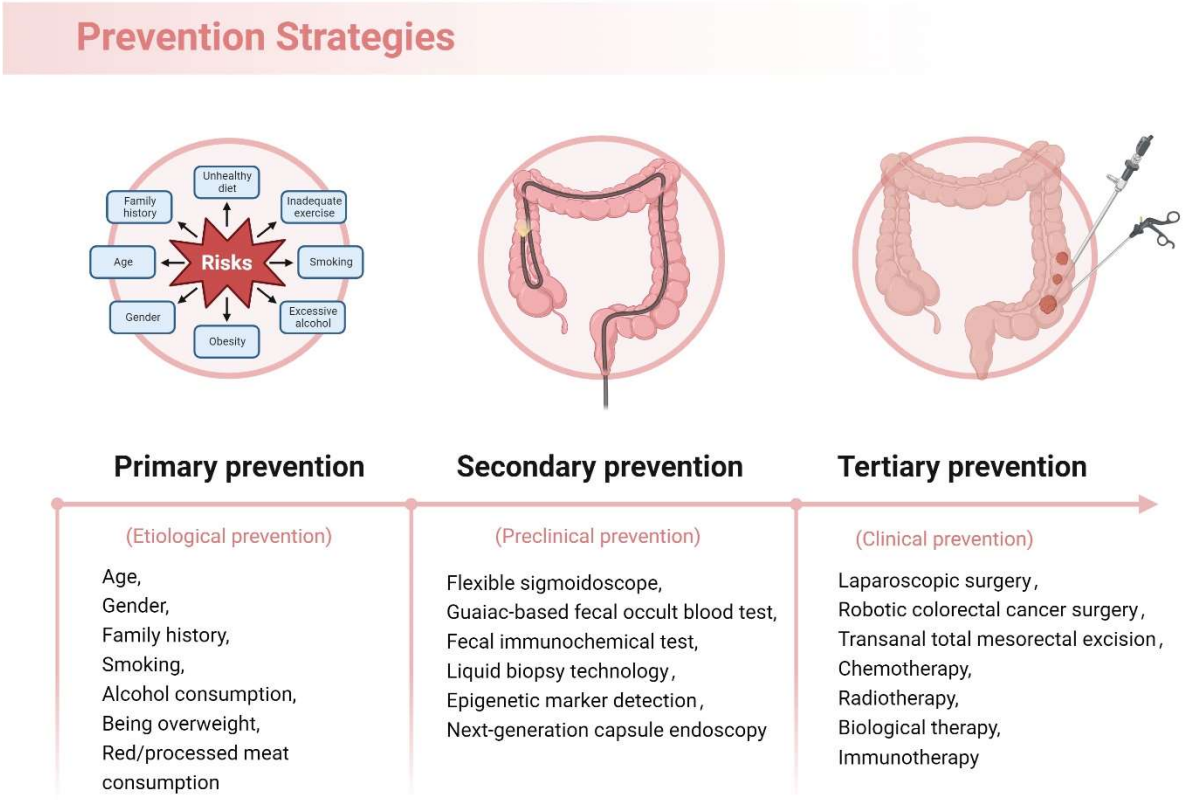

Figure 1. Three levels of prevention strategies for colorectal cancer. Here we list specific factors and interventions for etiological prevention, preclinical prevention, and clinical prevention. Created with BioRender.com

Primary (Etiological) prevention

Involves measures targeting the etiology or risk factors before the onset of the disease. Research to discern risk and protective factors provides a foundation for primary prevention in CRC. Identified risk factors include age, gender, family history, smoking (Botteri et al. 2008), alcohol consumption (Bagnardi et al. 2015), being overweight (Freisling et al. 2017), and red or processed meat consumption (Vieira et al. 2017). Conversely, protective factors comprise physical activity (Boyle et al. 2012), aspirin use (Algra and Rothwell 2012; Cao et al. 2016), hormone replacement therapy (Green et al. 2012), and consumption of milk or whole grains (Vieira et al. 2017).

Secondary (Preclinical) prevention

Applies to early detection, early diagnosis, and early treatment of diseases in the preclinical stage. Given the slow progression of CRC (Brenner et al. 2013), there is an opportunity for effective secondary prevention (Brenner and Chen 2018).

Screening, particularly through flexible sigmoidoscopy, has been demonstrated to reduce CRC mortality (Ladabaum et al. 2020). Flexible sigmoidoscopy every 5 years is recommended, reducing CRC morbidity and mortality by 21% and 27%, respectively (Ladabaum et al. 2020; Lin et al. 2016). Guaiac-based fecal occult blood test (gFOBT) and fecal immunochemical test (FIT) are also effective, with FIT offering advantages like higher compliance and substitution for gFOBT (Vart et al. 2012).

Novel screening strategies, including liquid biopsy technology, epigenetic marker detection, and next-generation capsule endoscopy, introduce promising approaches. Circulating tumor DNA (ctDNA) detection can predict clinical prognosis or recurrence in CRC patients (Chae and Oh 2019). Molecular analysis of circulating tumor cells (CTC) is another liquid biopsy method with predictive value in various cancers, including CRC (Jin et al. 2022; Rahbari et al. 2010).

Tertiary (Clinical) prevention

Actively treating patients to prevent further disease development and deterioration.

Surgical approaches, particularly minimally invasive techniques like laparoscopic surgery, are the mainstay for CRC treatment (Yamauchi et al. 2021). Laparoscopic colectomy is considered non-inferior to open surgery in technical and oncological safety (Acuna et al. 2019; Martel et al. 2012). Robotic colorectal cancer surgery has demonstrated safety feasibility since its inception in 2002. (Blumberg et al. 2019; Park et al. 2019; Weber et al. 2002). Transanal total mesorectal excision (TaTME) for middle and low rectal cancer is gaining attention (Butterworth et al. 2021; Liu et al. 2023; Penna et al. 2017), but the safety and therapeutic efficacy remain subjects of controversy, necessitating multicenter randomized controlled trials for validation (Larsen et al. 2019; Penna et al. 2019).

Advanced CRC is managed through chemotherapy, radiotherapy, biological therapy, and immunotherapy (Blumberg et al. 2021). The heterogeneous nature of CRC

demands a cost-benefit analysis to optimize treatment strategies and combinations (Ng et al. 2022). Robust biomarkers for assessing tumor behavior and predicting treatment response are also crucial for advancing CRC treatment.

1.1.3 Drug resistance mechanism of CRC

While various interventions, such as chemotherapy (e.g., oxaliplatin), targeted therapy, and immunotherapy, can extend the overall survival (OS) of CRC patients, the emergence of drug resistance over time poses a significant challenge. Tumor drug resistance mechanisms manifest in two forms: intrinsic and acquired. Intrinsic resistance may arise from inherent properties of tumor cells or genetic mutations, such as microsatellite instability in approximately 15% of CRC patients, rendering them naturally resistant to 5-fluorouracil (Sun 2021). Additionally, common mutations like B-Raf proto-oncogene (BRAF) contribute to intrinsic resistance to Epidermal Growth Factor Receptor (EGFR) inhibitors (De Roock et al. 2011). Acquired drug resistance develops during treatment, hindering the expected response of tumor cells to drugs. Mechanisms contributing to acquired resistance include: (1) Overexpression of drug pumps: P-glycoprotein (Pgp) actively expels drugs from tumor cells, reducing drug efficacy (Beklen et al. 2020). miR-26b increases the sensitivity of CRC to 5-fluorouracil in vivo and in vitro experiments by downregulating Pgp protein expression (Wang et al. 2018). (2) Gene mutations in drug targets: Mutations, such as in the RAS family (Kirsten rat sarcoma (KRAS) exons 3 and 4, NRAS proto-oncogene exons 2, 3, and 4), arising during treatment lead to resistance to EGFR-targeted therapies like cetuximab and panitumumab (Sorich et al. 2015). (3) DNA damage repair (DDR) mechanism: Cancer stem cells mediate acquired drug resistance by altering DDR activity (Lord and Ashworth 2012). In the absence of p53, cancer stem cells exhibit enhanced DNA repair activity, promoting survival after exposure to ionizing radiation (Diehn et al. 2009; Zhang et al. 2010). (4) Tumor microenvironment (TME): The TME is composed of a variety of stromal cells and extracellular matrix. By subcutaneously injecting SW480 cells into mice to establish xenografts, cancer-associated fibroblasts (CAFs) transfer exosomes (H19) to promote CRC resistance to oxaliplatin (Ren et al. 2018). CAFs also secrete cytokines, chemokines, and exosomes that recruit immunosuppressive cells, inhibiting cytotoxic lymphocyte-killing ability, and achieving immune evasion (Monteran and Erez 2019). The extracellular matrix (ECM) forms a physical barrier hindering drug access to cancer cells (Monteran and Erez 2018).

Changes in collagen content and distribution affect drug distribution and efficacy (Yoshimoto et al. 2023). Collagen alterations impact macrophage infiltration and differentiation, in vitro experiments using type I collagen as a matrix for culturing macrophages showed that the ability of macrophages to differentiate into the M1 phenotype and kill tumor cells was attenuated (Afik et al. 2016). Addressing CRC drug resistance requires continued research to comprehend its mechanisms, paving the way for new treatment strategies, including combination therapy and personalized approaches.

1.2 AT-rich interaction domain 1A (*ARID1A*) gene

1.2.1 Structure of switch/sucrose nonfermentable (SWI/SNF) complex and ARID1A protein

The SWI/SNF complex, a chromatin remodeling complex crucial in humans, consists of three subfamilies, with the BRG1/BRM-associated factor identified as the primary entity (Figure 2) (Jin et al. 2023). Initial identification of key components of the SWI/SNF complex occurred during the analysis of Saccharomyces cerevisiae mutants exhibiting fermentation defects (Wilson and Roberts 2011). The sucrose nonfermenting (SNF) is indispensable for SUC2 expression in sucrose metabolism, while the switch (SWI) facilitates mating-type switching (Neigeborn and Carlson 1984; Stern et al. 1984). Approximately 20-25% of human cancers exhibit subunit mutations within the SWI/SNF complex, correlating with heightened cancer risk and adverse survival outcomes (Monterde and Varela 2022; Savas and Skardasi 2018). The ARID1A gene undergoes mutations most frequently, constituting a well-documented occurrence (Jin et al. 2023). The functional integrity of the ARID1A protein relies on two vital conserved domains. The N-terminal DNA binding domain, characterized by evolutionary conservation, specifically binds AT-rich DNA sequences. Conversely, the C-terminal domain, containing multiple LXXLL sequence motifs, interacts predominantly with stimulatory proteins. This interaction regulates downstream transcription factor activity by binding to receptors (Wu et al. 2014).

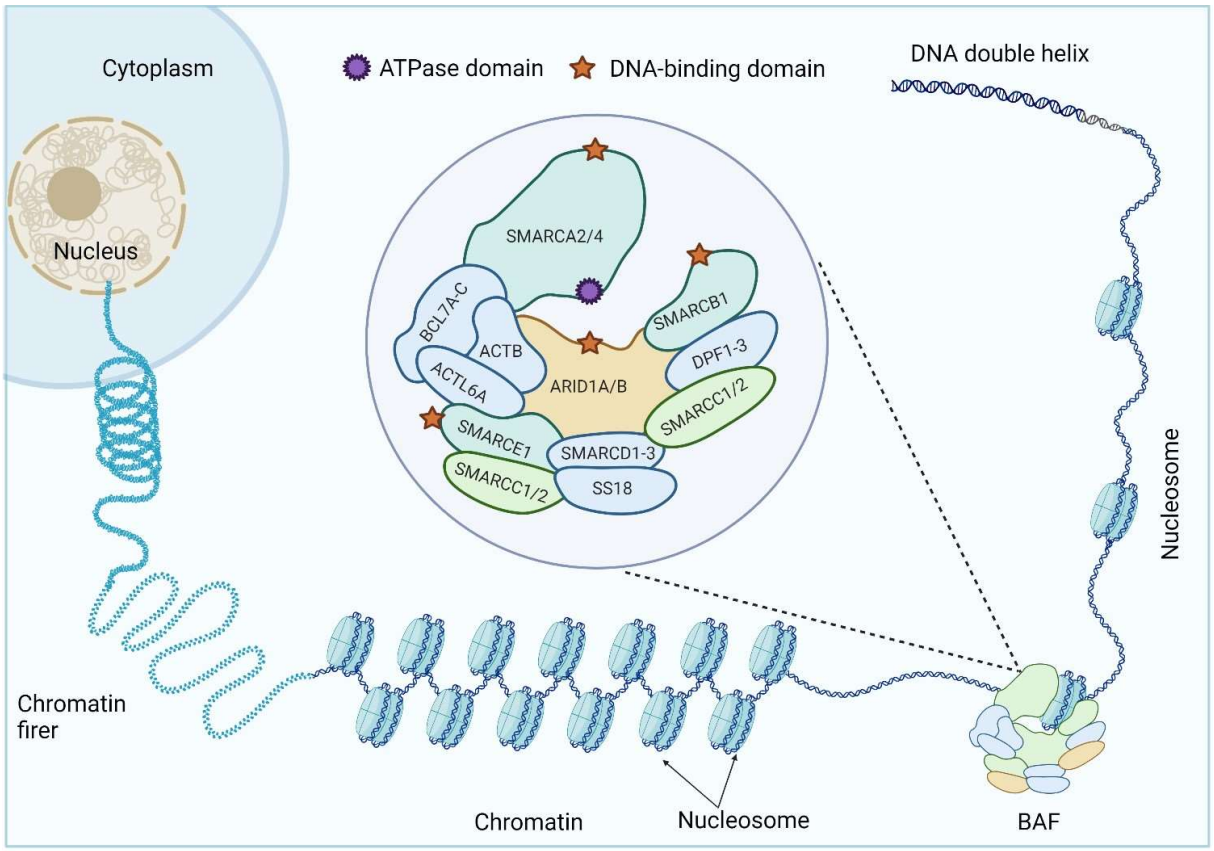

Figure 2. Structure and function of BRG1/BRM-associated factor complexes. The BRG1/BRM-associated factor complexes consist of multiple subunits, including ARID1A, SMARCC, and SMARCD, which slide or eject the nucleosomes using energy generated by ATP hydrolysis, thereby regulating nucleosome positioning and the accessibility of chromatin to a variety of related molecules. The current image is derived from the reference (Jin et al. 2023).

Abbreviations: ACTB: actin beta; ACTL6A: actin like 6A; ARID1A/B: AT-rich interaction domain 1A/B; ATPase: adenosine triphosphatase; BAF: BRG1/BRM-associated factor; BCL7A-C: B-cell CLL/lymphoma 7A-C (BAF chromatin remodeling complex subunit BCL7A-C); DNA: deoxyribonucleic acid; DPF1-3: Double PHD fingers 1-3; SMARCA2/4: SWI/SNF related, matrix associated, actin dependent regulator of chromatin, subfamily a, member 2/4; SMARCB1: SWI/SNF related, matrix associated, actin dependent regulator of chromatin, subfamily b, member; SMARCC1/2: SWI/SNF related, matrix associated, actin dependent regulator of chromatin subfamily c member 1/2; SMARCD1-3: SWI/SNF related, matrix associated, actin dependent regulator of chromatin, subfamily d, member 1-3; SMARCE1: SWI/SNF related, matrix associated, actin dependent regulator of chromatin, subfamily e, member 1; SS18: Synovial sarcoma translocation, chromosome 18 (SS18 subunit of BAF chromatin remodeling complex).

1.2.2 ARID1A loss and clinicopathological feature of CRC

The ARID1A gene mutation frequency in CRC ranges from 5-13% (Johnson et al. 2022; Kim et al. 2017). Analyzing The Cancer Genome Atlas Program (TCGA) CRC cohort revealed that the most prevalent ARID1A mutation occurred at D1850, constituting approximately 8.7% (24/275) of cases, with truncation mutations being the most common mutation type, accounting for about 62.2% (171/275) (Tokunaga et al. 2020). ARID1A protein loss is closely related to the clinicopathological features of CRC

(Wei et al. 2014). Immunohistochemical analysis of ARID1A protein expression demonstrated a higher prevalence of ARID1A loss in stage IV CRC compared to early CRC (35.2% vs. 25.8%). Additionally, patients with ARID1A loss exhibited a higher rate of distant metastasis compared to non-loss patients (46.3% vs. 29.7%) and a greater proportion of poorly differentiated tumors (25.9% vs. 14.2%) (Wei et al. 2014). Similar findings were reported in an independent study, which also noted associations between ARID1A loss and advanced patient age and lymph node metastasis (Lee et al. 2014). Contrasting results have been reported, indicating an association between ARID1A loss and younger CRC patients (Kishida et al. 2019). This discrepancy may arise from a study focusing solely on early CRC at the T1 stage.

1.2.3 Prognostic value of ARID1A loss in CRC

The correlation between ARID1A loss and CRC prognosis remains inconclusive. Despite several studies suggesting a potential reduction in survival for patients with ARID1A loss (Luchini et al. 2015; Shi et al. 2022), statistical significance is often lacking (Li et al. 2020; Ye et al. 2014). Conversely, ARID1A mutations have been identified as predictors of survival benefits in immune checkpoint inhibitor (ICI) therapy for CRC. Patients harboring ARID1A mutations exhibited significantly longer OS compared to wild-type patients (28 vs. 18 months, HR = 0.73, 95% CI: 0.61-0.93) (Jiang et al. 2020). Researchers posit that ARID1A mutations may impair mismatch repair, leading to an increased mutational burden conducive to ICI therapy (Shen et al. 2018).

However, conflicting results exist, as some studies fail to establish the predictive value of ARID1A loss for long-term survival in CRC. A study following 1,426 CRC patients (average follow-up time: 5.29 years) found no association between ARID1A loss and OS in multivariate analysis (HR = 0.60, 95% CI: 0.24 - 1.44) (Chou et al. 2014). This discrepancy may be attributed to the absence of disease-specific survival data, with only all-cause survival outcomes available. Similarly, another study with 196 patients (median follow-up: 48.5 months) reported no correlation between ARID1A loss and 5-year OS (83.3% vs. 54.2%), acknowledging the small sample size and the need for further validation with a larger cohort (Lee et al. 2015). A retrospective study of 578 stage I-II CRC patients (median follow-up: 49 months) also failed to find an association between ARID1A level and OS in univariate analysis (HR = 0.9, 95% CI: 0.5 - 1.6), highlighting limitations related to study design and sample size (Lee et al. 2016).

1.2.4 Mechanism of ARID1A loss in CRC

Research on the precise mechanism of ARID1A loss in CRC is increasing, offering potential therapeutic target identification. ARID1A loss induces extensive and intricate alterations in CRC cells, as illustrated in Figure 3. These changes will be discussed individually.

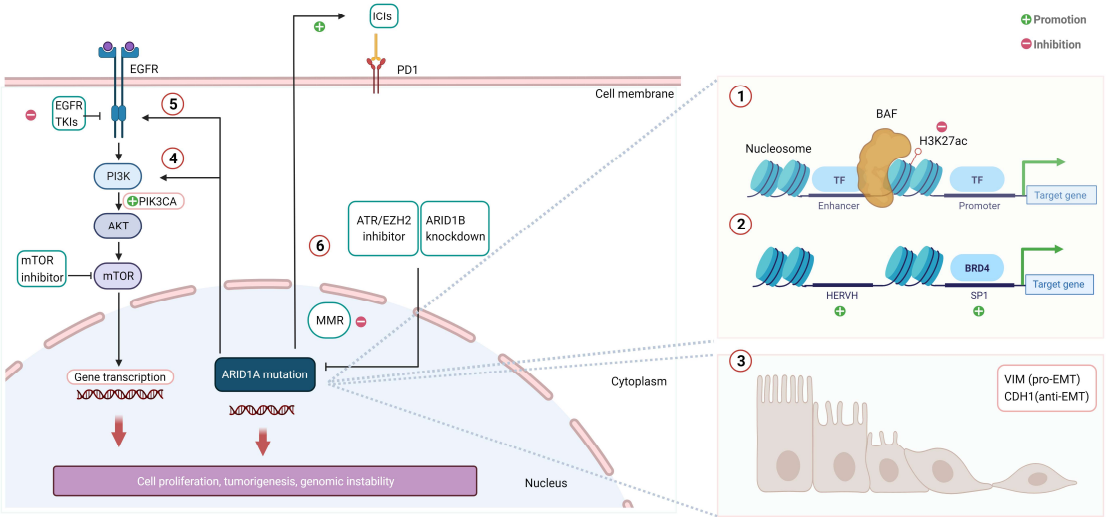

Figure 3. Mechanism and potential therapeutic target of *ARID1A* mutation in CRC cells. *ARID1A* mutations lead to impaired activity and position shift of the H3K27ac enhancer at the SWI/SNF binding site (1) and activate HERVH, which stimulates BRD4 transcription and promotes tumor progression (2). In addition, affects the EMT by adjusting the expression of VIM and CDH1 (3). ARID1A loss promotes PI3K/AKT signaling (4) and may confer resistance to EGFR therapy in CRC patients (5), but impaired MMR, which may ultimately contribute to ICI therapy (6). Created with BioRender.com

Abbreviations: AKT: Protein kinase B; ARID1A: AT-rich interacting domain containing protein 1A; ARID1B: AT-rich interacting domain containing protein 1B; ATR: Ataxia telangiectasia and Rad3-related serine/threonine kinase; BAF: BRG1/BRM-associated factor; BRD4: Bromodomain-containing protein 4; CDH1: Cadherin 1; EGFR: Epidermal growth factor receptor; EGFR-TKI: EGFR tyrosine kinase inhibitor; EMT: Epithelial-mesenchymal transition; EZH2: Enhancer of the polycomb repressive complex 2 subunit; H3K27ac: Histone H3 lysine 27 acetylation; HERVH: Human endogenous retrovirus H; ICIs: Immune checkpoint inhibitors; MMR: Mismatch repair; mTOR: Mammalian target of rapamycin kinase; PD-1: Programmed cell death protein 1; PI3K: Phosphatidylinositol 3-kinase; PIK3CA: Phosphatidylinositol-4,5-bisphosphate 3-kinase catalytic subunit alpha; SP1: Sp1 transcription factor; TF: Transcription factor; VIM: Vimentin.

Impaired activity and shifted position of histone H3 lysine 27 acetylation

In a previous investigation, *MX1-Cre Arid1a*$^{fl/fl}$ mice were employed to establish mouse models with *Arid1a* inactivation by inducing Cre enzyme activity with synthetic interferon (poly I: C) (Mathur et al. 2016). Verification of ARID1A loss in mice was achieved through histopathological (HE) staining and immunohistochemical staining, leading to the development of aggressive colon adenocarcinoma. Notably, the study

excluded interference from the Adenomatous polyposis coli (*Apc*) gene in the mouse model, affirming that ARID1A loss autonomously propels CRC without *Apc* mutation, thereby confirming that *Arid1a* plays a tumor suppressor role (Mathur et al. 2016).

Subsequent in vitro experiments using HCT116 *ARID1A*^{WT} and HCT116 *ARID1A*$^{-/-}$ cell lines verified that ARID1A biallelic deletion resulted in spindle morphology and filopodia, heightened invasiveness, and reduced E-cadherin expression. However, no observed changes were noted in proliferation ability and epithelial-mesenchymal transition (EMT). Furthermore, the study corroborated previous findings that mutations in ARID1A and AT-rich interaction domain 1B (ARID1B) are mutually exclusive, employing co-immunoprecipitation and chromatin immunoprecipitation-quantitative real-time PCR (ChIP-qPCR) methods. Knocking down ARID1B using short hairpin RNA (shRNA) demonstrated impaired *ARID1A*$^{-/-}$ cell proliferation, solidifying ARID1B as a synthetic lethal target of ARID1A (Helming et al. 2014b; Helming et al. 2014a).

To investigate alterations in histone modifications associated with active cis-regulatory elements upon ARID1A loss, chromatin immunoprecipitation-sequencing (ChIP-seq) analysis revealed impaired activity and a positional shift of the histone H3 lysine 27 acetylation (H3K27ac) enhancer at the SWI/SNF binding site (Mathur et al. 2016).

Human endogenous retrovirus H (HERVH) - Bromodomain-containing protein 4 (BRD4) regulatory axis

HERVH is a product of retroviruses that infiltrated human ancestors, integrating into the germ line genome and becoming incapable of infectious activity post-internalization. Consequently, these retroviruses transformed into endogenous retrovirus (ERV) sequences within the human genome, propagating solely through vertical transmission (Benveniste and Todaro 1974; Martin et al. 1981). Initially considered nonfunctional, ERV sequences, including HERVH, have been revealed to play roles in various cellular processes such as embryonic development, implantation, and the regulation of innate immune responses (Blaise et al. 2003; Chuong et al. 2016; Mi et al. 2000).

The loss of ARID1A results in aberrant activation of *HERVH*, leading to increased transcription of Bromodomain-containing protein 4 (BRD4) and facilitating tumor progression (Yu et al. 2014).

The generation of an ARID1A knockout (KO) CRC cell line involved transfecting HCT116 cells with the LentiCRISPR-V2 plasmid carrying sgARID1A. In light of the identified HERVH-BRD4 regulatory axis, this study proposes several alternative therapeutic targets, including the Sp1 transcription factor (SP1), ARID1B, BRD4, and HERVH. These targets hold potential for intervention in the context of aberrant *HERVH* activation and associated tumorigenesis.

Regulation of EMT by vimentin (VIM) and cadherin 1 (CDH1)

ARID1A knockdown (KD) enhances cell proliferation while reducing cell senescence and apoptosis. This effect was achieved by transfecting the Caco-2 cell line with small interfering RNA (siRNA) in an in vitro setting. Subsequent assessment revealed that ARID1A KD also promotes the invasion capability and multicellular sphere formation of Caco-2 cells (Peerapen et al. 2022).

In a separate investigation, researchers utilized siRNA to transfect HCT116, LS174T, and other cell lines in vitro, confirming that ARID1A KD acts as a transcription factor influencing the expression of VIM and CDH1. This regulatory activity subsequently impacts the EMT process in CRC (Baldi et al. 2022).

Phosphatidylinositol 3-kinase (PI3K) / AKT signaling pathway

In addition, after transfecting SW480 and SW620 cell lines with siRNA, ARID1A loss not only promotes CRC cell proliferation but also promotes 5-fluorouracil-induced apoptosis (Xie et al. 2014). Considering the previously detected association between ARID1A and the phosphatidylinositol 3-kinase (PI3K) / AKT signaling pathway in various cancers (Jin et al. 2023). the authors verified that the KD of ARID1A inhibits the phosphorylation level of AKT and vice versa.

Independent of KRAS mutation

ARID1A deletion effects on CRC proliferation differ from previously discussed inhibitory effects. CRISPR/Cas9-mediated ARID1A deletion in HT29 and COLO320DM CRC cell lines did not impact proliferation (Sen et al. 2019).

Comparative mRNA sequencing analysis revealed ARID1A loss-induced changes in the Wnt signaling pathway and cardiac differentiation gene expression in COLO320DM cells. Further exploration implicated gene set enrichment analysis on HCT116 and DLD1 cell lines, indicating specific downregulation in Mitogen-activated protein kinase kinase (MEK)/ Extracellular signal-regulated kinase (ERK) pathways (EGFR, MEK, and ERK) contrary to the transcriptional activation function of the ARID1A-containing BAF complex. Both cell lines harboring Kirsten rat sarcoma (KRAS) mutations prompted the screening of three candidate targets (Epiregulin, Tissue Factor III, and Jagged1) significantly increased in KRAS mutations. Identified as MEK/ERK downstream target genes using Trametinib (MEK inhibitor), they were also downregulated upon ARID1A loss, suggesting mutual exclusivity between *ARID1A* and *KRAS*, particularly G12 and G13 mutations. Analysis of the TCGA PanCancer Atlas cohort (526 CRC patients) confirmed these mutations in only 16 patients (Liu et al. 2018). ARID1A's tumor suppressor function was deemed independent of *KRAS* mutations, indicating its non-assertion of tumor suppressor function in the context of *KRAS* mutation.

Chromatin immunoprecipitation using a double cross-linking method, combined with ChIP-seq analysis, demonstrated ARID1A co-localization with various Activator protein 1 (AP1) transcription factors, supporting ARID1A's regulation of the MEK/ERK downstream pathway through AP1 transcription factor interaction. The study confirmed that ARID1A loss significantly reduces H3K27ac. The researchers emphasized careful consideration of tumor genetic background when evaluating treatment options for ARID1A-deficient cancers. Direct targeting of the BAF complex, potentially through PROTACS (Proteolytic Targeting Chimeras) for targeted cellular protein degradation, was suggested as a therapeutic option (Sen et al. 2019).

Association with tumor protein p53 (TP53) and APC mutation

The association between *ARID1A* and Tumor protein p53 (*TP53*) has been explored alongside the well-established link with the KRAS gene. Despite some studies suggesting a synergistic tumor-suppressive role for ARID1A and TP53 genes (Guan et al. 2011), they are generally considered mutually exclusive (Jones et al. 2012; Wang et al. 2011). In the TCGA CRC cohort evaluation of 20 mutated genes, specifically, *TP53* and *ARID1A* were found to be mutually exclusive (Tokunaga et al. 2020). This pattern aligns with observations in other cancers, such as gastric and ovarian cancers,

where ARID1A loss is inversely associated with *TP53* mutation (Guan et al. 2011). Notably, in CRC, the frequency of APC mutations ranges from approximately 27% to 71.7% (Huang et al. 2019; Huang et al. 2021), and ARID1A loss has been identified to inhibit tumor progression in the context of *APC* mutations (Sen et al. 2019).

Mutually exclusive with EGFR amplification

In a study utilizing circulating cell-free DNA (cfDNA) analysis of 333 metastatic CRC patients, *ARID1A* mutations were notably enriched in individuals who received cetuximab post-treatment compared to baseline, with no such enrichment observed in those treated with bevacizumab (Johnson et al. 2022). This implies that *ARID1A* mutations may confer resistance to EGFR therapy in CRC patients. After accounting for confounding factors such as age and gender, the study revealed that among CRC patients receiving cetuximab or panitumumab, those with *ARID1A* mutations experienced a worse prognosis than wild-type patients (HR = 2.2, 95% CI: 1.0 - 4.8, P = 0.04). Subsequent analysis of a database containing targeted DNA sequencing of 16,931 CRC tumors indicated mutual exclusivity between *ARID1A* mutation and *EGFR* amplification. Consequently, CRC patients with detected *ARID1A* mutations may not be suitable candidates for cetuximab treatment.

Close association with mismatch repair (MMR) deficiency

The strong correlation between ARID1A loss and Mismatch Repair (MMR) deficiency in CRC has been extensively documented. Notably, studies have indicated that ARID1A loss occurs in only 4-6% of MMR-intact CRCs, whereas in MMR-deficient cases, the loss of ARID1A expression rises to 15-25% (Agaimy et al. 2016). These findings were corroborated by another study (Lee et al. 2016). In CRC cases with MMR deficiency and ARID1A loss, hypermethylation of the mutL homolog 1 (*MLH1*) gene promoter and *BRAF V600E* mutation were observed. Furthermore, the prognosis for CRC patients with both MMR deficiency and ARID1A loss was notably poor (Ye et al. 2014). Studies spanning multiple cancers have indicated that the loss of ARID1A results in impaired MMR, potentially influencing the efficacy of ICI therapy (Jiang et al. 2020; Shen et al. 2018; Zhu et al. 2022).

1.2.5 Potential targets of synthetic lethality

Researchers are actively seeking therapeutic targets that demonstrate synthetic lethal effects with *ARID1A* mutations, aiming to uncover potential avenues for treatment. One such target is the enhancer of the polycomb repressive complex 2 subunit (EZH2), which, despite predicting poor prognosis in multiple cancers, has not yet been reported for use in colorectal cancer (CRC) (Jin et al. 2023). Ataxia telangiectasia and Rad3-related protein (ATR) stands out as a particularly promising synthetic lethal target for clinical applications. High-throughput RNA interference (RNAi) screens have unveiled a synthetic lethal relationship between ATR inhibitors (ATRi) and *ARID1A* mutations (Williamson et al. 2016). In vitro transfection of the HCT116 cell line with siRNA confirmed the selective toxicity of ATRi in ARID1A loss, and subsequent xenograft tumor formation in mice validated the synthetic lethality of ARID1A/ATR. Further mechanistic insights revealed that ARID1A loss led to the deficiency of the topoisomerase DNA topoisomerase II alpha (TOP2A), resulting in reduced TOP2A binding to chromatin. This led to a cell cycle defect characterized by a delay in the S phase and progression from G2 into mitosis (Williamson et al. 2016).

However, Loss-of-function mutations of the nonsense-mediated mRNA decay factor (SMG8) or SMG9 can lead to ATRi resistance through a mechanism mediated by SMG1 through genome-wide clustered regularly interspaced short palindromic repeats and CRISPR-associated protein 9 (CRISPR-Cas9) positive selection screening (Llorca-Cardenosa et al. 2022: 8). Additionally, loss of the nonsense-mediated decay factor UPF2 regulator of nonsense-mediated mRNA decay (UPF2), as well as cyclin C or cyclin-dependent kinase 8 (CDK8), has been reported to cause ATRi resistance (Lloyd et al. 2021; O'Leary et al. 2022).

1.3 Aim of our study

This study addresses the limited understanding of the impact mechanism of the ARID1A gene on CRC and aims to fill this knowledge gap. The primary objective is to investigate how the ARID1A gene influences essential cellular functions in CRC tumor cells, including proliferation, migration, invasion, and drug resistance. The study seeks to identify alternative targeted therapies and elucidate their specific mechanisms of action, thereby providing a scientific foundation for clinical applications.

Key objectives of the research include:

1. Establishing genetically modified mouse models with a clear genetic background and *Arid1a* gene mutation, along with designing stable mouse and human cell lines for comparative analysis.

2. Conducting comprehensive in vitro assessments to evaluate the impact of the *ARID1A* gene on CRC cell functions.

3. Investigating the specific mechanism through which the *ARID1A* gene affects CRC.

4. Identifying candidate drugs capable of targeting the *ARID1A* gene and evaluating their therapeutic effects.

The study employs cellular functional experiments initially conducted in genetically modified mouse models and subsequently extended to human CRC cell lines (Figure 4). Through these systematic investigations, the research aims to advance our understanding of the ARID1A gene's role in CRC and contribute valuable insights for the development of targeted therapeutic approaches in clinical settings.

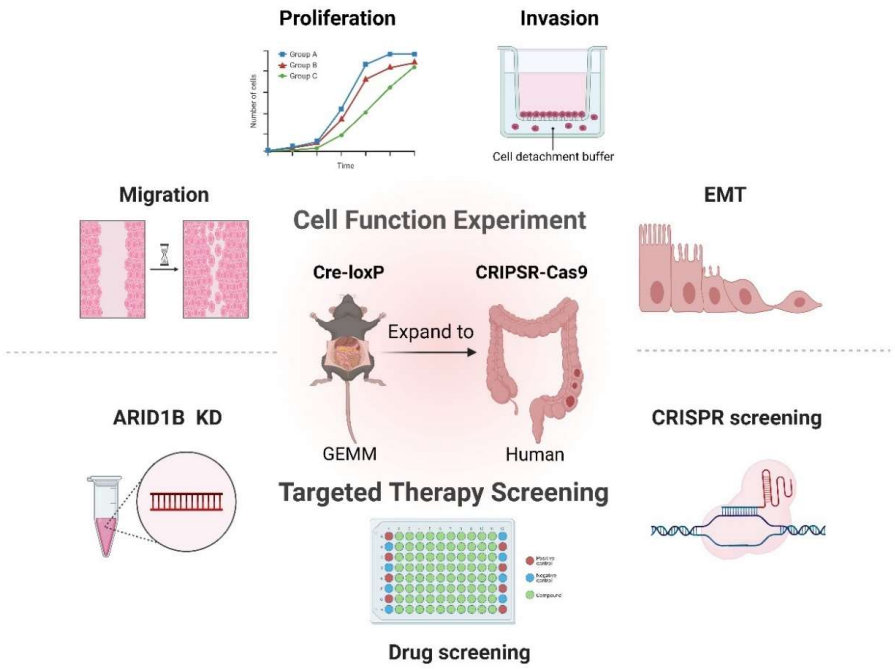

Figure 4. Overview of Experimental Design. We established colorectal organoids and 2D cell lines in genetically modified mouse models and performed various cell function experiments (proliferation, migration, metastasis, EMT, etc.), and extended the above experiments from mouse cell lines to human CRC cell lines. Search for potential drugs through methods such as ARID1B KD, drug screening, and CRISPR screening. Created with BioRender.com

2 MATERIAL AND METHODS

2.1 Materials and Reagents

2.1.1 Media and solutions

Product	Catalog number	Producer
Advanced dulbecco's modified eagle's medium/F-12 (1x)	11550446	Gibco
Annexin V binding buffer (1x)	422201	BIOLEGEND
Dimethylsulfoxide (DMSO)	PIER20688	VWR
Dulbecco's modified eagle medium (DMEM)	41966-029	Gibco
Dulbecco's phosphate-buffered saline	14190-094	Gibco
EDTA (0.5M)	11568896	Invitrogen
Ethidium bromide solution (1%)	1239-45-8	CARL ROTH
Fetal bovine serum (FBS)	10500-064	Gibco
LDS sample buffer (4x)	2045288	Thermo Fisher
Lipofectamine™ RNAiMAX	13778150	Thermo Fisher
L-WRN conditioned medium (2x)	SCM105	Sigma
Minimum essential medium (MEM) alpha medium	22561-021	Gibco
NuPAGE transfer buffer	NP0006-1	Thermo Fisher
OptiMEM (1x)	31985-062	Gibco
Organoid harvesting solution	3700-100-01	R&D Systems
Paraformaldehyd-Lösung (4 % in PBS)	J19943.K2	Thermo Fisher
RIPA lysis buffer	sc-24948	Santa Cruz
RPMI-1640 medium	RNBM0104	Sigma-Aldrich
Tris-acetate-EDTA (50x)	B49	Thermo Fisher
Tris-Acetate SDS running buffer	LA0041	Life Technologies
TrypE	12604-013	Gibco

2.1.2 Equipment, supplies and kits

Product	Catalog number	Producer
6/12/24/48/96-well culture plate	83.3925	Sarstedt
Azure 400 visible fluorescent western imaging system	AZI400	Azure Biosystems
BD FACSCanto™ II clinical flow cytometry system	-	BD
Cell counting kit-8 (cck-8)	CK04-20	Dojindo
Coomassie brilliant blue G-250 protein stain	46496364	CEPHAM
Cuvette (4mm)	620	BTX
QIAamp^{R} DNA mini kit	51306	QIAGEN
Electroporator	ECM399	BTX
Hydrophobic PVDF transfer membrane	IPVH00010	Fisher Scientific
LightCycler96 real-time system	-	Roche
Mouse epidermal growth factor (EGF)	5331	Cell signaling

MycoSPY® master mix - PCR mycoplasma test kit	MSL01	Biontex
NuPAGETM 3-8% Tris-Acetate gel	EA0375BOX	Thermo Fisher
Revert aid first strand cDNA synthesis kit	K1621	Thermo Fisher
RNeasy mini kit	74106	QIAGEN
TECAN System	-	Beckman Coulter
Transwell® insert (8 µm PET membrane)	662638	Greiner Bio-One

2.1.3 Antibodies and siRNA

Product	Catalog number	Producer
ARID1A/BAF250A (D2A8U)	12354	Cell signal tech
ARID1B/BAF250B (E1U7D)	65747	Cell signal tech
Arid1b siRNA	s109134, s109135	Thermo Fisher
Beta-Actin (13E5)	4970	Cell signal tech
Control siRNA	4390844	Thermo Fisher
E-Cadherin (4A2)	14472	Cell signal tech
N-Cadherin (D4R1H)	13116	Cell signal tech

2.1.4 Organoid culture medium supplementation factors

Product	Catalog number	Producer
A83-01	101327-5mg	Biotrend
Antibiotika-antimykotikum (100x)	15240-062	Gibco
B-27 (50x)	17504-044	Gibco
Brain-derived neurotrophic factor (BDNF,100x)	AF-450-02	Peprotech
CHIR-99021	HY-10182	MedChem
HEPES (1M)	15630-080	Gibco
L-WRN conditioned medium (2x)	SCM105	Sigma
Mouse epidermal growth factor (EGF)	5331	Cell signaling
N2 (100x)	17502048	Gibco
N-Acetyl-L-Cystein	616-91-1	Thermo Fisher
Primocin	ant-pm-1	InvivoGen
Y-27632	MCE-HY-10583-10mg	Hölzel Diagnostika Handels GmbH

2.1.5 Other reagents

Product	Catalog number	Producer
Annexin V-FITC	640920	BIOLEGEND
Cas9 protein	A36497	Life Technologies
Cultrex reduced growth factor basement membrane extract	3536-005-02	Bio-Techne
Fetal bovine serum (FBS)	10500-064	Gibco
Matrigel	3536-005-02	Bio-techne
Penicillin/streptomycin (10000 U/ml)	15140122	Gibco
Propidium iodide	421301	BIOLEGEND

Spectra multicolor high range protein ladder	26625	Thermo Fisher
SYBR® green supermix	S7586	Invitrogen

2.2 Methods

2.2.1 Animal experiments

All operating procedures on animals and tissues have been approved by the appropriate authorities (Regierungspräsidium Karlsruhe). The *Arid1a*$^{flox/flox}$*; Apc*$^{flox/flox}$*; Kras*$^{ki/wt}$*; Trp53*$^{flox/flox}$ (7291, ArAKPf)/*Apc*$^{flox/flox}$*; Kras*$^{ki/wt}$*; Trp53*$^{flox/flox}$ (0007, AKPf), *Arid1a*$^{flox/flox}$*; Apc*$^{flox/flox}$*; Kras*$^{ki/wt}$ (I610, ArAK)/*Apc* $^{flox/flox}$*; Kras*$^{ki/wt}$(3188, AK) and *Arid1a*$^{flox/flox}$*; Apc*$^{flox/flox}$*; Trp53*$^{flox/flox}$ (I628, ArAP)/*Apc*$^{flox/flox}$*; Trp53*$^{flox/flox}$ (9829, AP) models were generated by crossing, genotyping was provided by an external service provider (Transnetyx, Cordova, United States). All mice were kept in isolation cages that had been sterilized by high temperature and high pressure, and normal drinking water and food were provided ad libitum. The mice were housed in a 12h light/12h dark cycle, maintained at 22.5°C (±2°C) and about 50% (±5%) humidity.

2.2.2 Primary mouse colon organoid culture

The sacrificed mice were immobilized on the operating table, and the colorectum was dissected. After removing feces and minimizing fat tissue, the colorectum was longitudinally incised with scissors and sectioned into approximately 1 cm pieces. The tissues underwent three washes with 1x Dulbecco's phosphate-buffered saline (DPBS) and were subsequently transferred to a 10 mM EDTA/DPBS buffer. Incubation in a 37°C water bath for 20 minutes was followed by replacement with pre-cooled DPBS, and vigorous shaking for 20 seconds facilitated the separation of colonic crypts. The collected colonic crypts were quantified under a microscope, and the supernatant, containing the appropriate number of crypts, underwent centrifugation at 1000g for 10 minutes at 4 °C. Colon crypts were resuspended in Matrigel and seeded into a 48-well plate. Approximately 200 colon crypts in 15 µl of Matrigel were added to each well. The Matrigel polymerized at 37°C for 10-20 minutes, after which 200 µl of colon organoid medium (refer to Table 1) was supplemented.

To generate an L-WRN conditioned medium, L cells were cultured, and L cell supernatants were collected. The base medium used was DMEM/F-12. Wnt3A protein was incorporated into the culture medium at a concentration of 100-200 ng/ml. Additionally, R-spondin was added at a concentration of 100-200 ng/mL, and Noggin at a concentration of 50-100 ng/ml.

A83-01	0.5 µM
Antibiotika-Antimykotikum	1x
B-27	1x
BDNF	1x
CHIR-99021	1 µM
GlutaMAX™-I	10x
HEPES	10 mM
L-WRN conditioned medium	1x
N2	1x
N-Acetyl-L-Cystein	1.25 mM
Mouse epidermal growth factor (EGF)	50 ng/ml
Penicillin/streptomycin	1000 U/ml
Primocin	100 µg/ml
Y-27632	10 µM

Table 1. Formulation of the colon organoid medium in advanced dulbecco's modified eagle's medium/F-12.

Organoids are cultivated in a humidified incubator at 37 °C with a 5% CO2 atmosphere. The culture medium is refreshed every 2-3 days. During organoid passaging, Matrigel digestion is initiated using an organoid harvesting solution. Subsequently, the mixture is refrigerated at 4 degrees Celsius for 2 hours. An equal volume of TrypE solution is added, and the suspension is incubated at room temperature for 10 minutes. Following centrifugation at 1000g for 10 minutes at room temperature, the pellet is resuspended in Matrigel, and the inoculation process is carried out. All organoids utilized in the experiment have undergone more than three passages before commencement.

2.2.3 Transitioning from three-dimensional (3D) to two-dimensional (2D) cell culture

During the experiment, we opted to refresh the medium for the 3D organoids with a new medium (Tumor organoid medium: DMEM=1:1) after the standard passage. The organoids were then inoculated into a 6-well plate (with a 15 µl drop of Cultrex BME in each well). After a one-week incubation period, we observed 2D cells extending outward around the matrigel. Subsequently, trypsin was added for digestion, and passage expansion was carried out. Following the successful generation of 2D cell lines, single-cell clone selection was performed by inoculating a single cell into a 96-well plate and waiting for 1 - 2 weeks. Single-cell clones were selected for expansion, and DNA was then extracted for genotype verification, resulting in the acquisition of 2D subclonal cell lines with the correct genotype.

Mouse tumor cells were cultured in DMEM and 10% FBS and 1% penicillin/streptomycin at 37°C with 5% CO_2 in the incubator. Human tumor cells were cultured in RPMI-1640 medium and MEM alpha medium. The cell culture medium was changed every two or three days.

2.2.4 Organoid genotyping

Retrieve cell samples and execute DNA extraction following the prescribed procedures in the DNA extraction kit manual. Subsequently, amplify the DNA sequence at the target site using polymerase chain reaction (Table 2). Prepare a 1.5% agarose gel incorporating a DNA staining agent (Ethidium bromide). Apply 100 V for electrophoresis in Tris-acetate-EDTA buffer (1x) over 1 hour. Analyze and compare the molecular weights of DNA fragments in the samples using Azure 400 (Azure Biosystems).

Targeted allele	Primers	Sequence (5’ - 3’)
Apc^{tm2Rak}	Apc_Int13F2	GAGAAACCCTGTCTCGAAAAAA
	Apc_Int13R2	AGTGCTGTTTCTATGAGTCAAC
	Apc_Int14R4	TTGGCAGACTGTGTATATAAGC
$Kras^{tm4Tyj}$	y116-common	TCCGAATTCAGTGACTACAGATG
	y117-LSL	CTAGCCACCATGGCTTGAGT
	y118-wt	ATGTCTTTCCCCAGCACAGT
$Trp53^{tm1Brn}$	Int1F	CACAAAAACAGGTTAAACCCAG
	Int1R	AGCACATAGGAGGCAGAGAC
	Int10R	GAA GAC AGA AAA GGG GAG GG
$Arid1a^{tm1.1Zhwa}$	Forward	TGTTCATTTTTGTGGCGGGAG
	Reverse	TGTTCATTTTTGTGGCGGGAG

Cre	Forward	AGTGCGTTCGAACGCTAGAGCCTGT
	Reverse	AGTGCGTTCGAACGCTAGAGCCTGT

Table 2. PCR primers were used for genotype verification. Primer sequences are listed.

2.2.5 Mycoplasma infection detection method

The detection was performed using the MycoSPY® master mix-PCR mycoplasma test kit, following the provided instructions.

2.2.6 Transfection with siRNA

Confluent monolayers of CRC cells were obtained by culturing the seeded cells in 6-well plates for 24 hours. Transfection reagents consisting of 300 µl OptiMEM and 3 µl of a mixture containing 10 µM siRNA and 9 µl Lipofectamine RNAiMAX were employed. Following transfection, DMEM complete medium was introduced, and the cells were incubated for 48 hours. The evaluation of target protein expression was conducted through Western blotting. Arid1b siRNA (Thermo Fisher, Catalog number: s109134, s109135, abbreviated as siRNA34 and siRNA35, respectively), Control siRNA, lipofectamine™ RNAiMAX, and Opti-MEM I Reduced Serum Medium were utilized in this study. The final siRNA concentration per well during transfection was 5 pmol.

2.2.7 Quantitative reverse transcription PCR

RNA was extracted with the RNeasy mini kit. For quantitative reverse transcription PCR (RT-qPCR) analysis, RNA was reverse-transcribed with a revert aid first strand cDNA synthesis kit, and the relative amounts of each mRNA transcript were analyzed using the LightCycler96 real-time system (Roche) with SYBR® green supermix. The relative expression levels of specific genes were compared using the $2^{-\Delta\Delta Ct}$ calculation method, with the expression of Glyceraldehyde 3-phosphate dehydrogenase (GAPDH) serving as an internal control. Primer sequences were obtained from PrimerBank (Table 3).

Target gene	**Species**	**Primer name**	**Sequence (5' - 3')**	**Length**
Arid1a	Mouse	Arid1a_qPCR_F	TCCCAGCAAACTGCCTATTC	20
Arid1a	Mouse	Arid1a_qPCR_R	CATATCTTCTTGCCCTCCCTTAC	23
Arid1a	Mouse	Arid1a-qF2	GCCTAACTATAATGCCTTGCC	21
Arid1a	Mouse	Arid1a-qR2	GAGTTTTCCTGTTCATTCCCC	21
Arid1a	Mouse	Arid1a-qF3	TATGGGTGCTGGAGGTCAGA	20
Arid1a	Mouse	Arid1a-qR3	ACCTGAGGTGGCATATTGGC	20

Arid1b	Mouse	Arid1b_qF1	CGTGCGGAGCTTGTCTTTC	19
Arid1b	Mouse	Arid1b_qR1	CCTCCTTCTCATAGGTCTGTGG	22
Cdh1	Mouse	Cdh1_qF1	CAGGTCTCCTCATGGCTTTGC	21
Cdh1	Mouse	Cdh1_qR1	CTTCCGAAAAGAAGGCTGTCC	21
Cdh2	Mouse	Cdh2_qF1	AGCGCAGTCTTACCGAAGG	19
Cdh2	Mouse	Cdh2_qR1	TCGCTGCTTTCATACTGAACTTT	23
Egfr	Mouse	Egfr_qF1	GCCATCTGGGCCAAAGATACC	21
Egfr	Mouse	Egfr_qR1	GTCTTCGCATGAATAGGCCAAT	22
Epcam	Mouse	Epcam_qF1	GCGGCTCAGAGAGACTGTG	19
Epcam	Mouse	Epcam_qR1	CCAAGCATTTAGACGCCAGTTT	22
Fn1	Mouse	Fn1_qF1	ATGTGGACCCCTCCTGATAGT	21
Fn1	Mouse	Fn1_qR1	GCCCAGTGATTTCAGCAAAGG	21
Gapdh	Mouse	Gapdh_qF1	AGGTCGGTGTGAACGGATTTG	21
Gapdh	Mouse	Gapdh_qR1	TGTAGACCATGTAGTTGAGGTCA	23
Itgb1	Mouse	Itgb1_qF1	ATGCCAAATCTTGCGGAGAAT	21
Itgb1	Mouse	Itgb1_qR1	TTTGCTGCGATTGGTGACATT	21
Vim	Mouse	Vim_qF1	CGTCCACACGCACCTACAG	19
Vim	Mouse	Vim_qR1	GGGGGATGAGGAATAGAGGCT	21
Pik3ca	Mouse	Pik3ca_qF1	CCACGACCATCTTCGGGTG	19
Pik3ca	Mouse	Pik3ca_qR1	ACGGAGGCATTCTAAAGTCACTA	23
Akt1	Mouse	Akt1_qF1	ATGAACGACGTAGCCATTGTG	21
Akt1	Mouse	Akt1_qR1	TTGTAGCCAATAAAGGTGCCAT	22
Mtor	Mouse	Mtor_qF1	CAGTTCGCCAGTGGACTGAAG	21
Mtor	Mouse	Mtor_qR1	GCTGGTCATAGAAGCGAGTAGAC	23
Pten	Mouse	Pten_qF1	TGGATTCGACTTAGACTTGACCT	23
Pten	Mouse	Pten_qR1	GCGGTGTCATAATGTCTCTCAG	22
Eif4e	Mouse	Eif4e_qF1	ACCCCTACCACTAATCCCCC	20
Eif4e	Mouse	Eif4e_qR1	CAATCGAAGGTTTGCTTGCCA	21
Pik3r2	Mouse	Pik3r2_qF1	GGACAGTGAATGCTACAGTAAGC	23
Pik3r2	Mouse	Pik3r2_qR1	CCTGCAACCTCTCGAAGTG	19
Id1	Mouse	Id1_qF1	GGTCCGAGGCAGAGTATTACA	21
Id1	Mouse	Id1_qR1	CCTGAAAAGTAAGGAAGGGGGA	22

Table 3. Primers used in RT-qPCR test. The species and sequences corresponding to the primers are listed.

2.2.8 Western blot

For total cellular protein extraction, employ RIPA lysis buffer in accordance with the user manual. Afterward, collect the supernatant by separating cell debris in a 4°C centrifuge (14,000g, 30 min). Determine protein concentration using Coomassie Brilliant Blue G-250 protein stain. Subsequently, conduct a Western blot following standard procedures, with protein separation achieved using NuPAGETM 3-8% Tris-Acetate gel. Utilize 4x LDS sample buffer, Tris-Acetate SDS running buffer, Spectra Multicolor High Range Protein Ladder, and NuPAGE transfer buffer. Transfer the proteins onto a hydrophobic PVDF transfer membrane. Refer to Table 4 for antibody information.

Antibody	Species	Series No.	MW (kDa)	Company	Diluted
ARID1A/BAF250A (D2A8U)	Rabbit	#12354	270	Cell signal tech	1:1000
ARID1B/BAF250B (E1U7D)	Rabbi	#65747	250;280	Cell signal tech	1:1000
Beta-Actin (13E5)	Rabbit	#4970	45	Cell signal tech	1:1000
E-Cadherin (4A2)	Mouse	#14472	135	Cell signal tech	1:1000
N-Cadherin (D4R1H)	Rabbit	#13116	140	Cell signal tech	1:1000
Vimentin (D21H3)	Rabbit	#5741	57	Cell signal tech	1:1000

Table 4. Antibodies used in Western blot. The details of the antibodies are listed.

2.2.9 Cell counting kit-8 assay

At a density of 1,000 cells per 100 µl of medium, cells were seeded in each well of a 96-well culture plate. The cells were incubated at 37°C with 5% CO2. Every 24 hours, 10 µl of CCK-8 solution was added to each well without generating air bubbles. The cells were then incubated at 37°C with 5% CO2 for 2 hours, and the absorbance at 450 nm was measured using a TECAN System (Beckman Coulter, Brea, CA, United States).

2.2.10 Colony formation

For the colony formation assay, each well of 6-well plates was seeded with 400-800 cells and cultured at 37°C with 5% CO2. Following 14 days in culture, the cells were fixed in a 4% paraformaldehyde solution and stained with a 0.1% crystal violet solution. The colonies were then counted and photographed.

2.2.11 Cell apoptosis assay

The Annexin V assay was employed to detect apoptosis following the manufacturer's protocol. Apoptosis was induced by knocking down ARID1B in 7291 and 0007 cells using siRNA34 and siRNA35, respectively. After centrifugation (300g, 5 min), 2 x 10^5 cells were collected and resuspended in 500 µL of 1X annexin V binding buffer. Subsequently, 5 µL of annexin V-FITC and 5 µL of propidium iodide were added. The mixture was then incubated for 10 minutes at room temperature in the dark. Following the addition of a working buffer solution, the binding of annexin V-FITC was analyzed using flow cytometry (BD FACSCanto II).

2.2.12 Migration and invasion assays

2.2.12.1 Wound healing assay

Confluent monolayers with 90-100% confluence were established by seeding 5 × 10^4 cells per well in 6-well plates. Subsequently, a scratch was created across the surface

of the well using a 20 µL pipette. The detached cells were meticulously washed away by performing two rounds of washing with DPBS. Images were captured at different time points (0, 6, 12, 24h) and subsequently analyzed using ImageJ software (version 1.51s, NIH Image, NIH, Bethesda, MD, USA). Wound closure was quantified using the following equation:
Wound closure (%) = (Original wound area - area at each time point) / Original wound area.

2.2.12.2 Boyden chamber assay

The Cultrex reduced growth factor basement membrane extract (RGF BME) was diluted in serum-free DMEM medium to a final concentration of 200 µg/mL. Subsequently, 100 µL of the diluted RGF BME was carefully added to the center of each Transwell® insert and incubated at 37°C with 5% CO2 for 1 hour for invasion assays.

For the invasion assay, the upper chambers were loaded with 5×10^4 cells/well in 150 µl of serum-free DMEM, and then 800 µl of complete DMEM medium was added to the lower layer. The plates were incubated at 37˚C with 5% CO2 for 24-48 hours. Following incubation, the RGF BME was wiped from the upper membrane. The membranes were then fixed in 4% paraformaldehyde for 20 minutes. The cells that migrated to the lower side of the filter were stained with 0.5% crystal violet for 15 minutes and observed under a light microscope. The experiment was repeated three times.

2.2.13 CRISPR-Cas9 electroporation (Electroporation)

2.2.13.1 Prepare DNA constructs

Following Zhang's experiment protocol, the DNA sequence of the target site was cloned into the plasmid. Our project utilized three distinct sgRNA sequences (refer to Table 5) along with Cas9 protein.

Homo sapiens Gencode Release 26 (GRCh38.p10)	Target strand	PAM (5' - 3')	guide RNA sequence (5' - 3')	Target DNA sequence
ARID1A_gRNA_E19_1	+	CGG	GAGGUUUAUUUCAGAACCC	GAGGTTTATTTCAGAACCC
ARID1A_gRNA_E19_2	+	AGG	GUUUAUUUCAGAACCCCGG	GTTTATTTCAGAACCCCGG

ARID1A_gRNA_E19_3	-	GGG	CAUACCCGCCAUGCCUCCG	CATTACCCGCCATGCCTCCG

Table 5. Details of sgRNA used for electroporation.

2.2.13.2 Electroporation

The prepared DNA construct (CRISPR-Cas9 system) is introduced into the cells using an electroporator. A mixture of 2.5×10^5 cells in 25 µl, 180 pmol sgRNA in 6 µl and 20 pmol Cas-9 in 1 µl is placed in a 4 mm gap cuvette. Subsequently, the electroporation parameters are set to 270V voltage and a duration of 21-23 ms.

2.2.13.3 Cultured cells

Transfected cells are cultured and allowed to grow in the culture medium. Following one week, the cells are harvested, and single-cell sorting is performed. Expanded single-cell subclones are collected, and DNA is extracted from these subclones. Subsequently, the extracted DNA is analyzed using Sanger sequencing.

2.2.13.4 Sanger sequencing

The extracted DNA underwent PCR amplification, with primer information provided in Table 6. Subsequently, following the operational instructions of the TubeSeq Supreme sequencing service (Eurofins Genomics in Ebersberg, Germany), the PCR products were submitted for testing. The results were later provided by Eurofins.

Gene	Species	Primer name	Sequence (5’ - 3’)	Length
ARID1A	Human	Arid1a_sg_F1	ATT CGG CGG GAT ATC ACC TT	20
ARID1A	Human	Arid1a_sg_R1	ATC TTC CCC AGG CAC TGA TAC	21

Table 6. Primers of PCR amplification were used for Sanger sequencing.

2.2.14 Determination of dose-response curves

All inhibitors were procured from MedChemExpress. The drugs used in the experiment were dissolved in DMSO to obtain desired concentrations. To assess the potential influence of DMSO on the experimental outcomes, a vehicle control group was implemented. Within this group, both human and mouse CRC cells were exposed to an identical DMSO concentration as the experimental group, with the exception that

no drugs were introduced. This design enables us to differentiate between the effects induced by the drugs and any potential effects attributable to DMSO itself. Initially, cells were seeded at a density of 5×10^3 cells per well in a 96-well standard plate. B-cell lymphoma 2 (BCL-2) inhibitor and ATR inhibitor were applied at eight different dilutions, ranging from 0.2uM to 200uM. After 48 hours of exposure, cell viability was assessed using the CCK-8 kit.

Utilizing GraphPad Prism 9 software (GraphPad Software, Inc., Boston, USA), drug response curves were simulated employing a nonlinear log(inhibitor) versus slope equation of the response variable. Half-maximal inhibitor concentration values (IC50) were determined, considering IC50 values only when the software yielded unambiguous results and R^2 values were above 0.90. The experiment was iterated three times, each time with a minimum of three replicate wells.

2.2.15 Synergy was determined using Chou-Talalay and SynergyFinder

Following the determination of IC50 values for different inhibitors, two groups of drug combinations were prepared at a constant ratio (1:1). At least five dilution series of concentration gradients were established. Subsequently, cells were treated with both single drugs and the combined drugs for 48 hours, and cell viability was measured using the CCK-8 kit on the TECAN System (Beckman Coulter, Brea, CA, United States).

Combination index (CI) values were calculated utilizing CompuSyn software (ComboSyn, Inc., Paramus, USA). For determining synergy using the SynergyFinder method, the online SynergyFinder plus software (https://tangsoftwarelab.shinyapps.io › synergyfinder) was employed to calculate drug interaction relationships using the ZIP calculation method.

2.2.16 Statistical analysis

The means of two groups were compared utilizing an unpaired two-tailed Student's t-test, and experiments were replicated at least three times with more than two replicates. Data are presented as mean ± standard error (S.E.). One-way ANOVA tests were applied when comparing drug response curves, and all statistical analyses were conducted using GraphPad Prism 9 (GraphPad Software, Inc., Boston, USA). A

significance level of $p<0.05$ was considered statistically different, and all tests were two-sided.

3 RESULTS

3.1 Loss of ARID1A protein is prevalent in colorectal cancer and predicts poor survival.

We conducted an analysis of *ARID1A* gene mutation frequency in human cancers using TCGA cohort studies. *ARID1A* is frequently mutated across various human cancers, with notable prevalence in ovarian and endometrial cancers (up to 50%). In CRC, its mutation frequency is approximately 10% (cBioPortal calculation). Subsequently, we assessed the impact of *ARID1A* mutation on the clinical prognosis of CRC (Figure 5B). CRC patients harboring *ARID1A* mutations demonstrated a trend toward a poorer OS prognosis in comparison to wild-type patients. However, this observation did not reach statistical significance, consistent with similar findings reported by others (Li et al. 2020).

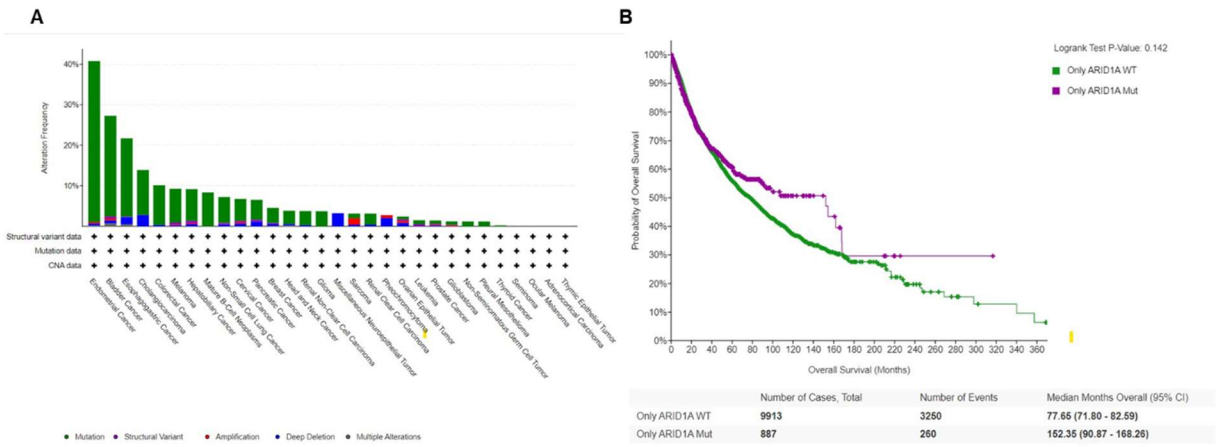

Figure 5. *ARID1A* mutation profile in human cancers (A) and impact on overall survival of CRC patients (B). A. Among human cancers, *ARID1A* mutations occur most frequently in women's endometrial cancers (more than 40%), while the mutation rate in CRC is about 10%. B. The overall survival of CRC patients carrying *ARID1A* mutations tended to decrease, but there was no statistical difference (p = 0.142). Mut: mutation. The current image is derived from the reference (Liu et al. 2018).

3.2 Establishment of animal models and cell lines

3.2.1 Generation of CRC organoids

The tumor-suppressive role of Arid1a in the mouse colon was demonstrated, and invasive Arid1a-deficient adenocarcinoma was shown to mimic human CRC (Mathur et al. 2016). In our study, the Cre-loxP system was employed to establish Arid1a mutant mice with a mutation in exon 8 and wild-type mice. Adenovirus-mediated Cre deletion of floxed sequences, a method previously utilized for inducing primary tumors,

was employed (Wang et al. 1996). CRC organoids were generated by introducing the Ad5CMV-Cre vector (The University of Iowa) into the organoids of the mouse colorectum in vitro models (Figure 6).

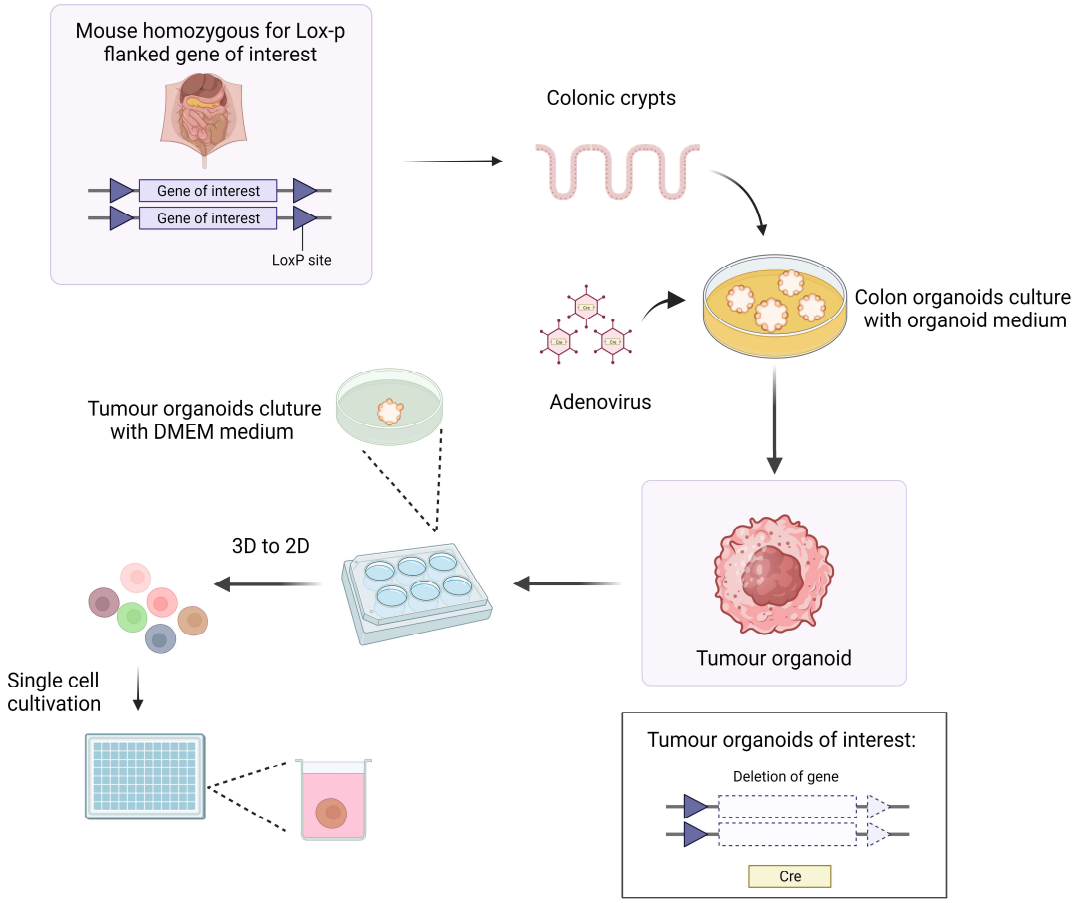

Figure 6. Flowchart for generating CRC organoids carrying mutations in the *ARID1A* gene. The colonic tissue was extracted from the genetic mouse model carrying the Cre-loxP system, the colonic crypt lumens were obtained after in vitro digestion, and the organoid tissue was generated after in vitro culture in organoid culture medium, and then transfected with adenovirus carrying Cre vector, and finally Obtain ARID1A KO organoids. Created with BioRender.com

The initial organoid culture system was pioneered by Sato using mouse intestinal epithelial cells (Sato et al. 2009). Subsequently, the establishment of tumor organoids has been extensively documented, demonstrating the ability to maintain key features of primary tumors even after prolonged passages (Sachs et al. 2018). Following cultivation with tumor organoid medium, we successfully generated and genotyped stably passaged organoids identified as ArAKPf and AKPf.

3.2.2 Single cell clone selection and genotype verification

Organoids are complex multicellular structures characterized by a high degree of cellular diversity (Takebe and Wells 2019). To minimize the impact of non-tumor or wrong-genotype cells, we isolated individual 2D cells through serial dilutions and established a clonal cell line after an expansion period. As a result, we tested the genotype of tumor cell colonies (Figure 7) and selected the ones with the right genotype, ensuring that we obtained a purified tumor sub-clonal cell line.

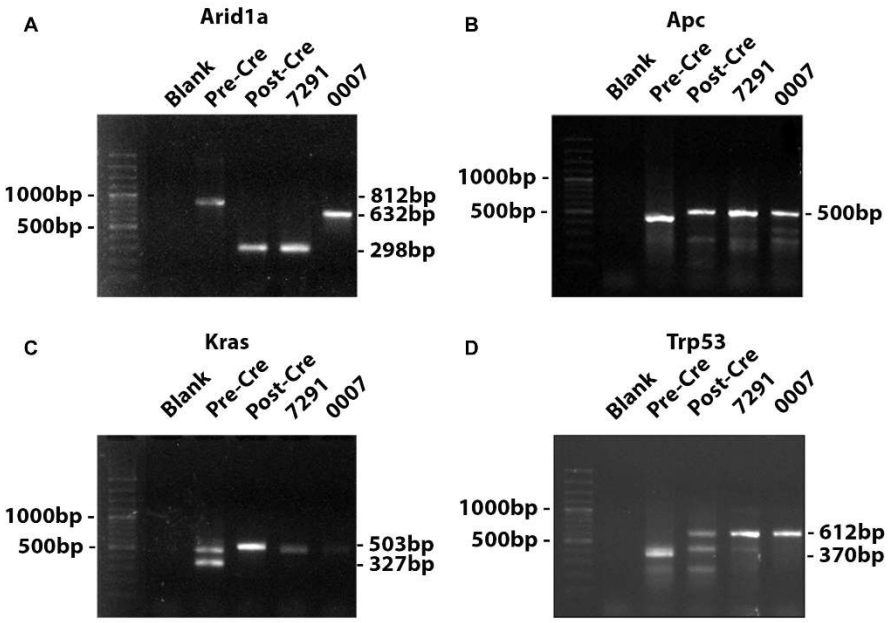

Figure 7. Genotype verification results of ArAKPf and AKPf cell lines. A. The *Arid1a* gene; B. The *Apc* gene; C. The *Kras* gene; D. The *Trp53* gene.

3.2.3 *Arid1a* gene expression

We assessed the mRNA and protein expression levels of *Arid1a* genes using real-time quantitative PCR and western blotting. The results unequivocally demonstrated a significant reduction in the expression of ARID1A in ArAKPf cells compared to AKPf cell lines, with statistical significance observed.

For the quantitative reverse transcription polymerase chain reaction (RT-qPCR) test, three different Arid1a primers targeting exons 2 and 8 were chosen. The results consistently revealed a substantial downregulation of ARID1A in the ArAKPf cell line in comparison to the AKPf cell line (Figure 8A). The Western blot (WB) analysis further confirmed the successful knockdown of ARID1A at the protein level (Figure 8B).

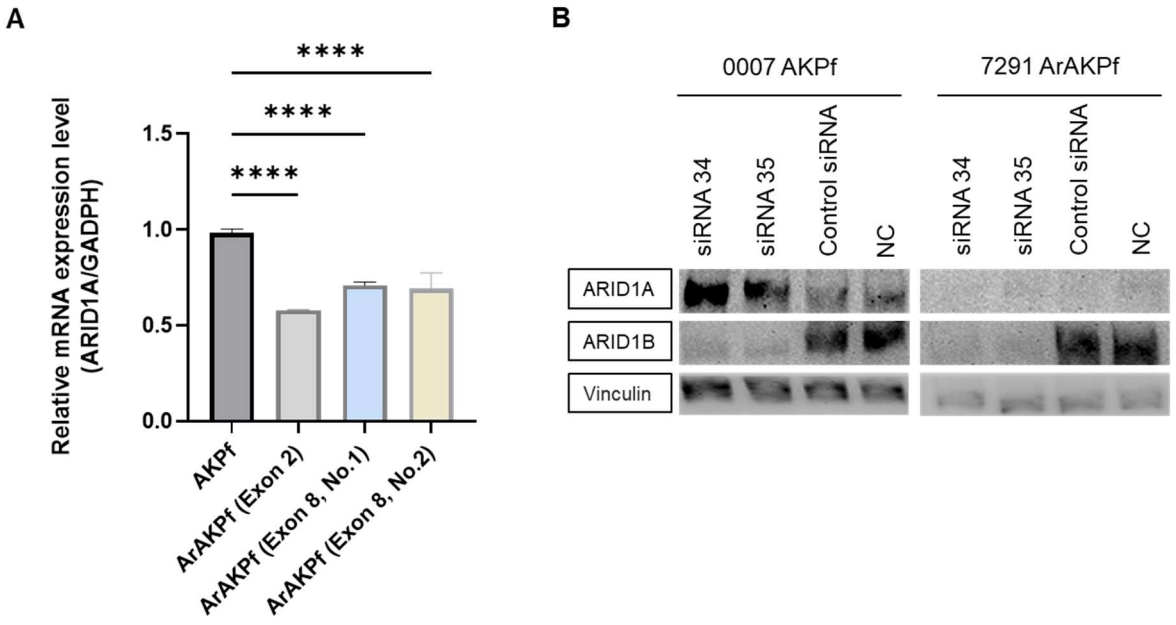

Figure 8. The results of ARID1A expression in AKPf and ArAKPf. A. ARID1A was significantly decreased in the ArAKPf cell line compared with the AKPf cell line. Three different Arid1a primers (target on exons 2 and 8) were tested by RT-qPCR. The experiment was repeated 3 times, mean ± SD are shown, ****: $p<0.0001$; B. Western Blot showed the protein expression levels of ARID1A and ARID1B in ArAKPf and AKPf cells. ARID1B was knocked down using two different siRNAs (No.34,35). ARID1A and ARID1B are co-expressed in the AKPf cell line. When ARID1B was knocked down, the expression responsiveness of ARID1A increased; while ARID1A was not expressed in the ArAKPf cell line, there was no change in ARID1A after knocking down ARID1B. Experiments were repeated twice.

Given the mutual exclusivity between ARID1A and ARID1B, we examined the expression of the *Arid1b* gene in AKPf and ArAKPf cell lines. The results aligned with prior studies, revealing a compensatory increase in the expression of the *Arid1b* gene in *Arid1a* mutant cell lines.

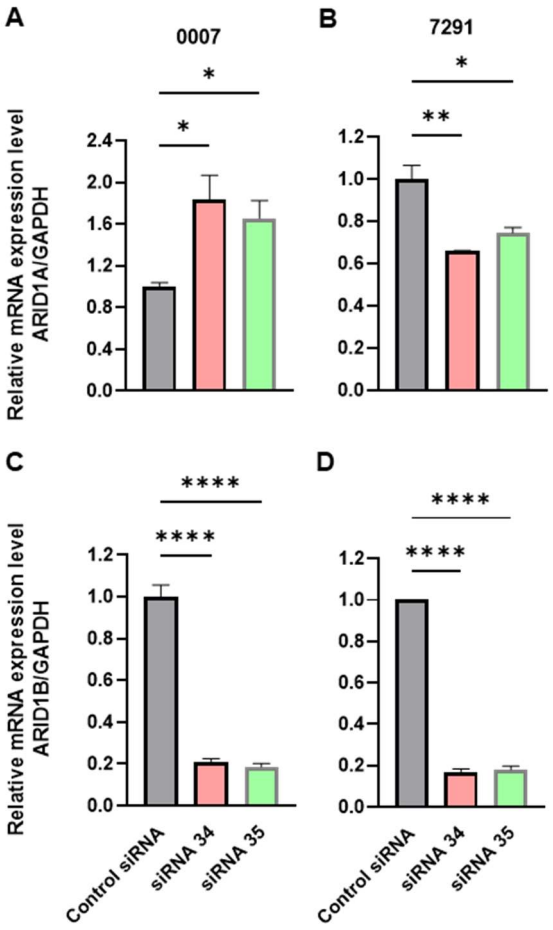

Figure 9. mRNA expression levels of ARID1A and ARID1B relative to GADPH. In the AKPf cell line, the mRNA expression level of ARID1A was compensatory increased after the knockdown of ARID1B (A), while the expression of ARID1B was confirmed to be decreased (C). Knockdown of ARID1B in the ArAKPf cell line means decreased expression of both ARID1A (B) and ARID1B (D). mean ± SD are shown, *: $p<0.05$, **: $p<0.01$; ****: $p<0.0001$.

Utilizing two validated siRNAs (siRNA 34 and siRNA 35) helps rule out non-specific effects in ARID1B KD and enhances the reliability of experimental results. Prior to conducting cellular functional experiments, we assessed the working efficiency of the siRNAs through RT-qPCR assay and Western blotting. The results demonstrated that the knockdown efficiency of the two different siRNAs reached 80% at the mRNA level (Figure 9). The knockdown effect at the protein level was also significant (Figure 8B).

We investigated whether ARID1B KD affects ARID1A. Interestingly, ARID1B KD leads to compensatory high expression of ARID1A in AKPf, but not in ArAKPf. According to previous reports, when ARID1A and ARID1B are lost simultaneously, the BAF complex cannot function normally (Helming et al. 2014b).

3.2.4 CRISPR/Cas9-mediated ARID1A knockout in human CRC cell line

To validate the aforementioned findings, we established human CRC cell line models with *ARID1A* mutations using CRISPR technology, which induces indel mutations during the cutting process, leading to a population of cells with mutated genes. Two different methods were attempted to deliver the CRISPR/Cas9 system into human CRC cells.

Initially, we designed three distinct sgRNAs (Figure 10), mixed them with Cas9 protein, and electroporated them into HCT116 cells to generate cell clones with ARID1A protein mutations (Figure 11). Single cells from the electroporated population were sorted into individual wells of a 96-well plate, followed by clonal expansion. The ARID1A indel in the sgRNA-targeted region was confirmed by Sanger sequencing (Figure 12). The loss of ARID1A expression in the cell clones was further confirmed by Western blotting (Figure 13), depicting the expression levels of ARID1A in multiple clones of HCT-116. Combining the results from Sanger sequencing and Western blotting, we selected subclone cell line No.5 as the ARID1A knockout experimental group.

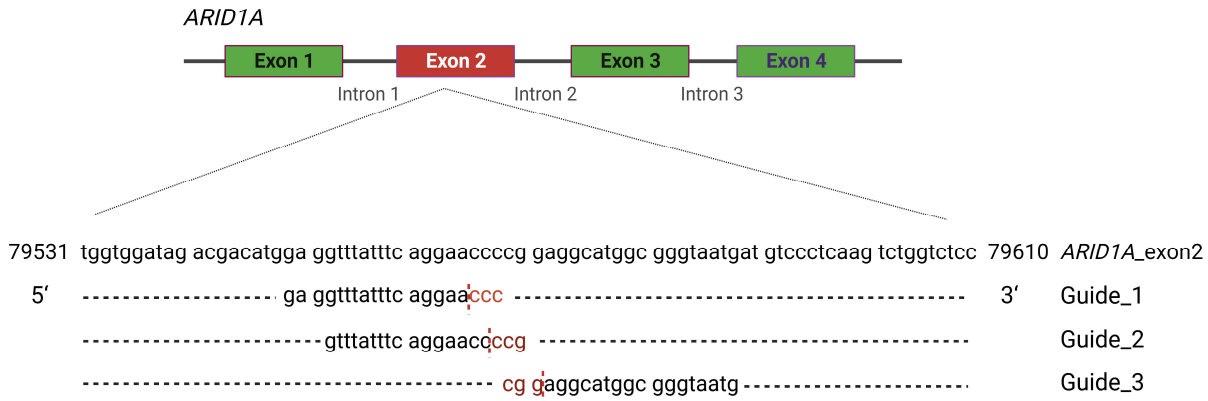

Figure 10. Sequences of three different sgRNAs. All three sgRNAs target exon 2 of the human *ARID1A* gene. Created with BioRender.com

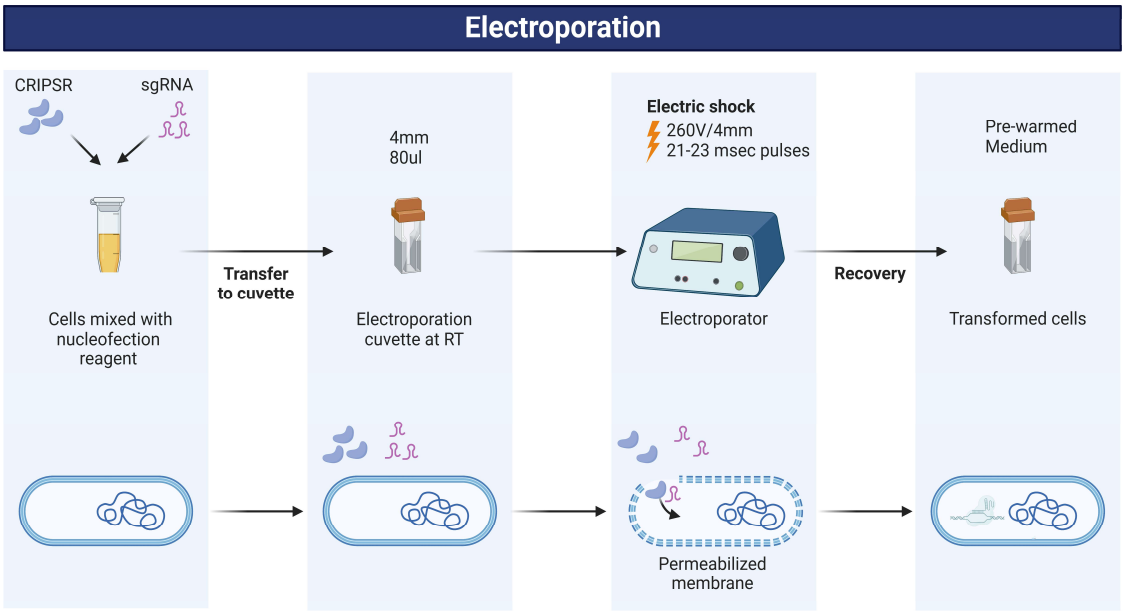

Figure 11. Main parameters and flowchart of electroporation. The detailed procedure is shown in Materials and Methods. Created with BioRender.com

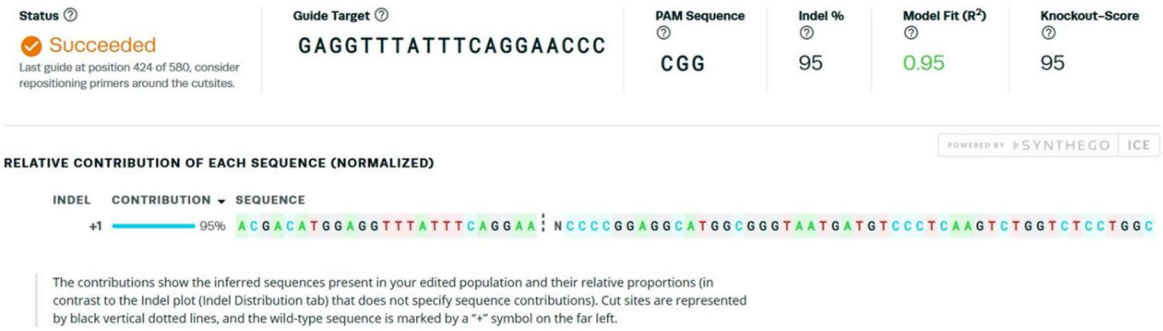

Figure 12. Sanger sequencing results of No.5 HCT116 subclone cells generated after electroporation. Indel %: The percentage of sequences that contain an indel in the sample. Model Fit (R2): is a measure of how well the proposed indel distribution fits the Sanger sequence data of the edited sample. Knockout Score: The proportion of sequences that are likely to result in functional protein knockout.

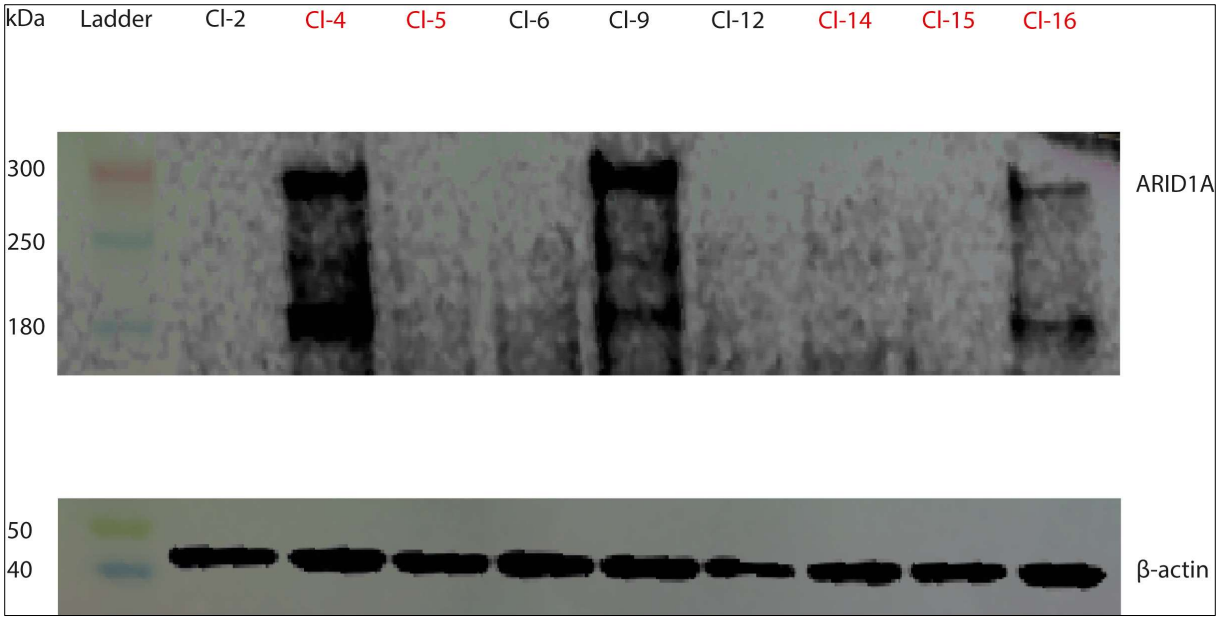

Figure 13. Western blot results confirmed that ARID1A was successfully knocked out in HCT116 subclone cells. Subcloned cells submitted for Sanger sequencing are marked in red. The results showed that ARID1A was knocked out in clones 5, 14, and 15. Cl: clone.

3.3 Impact and mechanism of *ARID1A* gene on the function of CRC tumor cells

3.3.1 Loss of ARID1A expression promotes proliferation in vitro

Given the tumor suppressor role of ARID1A, we proceeded to investigate the consequences of its loss in vitro using the CCK-8 assay. A phenotypic characterization was performed on the paired cell lines (ArAKPf/AKPf, ArAK/AK, and HCT116 ARID1AWT/ARID1AKO). In line with the known tumor-suppressive effects of ARID1A, the deletion of ARID1A resulted in a significant enhancement of cell proliferation (Figure 14).

Furthermore, we evaluated the impact of ARID1A loss on the organoid-forming ability of CRC. Quantification and comparison of the maximum observable organoid diameters validated that the deletion of ARID1A promotes organoid clonogenesis. (Figure 15).

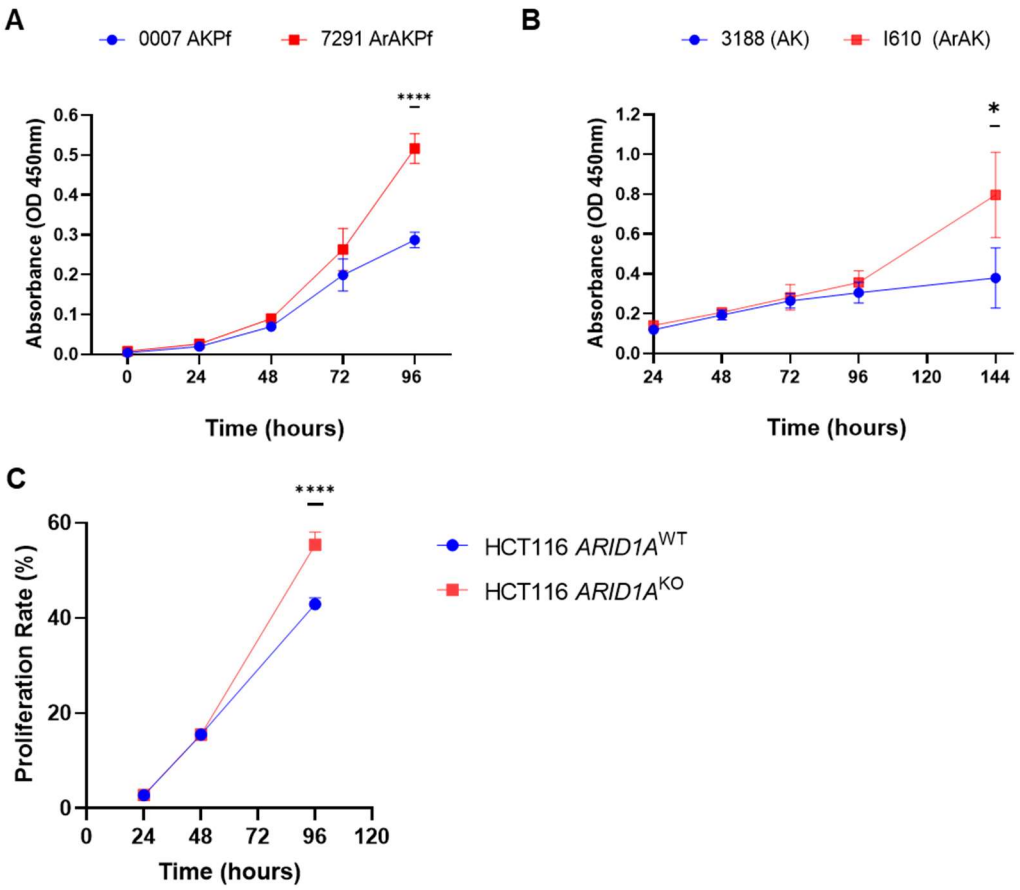

Figure 14. Loss of ARID1A resulted in significantly enhanced cell proliferation in CRC cells. The cck-8 assay was tested on AKPf/ArAKPf 2D cell line (A), AK/ArAK organoids (B), and HCT116 *ARID1A*^{WT}/*ARID1A*^{KO} 2D cell lines. Results from three independent experiments, mean ± SD are shown, *: p<0.05; ****: p<0.0001.

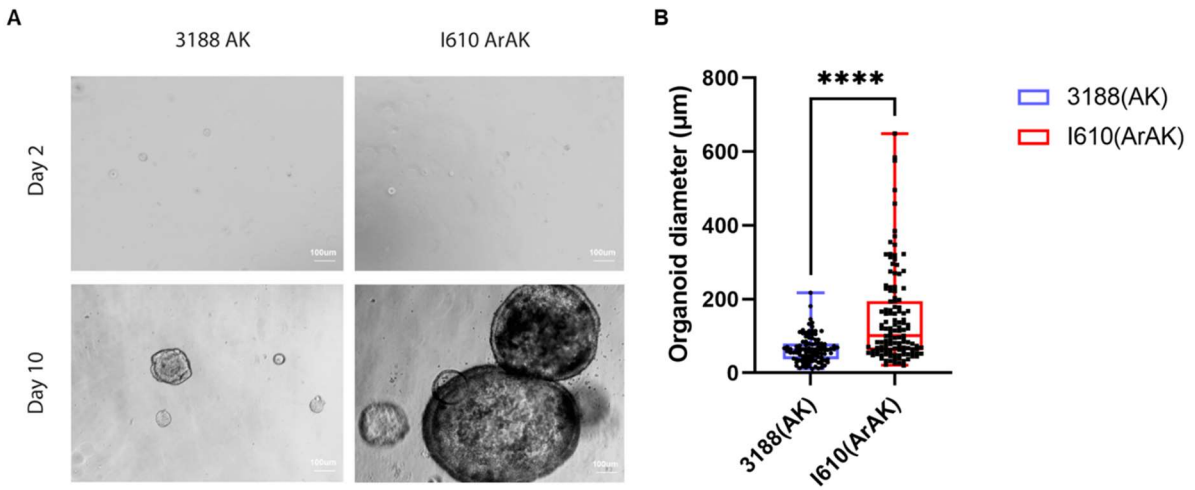

Figure 15. Diameter change of AK/ArAK organoids cultured for 10 days. A. Morphology of the organoids. Scale bar: 100um. B. Box plots were used to show the statistical difference in diameter. Results from two independent experiments. mean ± SD are shown, ****: p<0.0001.

3.3.2 Loss of ARID1A expression promotes migration and invasion in vitro

The Boyden Chamber assay was employed to verify the migration and invasion ability of the cells. The results consistently demonstrated that the loss of ARID1A promotes migration and invasion in both human and murine CRCs. Additionally, these findings were validated through a wound healing assay using ImageJ software to quantify digital images of migrating cells in the wound region. Our results confirmed that the ARID1A defect significantly increased the migration and invasion ability of CRCs, as illustrated in Figure 16-18.

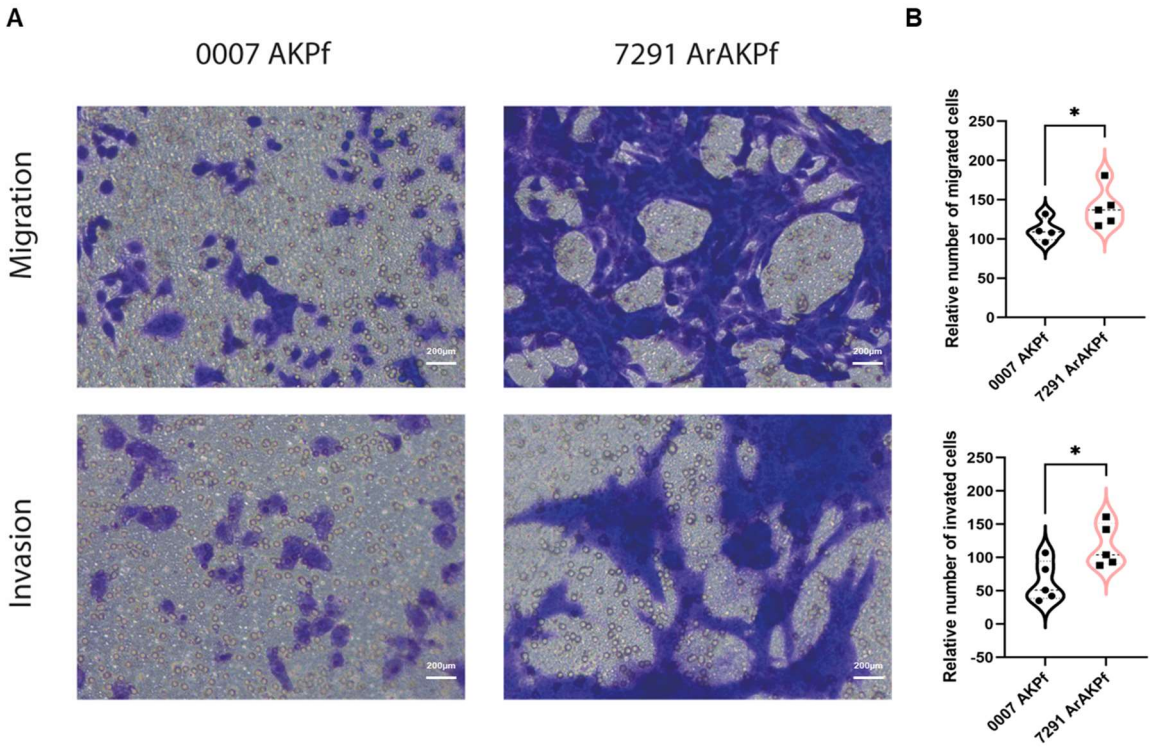

Figure 16. Migration and invasion assays of AKPf and ArAKPf cell lines using Boyden chamber. A. *Arid1a* mutations promote migratory and invasive abilities of mouse CRC cell lines. Scale bar: 200um. B. Violin plots showing the statistical results of migration and invasion assays. Results from three independent experiments. mean ± SD are shown, *: $p<0.05$.

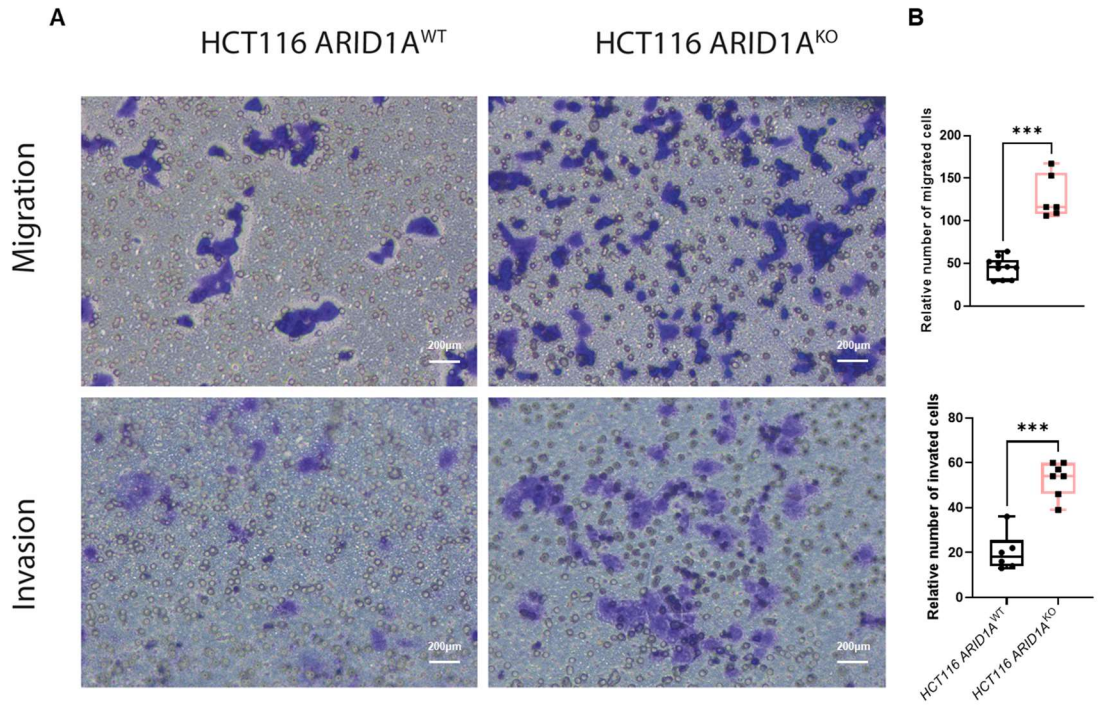

Figure 17. Migration and invasion assays of HCT116 *ARID1A*^{WT} and HCT116 *ARID1A*^{KO} cell lines using Boyden chamber. A. *ARID1A* mutations promote migratory and invasive abilities of HCT116 cell lines. Scale bar: 200um. B. Box plots showing the statistical results of migration and invasion assays. Results from three independent experiments. mean ± SD are shown, ***: p<0.001. WT: Wild-type; KO: Knock-out.

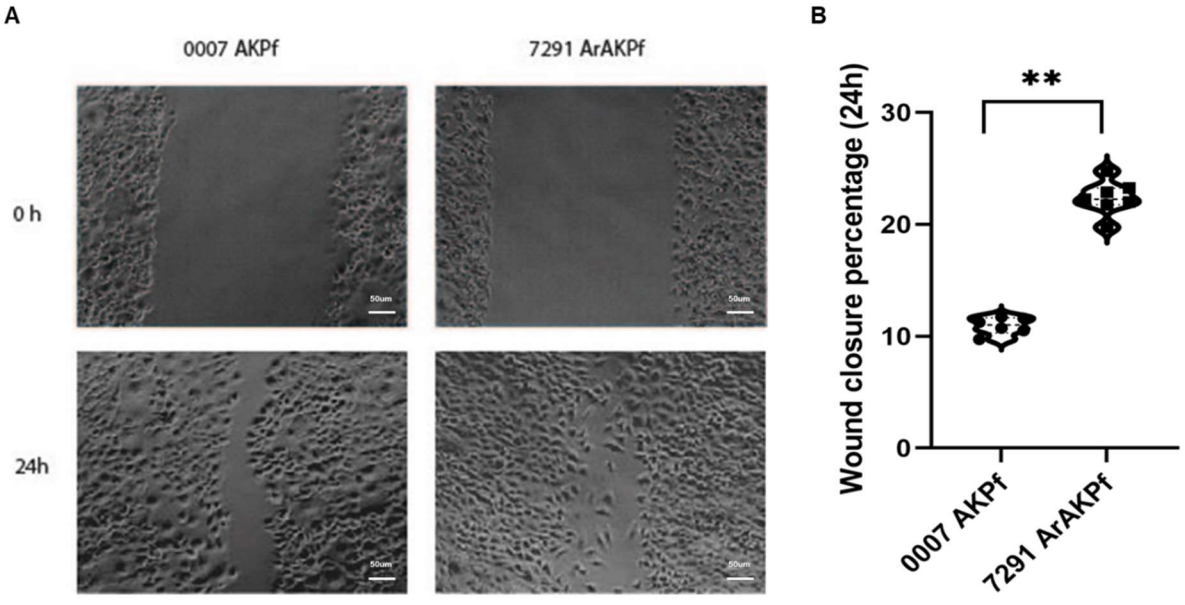

Figure 18. Wound healing assays of AKPf and ArAKPf cell lines were cultured for 24 hours. A. Light microscopy images revealed that mutations in *Arid1a* promote wound healing. Scale bar: 50um. B. Define the wound width at 0 h as 100%. Wound closure capacity was assessed by measuring the area without cell coverage as a percentage of the initial blank area after 24 hours. Three independent experiments were performed and mean ± SD are shown.

3.3.3 ARID1A loss regulates EMT by activating VIM and inhibiting CDH1

Cancer cells of epithelial origin typically exhibit a continuum between epithelial-mesenchymal phenotypes (Tam and Weinberg 2013). The epithelial-dominant phenotype is predominantly observed in primary cancers. As the metastatic process unfolds, tumor cells undergo a phenotypic shift, losing epithelial features such as cell-cell adhesion and adopting a mesenchymal phenotype. This phenomenon is referred to as EMT (Thiery et al. 2009).

VIM and CDH1 are commonly used markers for EMT, with the VIM/CDH1 ratio being a widely employed method to distinguish epithelial, mixed, and mesenchymal phenotypes of tumor cells (He et al. 2023: 2; Park et al. 2008; TANABE et al. 2014). Our study verified that the loss of ARID1A resulted in a significantly increased VIM/CDH1 ratio, while epidermal markers were not reduced. This suggests that the loss of ARID1A function contributes to the epithelial-mesenchymal transition (EMT) of colorectal cancer (CRC) cells (Figure 19A). Concurrent knockdown of ARID1B in Arid1a-mutated CRC cells did not reverse this trend (Figure 19B).

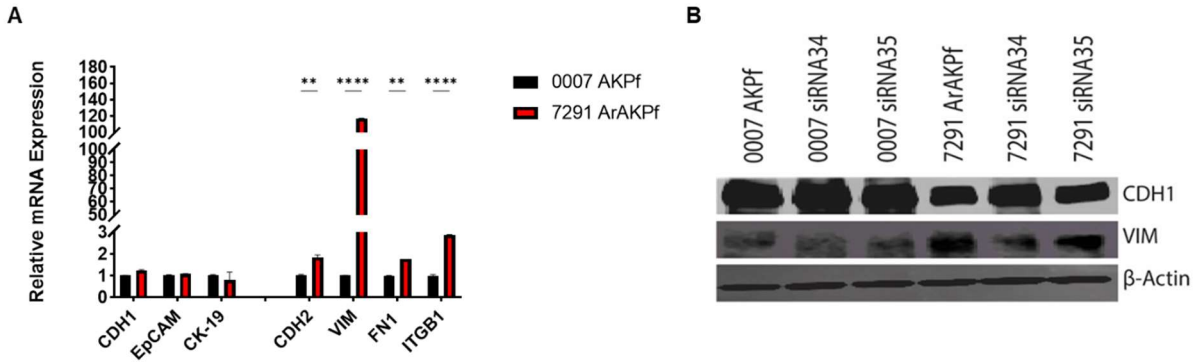

Figure 19. The results of EMT markers expression in AKPf and ArAKPf. A. Mesenchymal markers and transcription factors were significantly increased in the ArAKPf cell line compared with the AKPf cell line. The experiment was repeated 3 times, mean ± SD are shown, **: p<0.01; ****: p<0.0001; B. Western Blot showed the VIM and CDH1 protein expression levels of ARID1A and ARID1B in ArAKPf and AKPf cells. ARID1B was knocked down using two different siRNAs (No.34,35). ARID1A loss resulted in a significantly increased VIM/CDH1 ratio, but impairment of ARID1A and ARID1B does not reverse mesenchymal changes. Experiments were repeated twice. CDH1: cadherin 1; CDH2: cadherin 2; CK19: Cytokeratin 19; EpCAM: Epithelial cell adhesion molecule; FN1: Fibronectin 1; ITGB1: Integrin subunit beta 1; VIM: Vimentin.

3.3.4 *Arid1a* mutation enhances CRC metastasis in vitro via the PI3K signaling pathway

The bar plot in Figure 20B reveals that 210 genes (dark red dots) were significantly positively correlated with *ARID1A* mutations, while 128 genes (dark green dots) were

significantly negatively correlated (FDR<0.01, t-test followed by multiple testing correction). An enrichment analysis of the varied gene set was performed against multiple common signaling pathway sets to identify their overlap. The results indicated the activation of the PI3K/Akt signaling pathway. In line with prior research conclusions (Jin et al. 2023; Xie et al. 2014), we posit that the PI3K/Akt signaling pathway is one of the mechanisms by which ARID1A loss promotes CRC metastasis.

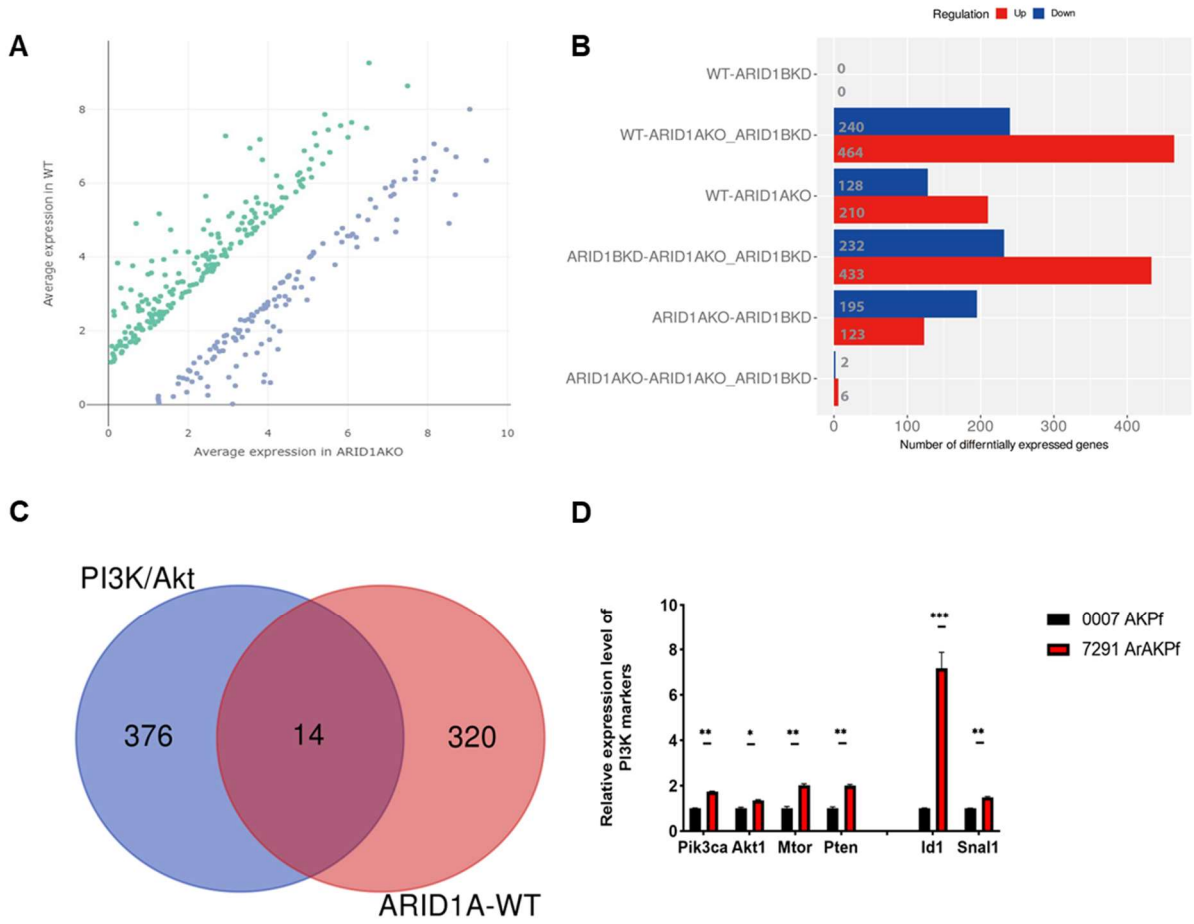

Figure 20. Bioinformatic analysis of RNA-seq results in GSE101966 data. A. Distribution of mRNA expression of different genes shown using a scatterplot. B. Histogram showing the set of differentially expressed genes. Red represents genes that are upregulated and blue represents downregulated genes. C. Venn diagram of PI3K/Akt signaling pathway and ARID1A mutations leading to differentially expressed genes. D. The mRNA expression levels of PI3K/Akt signaling pathway-related genes were significantly increased in the ArAKPf cell line compared with the AKPf cell line. The experiment was repeated 3 times, mean ± SD are shown, *: p<0.05; **: p<0.01; ***: p<0.001. WT: Wild-type; KO: Knock-out; Akt1: AKT serine/threonine kinase 1; Id1: Inhibitor of DNA binding 1; Mtor: Mechanistic target of rapamycin kinase; Pik3ca: Phosphatidylinositol-4,5-bisphosphate 3-kinase catalytic subunit alpha; Pten: Phosphatase and tensin homolog; Snal1: Snail family transcriptional repressor 1.

3.4 Potential therapeutic targets for ARID1A mutations

3.4.1 ARID1B loss results in reduced proliferation of ARID1A mutant cell lines

We initially verified whether clonogenicity could be affected. As expected, the knockdown of ARID1B in the AKPf cell line did not affect its clonogenic ability, but it significantly inhibited clonogenicity in the ArAKPf cell line (Figure 21)

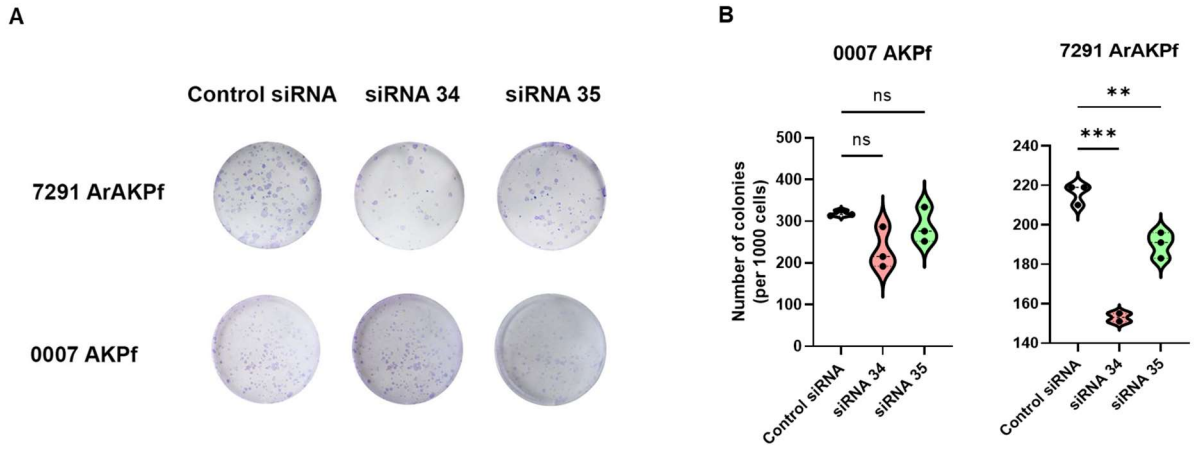

Figure 21. Colony formation experiment results. ARID1A deletion can enhance the clonogenic ability of ArAKPf cells, but knocking down ARID1B can inhibit the above changes. Cell lines with normal expression of ARID1A were not affected by knockdown of ARID1B. A. Colony formation assay results of 0007 and 7291 cells and the changes after ARID1B knockdown using siRNA. B. Violin plots show the results of the statistical analysis. Results from three independent experiments, mean ± SD are shown, ns: p>0.05; **: p<0.01; ***: p<0.001.

We evaluated the impact of ARID1B KD on CRC proliferation ability. The results demonstrated that knocking down ARID1B in the absence of ARID1A significantly inhibited cell proliferation. However, when ARID1B was knocked out alone, cell proliferation was not affected due to the compensatory effect of ARID1A (Figure 22).

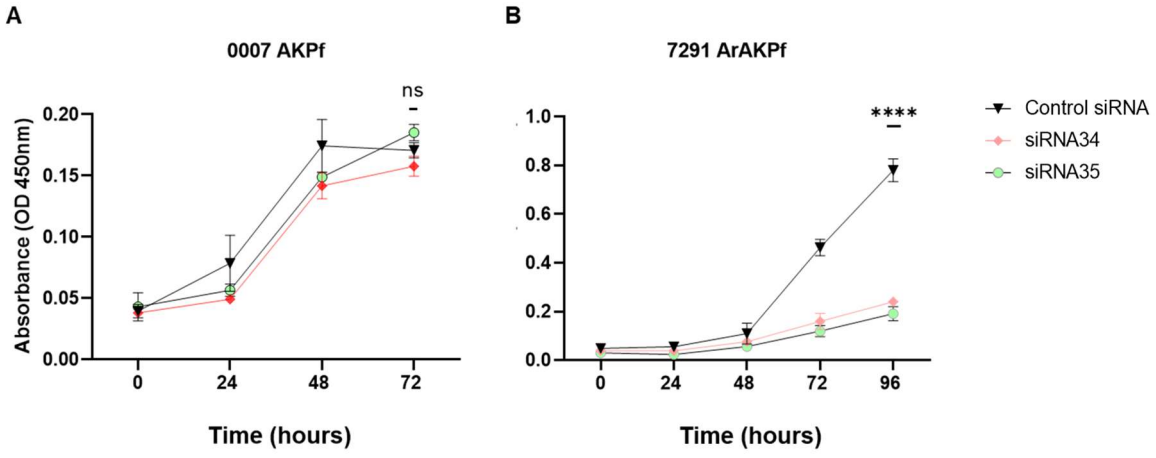

Figure 22. AKPf and ArAKPf cell proliferation test results obtained by cck-8 assay. A. The proliferation ability of the AKPf cell line is not affected by the expression level of ARID1B. B. The impaired expression of ARID1B can significantly inhibit the proliferation ability of ArAKPf cells. Results from three independent experiments, mean ± SD are shown, ns: $p>0.05$; ****: $p<0.0001$.

3.4.2 Dose-response assays of selected inhibitors on CRC cells

Simultaneous deletion of ARID1A and ARID1B has been shown to impair the SWI/SNF complex and inhibit CRC cell proliferation. However, designing specific inhibitors against ARID1B poses challenges due to the proteins sharing more than 60% homology (Helming et al. 2014b). Furthermore, the occurrence of co-mutations of both ARID1A and ARID1B in CRCs complicates the development of targeted therapies (Mathur 2018).

We assessed the efficacy of the conventional chemotherapeutic agent oxaliplatin in *ARID1A*-mutant CRC. The results indicated no specific effect on *ARID1A* mutations in mouse cell lines. In HCT116 cell line experiments, the *ARID1A* mutant line exhibited resistance to oxaliplatin (results not shown).

We also tested the targeted therapeutic effect of ATRi on *ARID1A* mutations. Utilizing insights gleaned from the vehicle control cohort, we maintained the DMSO concentration in the experimental group at or below 2.5%. This rigorous control was implemented to ascertain that the observed experimental results emanated from the pharmacological impact of the administered drug, mitigating any confounding non-specific effects attributable to DMSO. Interestingly, in mouse cell lines, two different ATRi were more lethal to *Arid1a* mutant cell lines (Figure 23 A and B). However, in the HCT116 cell line, ATRi did not show significant differences and even exhibited specific drug resistance (Figure 23 C and D). Given the multiple drug resistance mechanisms of ATRi reported in some studies, further clinical validation is essential before promoting ATRi as a treatment option.

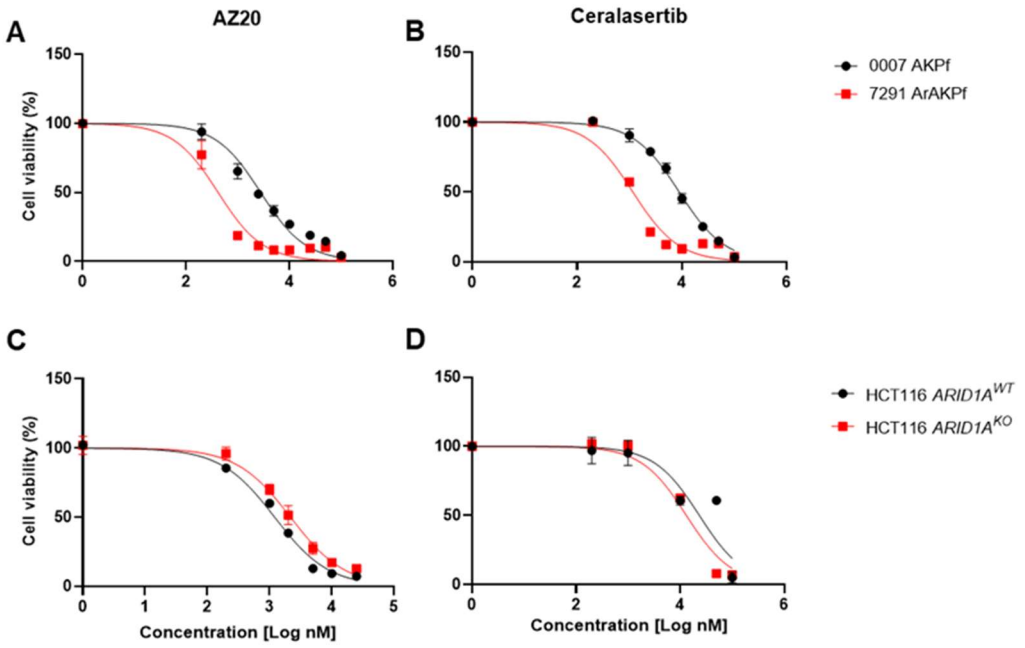

Figure 23. Drug response curves of mouse and human CRC cell lines treated with ART inhibitors for 48 hours. Cell viability was detected by the cck-8 assay. The survival rate of the control group was 100%, and the drug response curve showed the percentage of surviving cells after treatment with different drug concentrations. ARID1A deletion resulted in increased sensitivity of ArAKPf cells to two different ATRi (AZ20 and Ceralasertib) compared with wild-type controls (A and C) and concordantly in the HCT116 cell line (B and D). One-way ANOVA revealed significant differences ($P<0.05$). The experiment was repeated 3 times, and mean ± SD is shown.

A drug library consisting of 140 compounds was screened to identify potential therapeutics for addressing mutations in the *Arid1a* gene. The murine organoid cell lines (AKPf and ArAKPf) carrying the mutant *Arid1a* gene and their wild-type counterparts were subjected to drug screening. The ArAKPf cell line, with mutations in the Arid1a gene, exhibited greater resistance to most drugs compared to AKPf (Figure 24). This highlights the significance of screening therapeutic drugs targeting *Arid1a* gene mutations. Upon evaluating treatment effects, BCL-2 inhibitors were identified as more effective for CRC cell lines with *Arid1a* gene mutations.

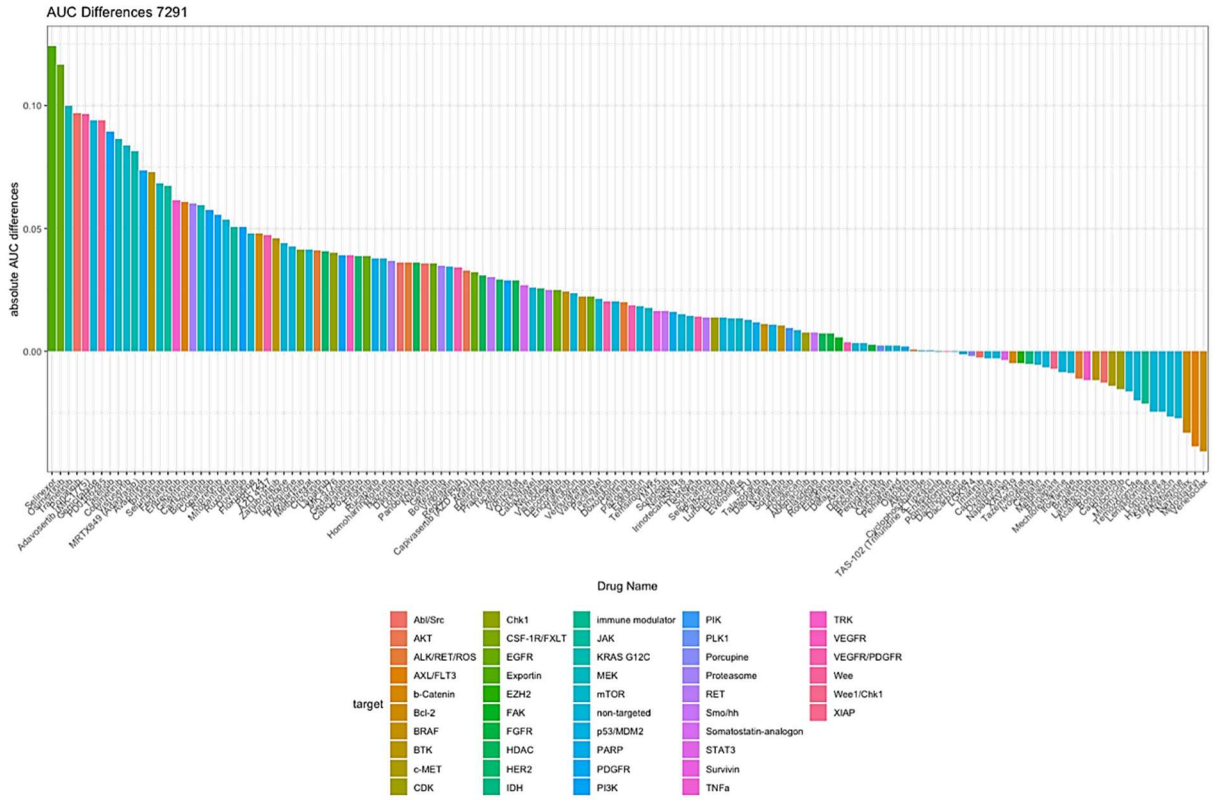

Figure 24. The result of the drug screening test on 140 compounds. The results showed that compared with Arid1a wild-type organoids (0007, AKPf), Arid1a mutant organoids (7291, ArAKPf) were relatively resistant to most types of drugs, and only a small number of drugs were relatively sensitive, among which the most obvious is BCL-2 inhibitor.

To validate the efficacy of BCL-2 inhibitors in the *ARID1A* gene mutant CRC cell line, we conducted in vitro viability assays using HCT116 *ARID1A*^{WT}/*ARID1A*^{KO} cells. A dose-response curve was generated to calculate the IC50 value (Figure 25). To corroborate these findings, we also tested another BCL-2 inhibitor in HCT116 cells. Considering the cell-killing potency, assay reproducibility, and the quality of dose-response curves, we conclusively determined that BCL-2 inhibitors can be effective against CRC with mutations in the *ARID1A* gene.

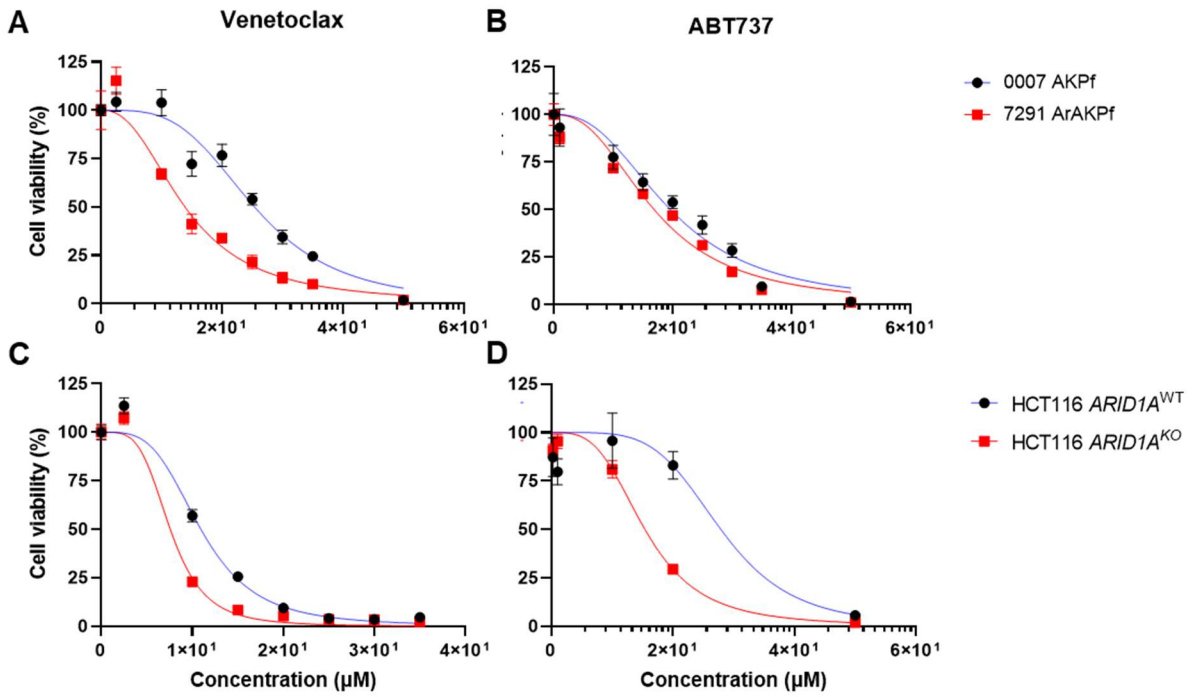

Figure 25. Drug response curves of mouse and human CRC cell lines treated with BCL-2 inhibitors for 48 hours. Cell viability was detected by the cck-8 assay. The survival rate of the control group was 100%, and the drug response curve showed the percentage of surviving cells after treatment with different drug concentrations. ARID1A deletion resulted in increased sensitivity of ArAKPf cells to two different BCL-2i (Venetoclax and ABT737) compared with wild-type controls (A, B) and concordantly in the HCT116 cell line (C, D). One-way ANOVA revealed significant differences ($P<0.05$). The experiment was repeated 3 times, and mean ± SD is shown.

3.4.3 The pairwise combinations of Bcl-2i, ATRi and Oxaliplatin did not demonstrate synergistic effects

Integrating our discoveries with prior studies indicating the lethal impact of ATR inhibitors on Arid1a-mutated mouse cells (Williamson et al. 2016), along with the efficacy of widely used clinical chemotherapy drugs, we sought to explore potential combination therapy strategies, we combined BCL-2i, ATRi and Oxaliplatin in pairs and administered them continuously to the HCT116 cell line for 48 hours. Drug-drug interactions were assessed using CompuSyn software based on the Chou-Talalay method and SynergyFinder software. The combination index (CI) was calculated by CompuSyn, where CI < 1, = 1, or > 1 indicated synergy, additivity, or antagonism, respectively. SynergyFinder software, employing ZIP, Loewe, Bliss, and HAS reference models, provided synergy scores. Results revealed antagonistic effects in all combinations, indicating that our findings do not support the use of combination therapy (Results not shown).

4 DISCUSSION

4.1 Summary of experimental results

In this investigation, we utilized a mouse model incorporating the Cre-loxP system and generated CRC tumor organoids with *ARID1A* gene mutations in vitro through Ad5CMV-Cre vector transfection. The objective was to elucidate the impact of *ARID1A* gene mutations on CRC using 2D and 3D cell culture models.

Our generated mouse CRC organoid models and human CRC cell lines bearing *ARID1A* mutations provided evidence that these mutations significantly modify the functional properties of CRC cells. Specifically, our findings indicate that *ARID1A* gene mutations promote cell proliferation, migration, and drug resistance in both 2D and 3D cell models, underscoring their diverse and profound impact on CRC.

Furthermore, we investigated the mechanistic basis for the promotion of EMT by *ARID1A* gene mutations. Our study demonstrates that these mutations regulate the expression of VIM and CDH1, enhancing the metastatic potential of CRC cells. This discovery enhances our understanding of CRC biology by delineating the molecular pathways through which *ARID1A* gene mutations exert their effects.

Bioinformatics analysis revealed activation of the PI3K/Akt pathway in CRC cells with *ARID1A* gene mutations, providing key insights into associated molecular mechanisms. To corroborate these findings, PCR experiments were conducted to assess the expression levels of key genes within the PI3K/Akt pathway. The results confirmed pathway activation in *ARID1A*-mutated CRC cells, reinforcing our bioinformatics data.

In pursuit of targeted therapies, traditional drug screens were performed, revealing BCL-2 inhibitors as promising candidates against *ARID1A* gene mutations. Notably, these inhibitors exhibited killing efficacy as single agents against CRC cell lines harboring *ARID1A* mutations, offering the potential for precision medicine strategies in treating CRC patients with this genetic alteration.

While our results demonstrate the efficacy of BCL-2 inhibitors alone, their lack of synergistic effects in combination suggests the need for further studies to optimize combination therapies for maximal therapeutic efficacy in *ARID1A*-mutated CRC.

In summary, our study provides valuable insights into the multifaceted effects of *ARID1A* gene mutations on CRC tumor cells, influencing cell proliferation, invasion, and drug resistance. By elucidating molecular pathways and identifying potential therapeutic targets, our investigation contributes to a deeper understanding of *ARID1A* gene mutations in the context of CRC, paving the way for more effective treatment strategies for patients with this genetic alteration.

4.2 Comparison and analysis of experimental results

The mutation rate of *ARID1A* in CRC is well documented and is indicative of a poor prognosis for patients. Initial analysis of CRC cohort data in ATCG revealed an approximate 10% incidence of *ARID1A* mutations, with patients bearing these mutations displaying a trend toward decreased survival, consistent with prior research (Li et al. 2020). However, these results lacked statistical significance, possibly due to the absence of subgroup analysis considering *ARID1A* mutation types, expression levels, tumor stage, etc., potentially leading to an underestimation of the prognostic value of ARID1A mutations.

KRAS and *APC* gene mutations are very common in CRC, *ARID1A* gene mutations and *KRAS* or APC mutations can significantly promote tumor progression (Huang et al. 2019; Sen et al. 2019). Therefore, we established ArAK/AK, ArAKPf/AKPf, and ArAP/AP mouse models. Despite previous observations of mutual exclusivity between *ARID1A* and *TP53* mutations (Jones et al. 2012; Wang et al. 2011), our established mouse cell lines demonstrated that concurrent mutations in *Arid1a* and *p53* heightened CRC malignancy, contingent upon the simultaneous presence of *Kras* and *Apc* mutations. This supports the argument that the exploration of the oncogenic role of the *ARID1A* gene in CRC should consider other genetic backgrounds (Sen et al. 2019).

ARID1A mutations were found to enhance the proliferation, migration, and invasion capabilities of CRC cells, consistent with previous studies. However, the impact of *ARID1A* mutations on epithelial-mesenchymal transition (EMT) remains contentious. While some studies failed to prove that *ARID1A* mutation promotes EMT (Mathur et al. 2016). Baldi et al. observed that ARID1A KD can affect the EMT process by regulating the expression of VIM and CDH1 in a variety of human CRC cell lines (Baldi et al. 2022). Since they used siRNA transcription to knock down ARID1A expression, we

hope to verify it by establishing a stable Arid1a KO mouse cell line. We found that ARID1A loss can lead to an increase in the VIM/CDH1 ratio, thereby regulating EMT conversion. We also explored whether ARID1B KD can reverse the above changes, and the results showed that the overall loss of ARID1 protein could not significantly reverse EMT, neither at the mRNA level (results not shown) nor at the protein level. Since we knocked down the expression of ARID1B using siRNA, we cannot determine whether this short-term knockdown effect limits the true effect.

Moreover, our analysis revealed that ARID1A mutations activate the PI3K/Akt pathway, aligning with previous findings (Xie et al. 2014). The comprehensive integration of bioinformatics analysis and RT-qPCR experiments supports the conclusion that ARID1A mutations induce changes in gene expression associated with the PI3K/Akt signaling pathway.

Exploring the chemotherapeutic response of ARID1A mutant CRC cell lines, we found increased resistance to most drugs, emphasizing the need for targeted therapies. While alternative targets like ARID1B and ATR inhibitors have been proposed (Helming et al. 2014b; Williamson et al. 2016), there are still challenges in developing drugs targeting ARID1B (Mathur et al. 2016). In addition, our study found that knocking down ARID1B in *Arid1a* mutant mouse cell lines could inhibit cell proliferation, but did not show the effect of promoting apoptosis and reversing EMT. ATR inhibition exhibited synthetic lethality in *Arid1a* mutant mouse cell lines but not in human CRC cell lines. Given the reported mechanisms of resistance to ATR inhibition (Llorca-Cardenosa et al. 2022; Lloyd et al. 2021; O'Leary et al. 2022), there remains a critical need to identify targeted drugs.

BCL-2 inhibitors, however, demonstrated specific lethality against ARID1A mutations in both in vitro validation and drug screening. BCL-2 assumes a pivotal role in apoptosis regulation, and its aberrant activation or overexpression is instrumental in sustaining the survival and drug resistance of cancer (Goff et al. 2013). BCL-2 inhibitors have demonstrated the capability to significantly enhance the apoptosis sensitivity of tumor cells (Davids and Letai 2013). Consequently, the inhibition of BCL-2 activity has emerged as one of the most compelling anti-cancer strategies (Zhang et al. 2021).

Unfortunately, combined treatment plans involving BCL-2 inhibitors, ATR inhibitors, and oxaliplatin did not exhibit notable synergy, discouraging the recommendation of combination therapy.

4.3 Significance and contribution of the results

The results of this study have important implications for the field of colorectal cancer (CRC) research, with far-reaching implications for both basic science and potential clinical applications. The main contributions and significance of the research results are as follows:

1. Understanding the role of *ARID1A* gene mutations in CRC: This study advances our understanding of the role of *ARID1A* gene mutations in CRC. By demonstrating that *ARID1A* mutations affect various aspects of CRC cell behavior, including proliferation, metastasis, and drug resistance, we provide valuable insights into the specific mechanisms underlying this genetic alteration.

2. Comprehensive evaluation: This study used 2D and 3D mouse cell culture models and human CRC 2D cell lines to conduct a comprehensive evaluation of the impact of *ARID1A* gene mutations on CRC. This multifaceted approach enhances the credibility and generalizability of the findings.

3. Mechanistic Insights: The identification of PI3K/Akt pathway activation in *ARID1A*-mutated CRC cells, as well as the molecular mechanisms regulating EMT, provides mechanistic insights into the effects of these mutations. This knowledge can serve as the basis for further research and drug development efforts.

4. Identification of potential therapeutic targets: The key finding of this study is that BCL-2 inhibitors are effective in treating *ARID1A*-mutated CRC. Through the implementation of a vehicle control group, we effectively mitigated the potential impact of DMSO on the observed effects, thereby reinforcing the reliability and reproducibility of our experimental findings.

5. Contribution to precision medicine: This study highlights the importance of personalized medicine in cancer treatment. It highlights the importance of identifying specific genetic alterations and tailoring treatments to an individual patient's unique genomic profile.

6. Foundation for future research: Insights gained from this study can serve as the basis for future research efforts in the field of CRC, allowing for a deeper exploration of *ARID1A* gene mutations and their broader impact on cancer biology.

Altogether, this study significantly advances our understanding of the impact of *ARID1A* gene mutations in CRC and provides a platform for future research and potential therapeutic intervention. The knowledge gained from this investigation has the potential to improve patient care and contribute to ongoing efforts to combat colorectal cancer.

4.4 Research shortcomings and open questions

While our study provides valuable insights into the role of *ARID1A* mutations in colorectal cancer (CRC), its limitations must be acknowledged as well as the open questions that remain for future research:

1. Limited clinical background: Our research mainly focuses on in vitro and mouse models, and the research results need to be verified with a clinical background. Further research is needed to understand how these molecular insights translate into actual patient outcomes.

2. Complex interactions: The mechanism by which ARID1A mutations affect CRC cells is undoubtedly multifaceted. Our study focused primarily on the PI3K/Akt pathway and EMT, but there may be other pathways and interactions that need to be explored.

3. Lack of in vivo data: Although our study used a mouse model, it did not address all aspects of the in vivo microenvironment. We have performed in vivo experiments in a CAM model. Although some evidence supporting this argument was observed (results not shown), further studies involving xenograft models or genetically engineered mouse models could provide a more comprehensive understanding of *ARID1A* mutations in a physiological context.

4. Interaction with other genetic alterations: CRC often involves multiple genetic mutations. The interaction between *ARID1A* mutations and other genetic alterations remains unclear and should be studied to provide a more accurate representation of the clinical situation.

5. Synergistic effects and clinical trials: Although we did not observe synergistic effects between BCL-2 inhibitors, it is still possible that combinatorial approaches involving different drug classes or timing may produce enhanced therapeutic effects. The identification of BCL-2 inhibitors as potential therapies for *ARID1A* mutant CRC is promising but has not been tested in the clinical setting. Clinical trials are needed to evaluate the safety and effectiveness of these targeted therapies.

6. Mechanistic details: Detailed mechanistic insights into how BCL-2 inhibitors target *ARDI1A* mutated CRC are areas where further research can provide valuable knowledge.

In summary, although our study makes a significant contribution to understanding the impact of *ARID1A* gene mutations on CRC, there are still unanswered questions and research gaps that require further investigation. Resolving these limitations and uncertainties will lead to a more complete understanding of ARID1A loss and its impact on CRC.

5 SUMMARY

The incidence of ARID1A mutation in human CRC is about 10%, and it indicates that there is a downward trend in the survival of patients.

Loss of ARID1A leads to morphological changes in CRC cells and can promote the proliferation activity, migration, and invasion of CRC cells, the mechanism behind which includes the activation of the PI3K/Akt pathway. ARID1A regulates the EMT transformation of CRC cells by regulating the expression ratio of VIM/CDH1.

Mutations in ARID1A lead to broad drug resistance in CRC cells, including traditional chemotherapeutics (oxaliplatin).

The therapeutic effect of ATR inhibitors on ARID1A-mutated CRC cell lines is still uncertain. Knockdown of ARID1B can produce synergistic lethal effects, but the clinical application prospect is still unclear.

BCL-2 inhibitors can be used as candidates for ARID1A mutations.

6 REFERENCES

Acuna, S. A., Chesney, T. R., Ramjist, J. K., Shah, P. S., Kennedy, E. D. and Baxter, N. N. (2019). **Laparoscopic Versus Open Resection for Rectal Cancer**. Ann Surg *269*, 849–855, doi:10.1097/SLA.0000000000003072.

Afik, R., Zigmond, E., Vugman, M., Klepfish, M., Shimshoni, E., Pasmanik-Chor, M., Shenoy, A., Bassat, E., Halpern, Z., Geiger, T., Sagi, I. and Varol, C. (2016). **Tumor macrophages are pivotal constructors of tumor collagenous matrix**. J Exp Med *213*, 2315–2331, doi:10.1084/jem.20151193.

Agaimy, A., Daum, O., Märkl, B., Lichtmannegger, I., Michal, M. and Hartmann, A. (2016). **SWI/SNF Complex–deficient Undifferentiated/Rhabdoid Carcinomas of the Gastrointestinal Tract**. Am J Surg Pathol *40*, 544–553, doi:10.1097/PAS.0000000000000554.

Algra, A. M. and Rothwell, P. M. (2012). **Effects of regular aspirin on long-term cancer incidence and metastasis: a systematic comparison of evidence from observational studies versus randomised trials**. The Lancet Oncology *13*, 518–527, doi:10.1016/S1470-2045(12)70112-2.

Araghi, M., Soerjomataram, I., Bardot, A., Ferlay, J., Cabasag, C. J., Morrison, D. S., De, P., Tervonen, H., Walsh, P. M., Bucher, O., Engholm, G., Jackson, C., McClure, C., Woods, R. R., Saint-Jacques, N., Morgan, E., Ransom, D., Thursfield, V., Møller, B., Leonfellner, S., Guren, M. G., Bray, F. and Arnold, M. (2019). **Changes in colorectal cancer incidence in seven high-income countries: a population-based study**. The Lancet Gastroenterology & Hepatology *4*, 511–518, doi:10.1016/S2468-1253(19)30147-5.

Arnold, M., Abnet, C. C., Neale, R. E., Vignat, J., Giovannucci, E. L., McGlynn, K. A. and Bray, F. (2020). **Global Burden of 5 Major Types of Gastrointestinal Cancer**. Gastroenterology *159*, 335-349.e15, doi:10.1053/j.gastro.2020.02.068.

Bagnardi, V., Rota, M., Botteri, E., Tramacere, I., Islami, F., Fedirko, V., Scotti, L., Jenab, M., Turati, F., Pasquali, E., Pelucchi, C., Galeone, C., Bellocco, R., Negri, E., Corrao, G., Boffetta, P. and La Vecchia, C. (2015). **Alcohol consumption and site-specific cancer risk: a comprehensive dose–response meta-analysis**. Br J Cancer *112*, 580–593, doi:10.1038/bjc.2014.579.

Baldi, S., Zhang, Q., Zhang, Z., Safi, M., Khamgan, H., Wu, H., Zhang, M., Qian, Y., Gao, Y., Shopit, A., Al‐Danakh, A., Alradhi, M., Al‐Nusaif, M. and Zuo, Y. (2022). **ARID1A downregulation promotes cell proliferation and migration of colon cancer via VIM activation and CDH1 suppression**. J Cell Mol Med *26*, 5984–5997, doi:10.1111/jcmm.17590.

Beklen, H., Gulfidan, G., Arga, K. Y., Mardinoglu, A. and Turanli, B. (2020). **Drug Repositioning for P-Glycoprotein Mediated Co-Expression Networks in Colorectal Cancer**. Front Oncol *10*, 1273, doi:10.3389/fonc.2020.01273.

Benveniste, R. E. and Todaro, G. J. (1974). **Evolution of Type C Viral Genes: I. Nucleic Acid from Baboon Type C Virus as a Measure of Divergence among Primate Species**. Proc Natl Acad Sci USA *71*, 4513–4518, doi:10.1073/pnas.71.11.4513.

Blaise, S., de Parseval, N., Bénit, L. and Heidmann, T. (2003). **Genomewide screening for fusogenic human endogenous retrovirus envelopes identifies syncytin 2, a gene conserved on primate evolution**. Proc Natl Acad Sci USA *100*, 13013–13018, doi:10.1073/pnas.2132646100.

Blumberg, D., Biller, L. H. and Schrag, D. (2019). **Robotic colectomy with intracorporeal anastomosis is feasible with no operative conversions during the learning curve for an experienced laparoscopic surgeon developing a robotics program**. JAMA *13*, 545–555, doi:10.1007/s11701-018-0895-1.

Blumberg, D., Biller, L. H. and Schrag, D. (2021). **Diagnosis and Treatment of Metastatic Colorectal Cancer**. JAMA *325*, 669, doi:10.1001/jama.2021.0106.

Botteri, E., Iodice, S., Bagnardi, V., Raimondi, S., Lowenfels, A. B. and Maisonneuve, P. (2008). **Smoking and Colorectal Cancer**. JAMA *300*, 2765, doi:10.1001/jama.2008.839.

Boyle, T., Keegel, T., Bull, F., Heyworth, J. and Fritschi, L. (2012). **Physical Activity and Risks of Proximal and Distal Colon Cancers: A Systematic Review and Meta-analysis**. J Natl Cancer Inst *104*, 1548–1561, doi:10.1093/jnci/djs354.

Brenner, H., Altenhofen, L., Stock, C. and Hoffmeister, M. (2013). **Natural History of Colorectal Adenomas: Birth Cohort Analysis Among 3.6 Million Participants of Screening Colonoscopy**. Cancer Epidemiol Biomarkers Prev *22*, 1043–1051, doi:10.1158/1055-9965.EPI-13-0162.

Brenner, H. and Chen, C. (2018). **The colorectal cancer epidemic: challenges and opportunities for primary, secondary and tertiary prevention**. Br J Cancer *119*, 785–792, doi:10.1038/s41416-018-0264-x.

Butterworth, J. W., Butterworth, W. A., Meyer, J., Giacobino, C., Buchs, N., Ris, F. and Scarpinata, R. (2021). **A systematic review and meta-analysis of robotic-assisted transabdominal total mesorectal excision and transanal total mesorectal excision: which approach offers optimal short-term outcomes for mid-to-low rectal adenocarcinoma?** Tech Coloproctol *25*, 1183–1198, doi:10.1007/s10151-021-02515-7.

Cao, Y., Nishihara, R., Wu, K., Wang, M., Ogino, S., Willett, W. C., Spiegelman, D., Fuchs, C. S., Giovannucci, E. L. and Chan, A. T. (2016). **Population-wide Impact of Long-term Use of Aspirin and the Risk for Cancer**. JAMA Oncol *2*, 762, doi:10.1001/jamaoncol.2015.6396.

Chae, Y. K. and Oh, M. S. (2019). **Detection of Minimal Residual Disease Using ctDNA in Lung Cancer: Current Evidence and Future Directions**. Journal of Thoracic Oncology *14*, 16–24, doi:10.1016/j.jtho.2018.09.022.

Chou, A., Toon, C. W., Clarkson, A., Sioson, L., Houang, M., Watson, N., DeSilva, K. and Gill, A. J. (2014). **Loss of ARID1A expression in colorectal carcinoma is strongly associated with mismatch repair deficiency**. Human Pathology *45*, 1697–1703, doi:10.1016/j.humpath.2014.04.009.

Chuong, E. B., Elde, N. C. and Feschotte, C. (2016). **Regulatory evolution of innate immunity through co-option of endogenous retroviruses**. Science *351*, 1083–1087, doi:10.1126/science.aad5497.

Davids, M. S. and Letai, A. (2013). **ABT-199: Taking Dead Aim at BCL-2**. Cancer Cell *23*, 139–141, doi:10.1016/j.ccr.2013.01.018.

De Roock, W., De Vriendt, V., Normanno, N., Ciardiello, F. and Tejpar, S. (2011). **KRAS, BRAF, PIK3CA, and PTEN mutations: implications for targeted therapies in metastatic colorectal cancer**. Lancet Oncol *12*, 594–603, doi:10.1016/S1470-2045(10)70209-6.

Delbridge, A. R. D., Grabow, S., Strasser, A. and Vaux, D. L. (2016). **Thirty years of BCL-2: translating cell death discoveries into novel cancer therapies**. Nat Rev Cancer *16*, 99–109, doi:10.1038/nrc.2015.17.

Diehn, M., Cho, R. W., Lobo, N. A., Kalisky, T., Dorie, M. J., Kulp, A. N., Qian, D., Lam, J. S., Ailles, L. E., Wong, M., Joshua, B., Kaplan, M. J., Wapnir, I., Dirbas, F. M., Somlo, G., Garberoglio, C., Paz, B., Shen, J., Lau, S. K., Quake, S. R., Brown, J. M., Weissman, I. L. and Clarke, M. F. (2009). **Association of reactive oxygen species levels and radioresistance in cancer stem cells**. Nature *458*, 780–783, doi:10.1038/nature07733.

Edwards, B. K., Ward, E., Kohler, B. A., Eheman, C., Zauber, A. G., Anderson, R. N., Jemal, A., Schymura, M. J., Lansdorp-Vogelaar, I., Seeff, L. C., van Ballegooijen, M., Goede, S. L. and Ries, L. A. G. (2010). **Annual report to the nation on the status of cancer, 1975-2006, featuring colorectal cancer trends and impact of interventions (risk factors, screening, and treatment) to reduce future rates**. Cancer *116*, 544–573, doi:10.1002/cncr.24760.

Freisling, H., Arnold, M., Soerjomataram, I., O'Doherty, M. G., Ordóñez-Mena, J. M., Bamia, C., Kampman, E., Leitzmann, M., Romieu, I., Kee, F., Tsilidis, K., Tjønneland, A., Trichopoulou, A., Boffetta, P., Benetou, V., Bueno-de-Mesquita, H. B., Huerta, J. M., Brenner, H., Wilsgaard, T. and Jenab, M. (2017). **Comparison of general obesity and measures of body fat distribution in older adults in relation to cancer risk: meta-analysis of individual participant data of seven prospective cohorts in Europe**. Br J Cancer *116*, 1486–1497, doi:10.1038/bjc.2017.106.

Goff, D. J., Recart, A. C., Sadarangani, A., Chun, H.-J., Barrett, C. L., Krajewska, M., Leu, H., Low-Marchelli, J., Ma, W., Shih, A. Y., Wei, J., Zhai, D., Geron, I., Pu, M., Bao, L., Chuang, R., Balaian, L., Gotlib, J., Minden, M., Martinelli, G., Rusert, J., Dao, K.-H., Shazand, K., Wentworth, P., Smith, K. M., Jamieson, C. A. M., Morris, S. R., Messer, K., Goldstein, L. S. B., Hudson, T. J., Marra, M., Frazer, K. A., Pellecchia, M., Reed, J. C. and Jamieson, C. H. M. (2013). **A Pan-BCL2 Inhibitor Renders Bone-Marrow-Resident Human Leukemia Stem**

Cells Sensitive to Tyrosine Kinase Inhibition. Cell Stem Cell *12*, 316–328, doi:10.1016/j.stem.2012.12.011.

Green, J., Czanner, G., Reeves, G., Watson, J., Wise, L., Roddam, A. and Beral, V. (2012). **Menopausal hormone therapy and risk of gastrointestinal cancer: Nested case-control study within a prospective cohort, and meta-analysis**. Int J Cancer *130*, 2387–2396, doi:10.1002/ijc.26236.

Guan, B., Wang, T.-L. and Shih, I.-M. (2011). **ARID1A, a factor that promotes formation of SWI/SNF-mediated chromatin remodeling, is a tumor suppressor in gynecologic cancers**. Cancer Res *71*, 6718–6727, doi:10.1158/0008-5472.CAN-11-1562.

He, Y., Zhang, Q., Chen, Y., Wu, Y., Quan, Y., Chen, W., Yao, J. and Zhang, P. (2023). **ZHX2 deficiency enriches hybrid MET cells through regulating E-cadherin expression**. Cell Death Dis *14*, 444, doi:10.1038/s41419-023-05974-y.

Helming, K. C., Wang, X. and Roberts, C. W. M. (2014a). **Vulnerabilities of Mutant SWI/SNF Complexes in Cancer**. Cancer Cell *26*, 309–317, doi:10.1016/j.ccr.2014.07.018.

Helming, K. C., Wang, X., Wilson, B. G., Vazquez, F., Haswell, J. R., Manchester, H. E., Kim, Y., Kryukov, G. V., Ghandi, M., Aguirre, A. J., Jagani, Z., Wang, Z., Garraway, L. A., Hahn, W. C. and Roberts, C. W. M. (2014b). **ARID1B is a specific vulnerability in ARID1A-mutant cancers**. Nat Med *20*, 251–254, doi:10.1038/nm.3480.

Huang, W., Li, H., Shi, X., Lin, M., Liao, C., Zhang, S., Shi, W., Zhang, L., Zhang, X. and Gan, J. (2021). **Characterization of genomic alterations in Chinese colorectal cancer patients**. Oncotarget *51*, 120–129, doi:10.1093/jjco/hyaa182.

Huang, W., Li, H., Shi, X., Lin, M., Liao, C., Zhang, S., Shi, W., Zhang, L., Zhang, X., Gan, J., Ashktorab, H., Azimi, H., Varma, S., Lee, E. L., Laiyemo, A. O., Nickerson, M. L. and Brim, H. (2019). **Driver genes exome sequencing reveals distinct variants in African Americans with colorectal neoplasia**. Oncotarget *10*, 2607–2624, doi:10.18632/oncotarget.26721.

Hyuna S (n.d.). *Global Cancer Statistics 2020: GLOBOCAN Estimates of Incidence and Mortality Worldwide for 36 Cancers in 185 Countries. CA Cancer J. Clin. 71, 209-249(2021)*.

Jiang, T., Chen, X., Su, C., Ren, S. and Zhou, C. (2020). **Pan-cancer analysis of *ARID1A* Alterations as Biomarkers for Immunotherapy Outcomes**. J Cancer *11*, 776–780, doi:10.7150/jca.41296.

Jin, F., Yang, Z., Shao, J., Tao, J., Reißfelder, C., Loges, S., Zhu, L. and Schölch, S. (2023). **ARID1A mutations in lung cancer: biology, prognostic role, and therapeutic implications**. Trends in Molecular Medicine *29*, 646–658, doi:10.1016/j.molmed.2023.04.005.

Jin, F., Zhu, L., Shao, J., Yakoub, M., Schmitt, L., Reißfelder, C., Loges, S., Benner, A. and Schölch, S. (2022). **Circulating tumour cells in patients with lung**

cancer universally indicate poor prognosis. Eur Respir Rev *31*, 220151, doi:10.1183/16000617.0151-2022.

Johnson, R. M., Qu, X., Lin, C.-F., Huw, L.-Y., Venkatanarayan, A., Sokol, E., Ou, F.-S., Ihuegbu, N., Zill, O. A., Kabbarah, O., Wang, L., Bourgon, R., de Sousa E Melo, F., Bolen, C., Daemen, A., Venook, A. P., Innocenti, F., Lenz, H.-J. and Bais, C. (2022). **ARID1A mutations confer intrinsic and acquired resistance to cetuximab treatment in colorectal cancer**. Nat Commun *13*, 5478, doi:10.1038/s41467-022-33172-5.

Jones, S., Li, M., Parsons, D. W., Zhang, X., Wesseling, J., Kristel, P., Schmidt, M. K., Markowitz, S., Yan, H., Bigner, D., Hruban, R. H., Eshleman, J. R., Iacobuzio-Donahue, C. A., Goggins, M., Maitra, A., Malek, S. N., Powell, S., Vogelstein, B., Kinzler, K. W., Velculescu, V. E. and Papadopoulos, N. (2012). **Somatic mutations in the chromatin remodeling gene ARID1A occur in several tumor types**. Hum Mutat *33*, 100–103, doi:10.1002/humu.21633.

Kim, Y.-S., Jeong, H., Choi, J.-W., Oh, H. E. and Lee, J.-H. (2017). **Unique characteristics of ARID1A mutation and protein level in gastric and colorectal cancer: A meta-analysis**. Nat Commun *23*, 268, doi:10.4103/sjg.SJG_184_17.

Kishida, Y., Oishi, T., Sugino, T., Shiomi, A., Urakami, K., Kusuhara, M., Yamaguchi, K., Kitagawa, Y. and Ono, H. (2019). **Associations Between Loss of ARID1A Expression and Clinicopathologic and Genetic Variables in T1 Early Colorectal Cancer**. Am J Clin Pathol *152*, 463–470, doi:10.1093/ajcp/aqz062.

Ladabaum, U., Dominitz, J. A., Kahi, C. and Schoen, R. E. (2020). **Strategies for Colorectal Cancer Screening**. Gastroenterology *158*, 418–432, doi:10.1053/j.gastro.2019.06.043.

Larsen, S. G., Pfeffer, F., Kørner, H., and Norwegian Colorectal Cancer Group (2019). **Norwegian moratorium on transanal total mesorectal excision**. Tech Coloproctol *106*, 1120–1121, doi:10.1002/bjs.11287.

Lee, J.-H., Kim, Y.-S., Jeong, H., Choi, J.-W. and Oh, H. (2014). **Immunohistochemical detection of ARID1A in colorectal carcinoma: loss of staining is associated with sporadic microsatellite unstable tumors with medullary histology and high TNM stage**. WJG *45*, 2430–2436, doi:10.1016/j.humpath.2014.08.007.

Lee, L. H., Sadot, E., Ivelja, S., Vakiani, E., Hechtman, J. F., Sevinsky, C. J., Klimstra, D. S., Ginty, F. and Shia, J. (2016). **ARID1A expression in early stage colorectal adenocarcinoma: an exploration of its prognostic significance**. Human Pathology *53*, 97–104, doi:10.1016/j.humpath.2016.02.004.

Lee, S. Y., Kim, D.-W., Lee, H. S., Ihn, M. H., Oh, H.-K., Park, D. J., Kim, H.-H. and Kang, S.-B. (2015). **Loss of AT-Rich Interactive Domain 1A Expression in Gastrointestinal Malignancies**. Oncology *88*, 234–240, doi:10.1159/000369140.

Li, J., Wang, Weichao, Zhang, Y., Cieślik, M., Guo, J., Tan, M., Green, M. D., Wang, Weimin, Lin, H., Li, W., Wei, S., Zhou, J., Li, G., Jing, X., Vatan, L., Zhao, L.,

Bitler, B., Zhang, R., Cho, K. R., Dou, Y., Kryczek, I., Chan, T. A., Huntsman, D., Chinnaiyan, A. M. and Zou, W. (2020). 1 May 2020 Epigenetic driver mutations in ARID1A shape cancer immune phenotype and immunotherapy, , doi:10.1172/JCI134402.

Lin, J. S., Piper, M. A., Perdue, L. A., Rutter, C., Webber, E. M., O'Connor, E., Smith, N. and Whitlock, E. P. (2016). Screening for Colorectal Cancer: A Systematic Review for the U.S. Preventive Services Task Force, Agency for Healthcare Research and Quality (US), Rockville (MD), URL: http://www.ncbi.nlm.nih.gov/books/NBK373584/ [Accessed August 2023].

Liu, H., Zeng, Z., Zhang, H., Wu, M., Ma, D., Wang, Q., Xie, M., Xu, Qing, Ouyang, J., Xiao, Y., Song, Y., Feng, B., Xu, Qingwen, Wang, Y., Zhang, Y., Hao, Y., Luo, S., Zhang, X., Yang, Z., Peng, J., Wu, X., Ren, D., Huang, M., Lan, P., Tong, W., Ren, M., Wang, J., Kang, L., and Chinese Transanal Endoscopic Surgery Collaborative (CTESC) Group (2023). **Morbidity, Mortality, and Pathologic Outcomes of Transanal Versus Laparoscopic Total Mesorectal Excision for Rectal Cancer Short-term Outcomes From a Multicenter Randomized Controlled Trial**. Ann Surg *277*, 1–6, doi:10.1097/SLA.0000000000005523.

Liu, Jianfang, Lichtenberg, T., Hoadley, K. A., Poisson, L. M., Lazar, A. J., Cherniack, A. D., Kovatich, A. J., Benz, C. C., Levine, D. A., Lee, A. V., Omberg, L., Wolf, D. M., Shriver, C. D., Thorsson, V., Hu, H., Caesar-Johnson, S. J., Demchok, J. A., Felau, I., Kasapi, M., Ferguson, M. L., Hutter, C. M., Sofia, H. J., Tarnuzzer, R., Wang, Z., Yang, L., Zenklusen, J. C., Zhang, J. (Julia), Chudamani, S., Liu, Jia, Lolla, L., Naresh, R., Pihl, T., Sun, Q., Wan, Y., Wu, Y., Cho, J., DeFreitas, T., Frazer, S., Gehlenborg, N., Getz, G., Heiman, D. I., Kim, J., Lawrence, M. S., Lin, P., Meier, S., Noble, M. S., Saksena, G., Voet, D., Zhang, Hailei, Bernard, B., Chambwe, N., Dhankani, V., Knijnenburg, T., Kramer, R., Leinonen, K., Liu, Y., Miller, M., Reynolds, S., Shmulevich, I., Thorsson, V., Zhang, W., Akbani, R., Broom, B. M., Hegde, A. M., Ju, Z., Kanchi, R. S., Korkut, A., Li, J., Liang, H., Ling, S., Liu, W., Lu, Y., Mills, G. B., Ng, K.-S., Rao, A., Ryan, M., Wang, Jing, Weinstein, J. N., Zhang, J., Abeshouse, A., Armenia, J., Chakravarty, D., Chatila, W. K., de Bruijn, I., Gao, J., Gross, B. E., Heins, Z. J., Kundra, R., La, K., Ladanyi, M., Luna, A., Nissan, M. G., Ochoa, A., Phillips, S. M., Reznik, E., Sanchez-Vega, F., Sander, C., Schultz, N., Sheridan, R., Sumer, S. O., Sun, Y., Taylor, B. S., Wang, Jioajiao, Zhang, Hongxin, Anur, P., Peto, M., Spellman, P., Benz, C., Stuart, J. M., Wong, C. K., Yau, C., Hayes, D. N., Parker, J. S., Wilkerson, M. D., Ally, A., Balasundaram, M., Bowlby, R., Brooks, D., Carlsen, R., Chuah, E., Dhalla, N., Holt, R., Jones, S. J. M., Kasaian, K., Lee, D., Ma, Y., Marra, M. A., Mayo, M., Moore, R. A., Mungall, A. J., Mungall, K., Robertson, A. G., Sadeghi, S., Schein, J. E., Sipahimalani, P., Tam, A., Thiessen, N., Tse, K., Wong, T., Berger, A. C., Beroukhim, R., Cherniack, A. D., Cibulskis, C., Gabriel, S. B., Gao, G. F., Ha, G., Meyerson, M., Schumacher, S. E., Shih, J., Kucherlapati, M. H., Kucherlapati, R. S., Baylin, S., Cope, L., Danilova, L., Bootwalla, M. S., Lai, P. H., Maglinte, D. T., Van Den Berg, D. J., Weisenberger, D. J., Auman, J. T., Balu, S., Bodenheimer, T., Fan, C., Hoadley, K. A., Hoyle, A. P., Jefferys, S. R., Jones, C. D., Meng, S., Mieczkowski, P. A., Mose, L. E., Perou, A. H., Perou, C. M., Roach, J., Shi, Y., Simons, J. V., Skelly, T., Soloway, M. G., Tan, D., Veluvolu, U., Fan, H., Hinoue, T., Laird, P. W., Shen, H., Zhou, W., Bellair, M., Chang, K., Covington, K., Creighton, C. J., Dinh, H., Doddapaneni, H., Donehower, L. A., Drummond, J., Gibbs, R. A., Glenn, R.,

Hale, W., Han, Y., Hu, J., Korchina, V., Lee, S., Lewis, L., Li, W., Liu, X., Morgan, M., Morton, D., Muzny, D., Santibanez, J., Sheth, M., Shinbro, E., Wang, L., Wang, M., Wheeler, D. A., Xi, L., Zhao, F., Hess, J., Appelbaum, E. L., Bailey, M., Cordes, M. G., Ding, L., Fronick, C. C., Fulton, L. A., Fulton, R. S., Kandoth, C., Mardis, E. R., McLellan, M. D., Miller, C. A., Schmidt, H. K., Wilson, R. K., Crain, D., Curley, E., Gardner, J., Lau, K., Mallery, D., Morris, S., Paulauskis, J., Penny, R., Shelton, C., Shelton, T., Sherman, M., Thompson, E., Yena, P., Bowen, J., Gastier-Foster, J. M., Gerken, M., Leraas, K. M., Lichtenberg, T. M., Ramirez, N. C., Wise, L., Zmuda, E., Corcoran, N., Costello, T., Hovens, C., Carvalho, A. L., de Carvalho, A. C., Fregnani, J. H., Longatto-Filho, A., Reis, R. M., Scapulatempo-Neto, C., Silveira, H. C. S., Vidal, D. O., Burnette, A., Eschbacher, J., Hermes, B., Noss, A., Singh, R., Anderson, M. L., Castro, P. D., Ittmann, M., Huntsman, D., Kohl, B., Le, X., Thorp, R., Andry, C., Duffy, E. R., Lyadov, V., Paklina, O., Setdikova, G., Shabunin, A., Tavobilov, M., McPherson, C., Warnick, R., Berkowitz, R., Cramer, D., Feltmate, C., Horowitz, N., Kibel, A., Muto, M., Raut, C. P., Malykh, A., Barnholtz-Sloan, J. S., Barrett, W., Devine, K., Fulop, J., Ostrom, Q. T., Shimmel, K., Wolinsky, Y., Sloan, A. E., De Rose, A., Giuliante, F., Goodman, M., Karlan, B. Y., Hagedorn, C. H., Eckman, J., Harr, J., Myers, J., Tucker, K., Zach, L. A., Deyarmin, B., Hu, H., Kvecher, L., Larson, C., Mural, R. J., Somiari, S., Vicha, A., Zelinka, T., Bennett, J., Iacocca, M., Rabeno, B., Swanson, P., Latour, M., Lacombe, L., Têtu, B., Bergeron, A., McGraw, M., Staugaitis, S. M., Chabot, J., Hibshoosh, H., Sepulveda, A., Su, T., Wang, T., Potapova, O., Voronina, O., Desjardins, L., Mariani, O., Roman-Roman, S., Sastre, X., Stern, M.-H., Cheng, F., Signoretti, S., Berchuck, A., Bigner, D., Lipp, E., Marks, J., McCall, S., McLendon, R., Secord, A., Sharp, A., Behera, M., Brat, D. J., Chen, A., Delman, K., Force, S., Khuri, F., Magliocca, K., Maithel, S., Olson, J. J., Owonikoko, T., Pickens, A., Ramalingam, S., Shin, D. M., Sica, G., Van Meir, E. G., Zhang, Hongzheng, Eijckenboom, W., Gillis, A., Korpershoek, E., Looijenga, L., Oosterhuis, W., Stoop, H., van Kessel, K. E., Zwarthoff, E. C., Calatozzolo, C., Cuppini, L., Cuzzubbo, S., DiMeco, F., Finocchiaro, G., Mattei, L., Perin, A., Pollo, B., Chen, C., Houck, J., Lohavanichbutr, P., Hartmann, A., Stoehr, C., Stoehr, R., Taubert, H., Wach, S., Wullich, B., Kycler, W., Murawa, D., Wiznerowicz, M., Chung, K., Edenfield, W. J., Martin, J., Baudin, E., Bubley, G., Bueno, R., De Rienzo, A., Richards, W. G., Kalkanis, S., Mikkelsen, T., Noushmehr, H., Scarpace, L., Girard, N., Aymerich, M., Campo, E., Giné, E., Guillermo, A. L., Van Bang, N., Hanh, P. T., Phu, B. D., Tang, Y., Colman, H., Evason, K., Dottino, P. R., Martignetti, J. A., Gabra, H., Juhl, H., Akeredolu, T., Stepa, S., Hoon, D., Ahn, K., Kang, K. J., Beuschlein, F., Breggia, A., Birrer, M., Bell, D., Borad, M., Bryce, A. H., Castle, E., Chandan, V., Cheville, J., Copland, J. A., Farnell, M., Flotte, T., Giama, N., Ho, T., Kendrick, M., Kocher, J.-P., Kopp, K., Moser, C., Nagorney, D., O'Brien, D., O'Neill, B. P., Patel, T., Petersen, G., Que, F., Rivera, M., Roberts, L., Smallridge, R., Smyrk, T., Stanton, M., Thompson, R. H., Torbenson, M., Yang, J. D., Zhang, L., Brimo, F., Ajani, J. A., Angulo Gonzalez, A. M., Behrens, C., Bondaruk, J., Broaddus, R., Czerniak, B., Esmaeli, B., Fujimoto, J., Gershenwald, J., Guo, C., Lazar, A. J., Logothetis, C., Meric-Bernstam, F., Moran, C., Ramondetta, L., Rice, D., Sood, A., Tamboli, P., Thompson, T., Troncoso, P., Tsao, A., Wistuba, I., Carter, C., Haydu, L., Hersey, P., Jakrot, V., Kakavand, H., Kefford, R., Lee, K., Long, G., Mann, G., Quinn, M., Saw, R., Scolyer, R., Shannon, K., Spillane, A., Stretch, J., Synott, M., Thompson, J., Wilmott, J., Al-Ahmadie, H., Chan, T. A., Ghossein, R.,

Gopalan, A., Levine, D. A., Reuter, V., Singer, S., Singh, B., Tien, N. V., Broudy, T., Mirsaidi, C., Nair, P., Drwiega, P., Miller, J., Smith, J., Zaren, H., Park, J.-W., Hung, N. P., Kebebew, E., Linehan, W. M., Metwalli, A. R., Pacak, K., Pinto, P. A., Schiffman, M., Schmidt, L. S., Vocke, C. D., Wentzensen, N., Worrell, R., Yang, H., Moncrieff, M., Goparaju, C., Melamed, J., Pass, H., Botnariuc, N., Caraman, I., Cernat, M., Chemencedji, I., Clipca, A., Doruc, S., Gorincioi, G., Mura, S., Pirtac, M., Stancul, I., Tcaciuc, D., Albert, M., Alexopoulou, I., Arnaout, A., Bartlett, J., Engel, J., Gilbert, S., Parfitt, J., Sekhon, H., Thomas, G., Rassl, D. M., Rintoul, R. C., Bifulco, C., Tamakawa, R., Urba, W., Hayward, N., Timmers, H., Antenucci, A., Facciolo, F., Grazi, G., Marino, M., Merola, R., de Krijger, R., Gimenez-Roqueplo, A.-P., Piché, A., Chevalier, S., McKercher, G., Birsoy, K., Barnett, G., Brewer, C., Farver, C., Naska, T., Pennell, N. A., Raymond, D., Schilero, C., Smolenski, K., Williams, F., Morrison, C., Borgia, J. A., Liptay, M. J., Pool, M., Seder, C. W., Junker, K., Omberg, L., Dinkin, M., Manikhas, G., Alvaro, D., Bragazzi, M. C., Cardinale, V., Carpino, G., Gaudio, E., Chesla, D., Cottingham, S., Dubina, M., Moiseenko, F., Dhanasekaran, R., Becker, K.-F., Janssen, K.-P., Slotta-Huspenina, J., Abdel-Rahman, M. H., Aziz, D., Bell, S., Cebulla, C. M., Davis, A., Duell, R., Elder, J. B., Hilty, J., Kumar, B., Lang, J., Lehman, N. L., Mandt, R., Nguyen, P., Pilarski, R., Rai, K., Schoenfield, L., Senecal, K., Wakely, P., Hansen, P., Lechan, R., Powers, J., Tischler, A., Grizzle, W. E., Sexton, K. C., Kastl, A., Henderson, J., Porten, S., Waldmann, J., Fassnacht, M., Asa, S. L., Schadendorf, D., Couce, M., Graefen, M., Huland, H., Sauter, G., Schlomm, T., Simon, R., Tennstedt, P., Olabode, O., Nelson, M., Bathe, O., Carroll, P. R., Chan, J. M., Disaia, P., Glenn, P., Kelley, R. K., Landen, C. N., Phillips, J., Prados, M., Simko, J., Smith-McCune, K., VandenBerg, S., Roggin, K., Fehrenbach, A., Kendler, A., Sifri, S., Steele, R., Jimeno, A., Carey, F., Forgie, I., Mannelli, M., Carney, M., Hernandez, B., Campos, B., Herold-Mende, C., Jungk, C., Unterberg, A., von Deimling, A., Bossler, A., Galbraith, J., Jacobus, L., Knudson, M., Knutson, T., Ma, D., Milhem, M., Sigmund, R., Godwin, A. K., Madan, R., Rosenthal, H. G., Adebamowo, C., Adebamowo, S. N., Boussioutas, A., Beer, D., Giordano, T., Mes-Masson, A.-M., Saad, F., Bocklage, T., Landrum, L., Mannel, R., Moore, K., Moxley, K., Postier, R., Walker, J., Zuna, R., Feldman, M., Valdivieso, F., Dhir, R., Luketich, J., Mora Pinero, E. M., Quintero-Aguilo, M., Carlotti, Jr, C. G., Dos Santos, J. S., Kemp, R., Sankarankuty, A., Tirapelli, D., Catto, J., Agnew, K., Swisher, E., Creaney, J., Robinson, B., Shelley, C. S., Godwin, E. M., Kendall, S., Shipman, C., Bradford, C., Carey, T., Haddad, A., Moyer, J., Peterson, L., Prince, M., Rozek, L., Wolf, G., Bowman, R., Fong, K. M., Yang, I., Korst, R., Rathmell, W. K., Fantacone-Campbell, J. L., Hooke, J. A., Kovatich, A. J., Shriver, C. D., DiPersio, J., Drake, B., Govindan, R., Heath, S., Ley, T., Van Tine, B., Westervelt, P., Rubin, M. A., Lee, J. I., Aredes, N. D. and Mariamidze, A. (2018). **An Integrated TCGA Pan-Cancer Clinical Data Resource to Drive High-Quality Survival Outcome Analytics**. Cell *173*, 400-416.e11, doi:10.1016/j.cell.2018.02.052.

Llorca-Cardenosa, M. J., Aronson, L. I., Krastev, D. B., Nieminuszczy, J., Alexander, J., Song, F., Dylewska, M., Broderick, R., Brough, R., Zimmermann, A., Zenke, F. T., Gurel, B., Riisnaes, R., Ferreira, A., Roumeliotis, T., Choudhary, J., Pettitt, S. J., de Bono, J., Cervantes, A., Haider, S., Niedzwiedz, W., Lord, C. J. and Chong, I. Y. (2022). **SMG8/SMG9 Heterodimer Loss Modulates SMG1**

Kinase to Drive ATR Inhibitor Resistance. Cancer Res *82*, 3962–3973, doi:10.1158/0008-5472.CAN-21-4339.

Lloyd, R. L., Urban, V., Muñoz-Martínez, F., Ayestaran, I., Thomas, J. C., de Renty, C., O'Connor, M. J., Forment, J. V., Galanty, Y. and Jackson, S. P. (2021). **Loss of Cyclin C or CDK8 provides ATR inhibitor resistance by suppressing transcription-associated replication stress**. Nucleic Acids Res *49*, 8665–8683, doi:10.1093/nar/gkab628.

Lord, C. J. and Ashworth, A. (2012). **The DNA damage response and cancer therapy**. Nature *481*, 287–294, doi:10.1038/nature10760.

Luchini, C., Veronese, N., Solmi, M., Cho, H., Kim, J.-H., Chou, A., Gill, A. J., Faraj, S. F., Chaux, A., Netto, G. J., Nakayama, K., Kyo, S., Lee, S. Y., Kim, D.-W., Yousef, G. M., Scorilas, A., Nelson, G. S., Köbel, M., Kalloger, S. E., Schaeffer, D. F., Yan, H.-B., Liu, F., Yokoyama, Y., Zhang, X., Pang, D., Lichner, Z., Sergi, G., Manzato, E., Capelli, P., Wood, L. D., Scarpa, A. and Correll, C. U. (2015). **Prognostic role and implications of mutation status of tumor suppressor gene ARID1A in cancer: a systematic review and meta-analysis**. Oncotarget *6*, 39088–39097, doi:10.18632/oncotarget.5142.

Martel, G., Crawford, A., Barkun, J. S., Boushey, R. P., Ramsay, C. R. and Fergusson, D. A. (2012). **Expert Opinion on Laparoscopic Surgery for Colorectal Cancer Parallels Evidence from a Cumulative Meta-Analysis of Randomized Controlled Trials**. PLoS ONE *7*, e35292, doi:10.1371/journal.pone.0035292.

Martin, M. A., Bryan, T., Rasheed, S. and Khan, A. S. (1981). **Identification and cloning of endogenous retroviral sequences present in human DNA.** Proc Natl Acad Sci USA *78*, 4892–4896, doi:10.1073/pnas.78.8.4892.

Mathur, R. (2018). **ARID1A loss in cancer: Towards a mechanistic understanding**. Pharmacol Ther *190*, 15–23, doi:10.1016/j.pharmthera.2018.05.001.

Mathur, R., Alver, B. H., San Roman, A. K., Wilson, B. G., Wang, X., Agoston, A. T., Park, P. J., Shivdasani, R. A. and Roberts, C. W. M. (2016). **ARID1A loss impairs enhancer-mediated gene regulation and drives colon cancer in mice**. Nat Genet, doi:10.1038/ng.3744.

Mi, S., Lee, X., Li, X., Veldman, G. M., Finnerty, H., Racie, L., LaVallie, E., Tang, X.-Y., Edouard, P., Howes, S., Keith, J. C. and McCoy, J. M. (2000). **Syncytin is a captive retroviral envelope protein involved in human placental morphogenesis**. Nature *403*, 785–789, doi:10.1038/35001608.

Monteran, L. and Erez, N. (2018). **Targeting the tumour stroma to improve cancer therapy**. Nat Rev Clin Oncol *15*, 366–381, doi:10.1038/s41571-018-0007-1.

Monteran, L. and Erez, N. (2019). **The Dark Side of Fibroblasts: Cancer-Associated Fibroblasts as Mediators of Immunosuppression in the Tumor Microenvironment**. Front Immunol *10*, 1835, doi:10.3389/fimmu.2019.01835.

Monterde, B. and Varela, I. (2022). **Role of SWI/SNF chromatin remodeling genes in lung cancer development**. Biochemical Society Transactions *50*, 1143–1150, doi:10.1042/BST20211084.

Neigeborn, L. and Carlson, M. (1984). **GENES AFFECTING THE REGULATION OF *SUC2* GENE EXPRESSION BY GLUCOSE REPRESSION IN *SACCHAROMYCES CEREVISIAE***. Genetics *108*, 845–858, doi:10.1093/genetics/108.4.845.

Ng, S. P., Ngan, S. Y. and Leong, T. (2022). **Current State of Neoadjuvant Radiotherapy for Rectal Cancer**. Clinical Colorectal Cancer *21*, 63–70, doi:10.1016/j.clcc.2021.10.008.

O'Leary, P. C., Chen, H., Doruk, Y. U., Williamson, T., Polacco, B., McNeal, A. S., Shenoy, T., Kale, N., Carnevale, J., Stevenson, E., Quigley, D. A., Chou, J., Feng, F. Y., Swaney, D. L., Krogan, N. J., Kim, M., Diolaiti, M. E. and Ashworth, A. (2022). **Resistance to ATR Inhibitors Is Mediated by Loss of the Nonsense-Mediated Decay Factor UPF2**. Cancer Res *82*, 3950–3961, doi:10.1158/0008-5472.CAN-21-4335.

Park, J. S., Kang, H., Park, S. Y., Kim, H. J., Woo, I. T., Park, I.-K., Choi, G.-S., Sylla, P., Rattner, D. W., Delgado, S. and Lacy, A. M. (2019). **Long-term oncologic after robotic versus laparoscopic right colectomy: a prospective randomized study**. Surg Endosc *33*, 2975–2981, doi:10.1007/s00464-018-6563-8.

Park, S.-M., Gaur, A. B., Lengyel, E. and Peter, M. E. (2008). **The miR-200 family determines the epithelial phenotype of cancer cells by targeting the E-cadherin repressors ZEB1 and ZEB2**. Genes Dev *22*, 894–907, doi:10.1101/gad.1640608.

Peerapen, P., Sueksakit, K., Boonmark, W., Yoodee, S. and Thongboonkerd, V. (2022). **ARID1A knockdown enhances carcinogenesis features and aggressiveness of Caco-2 colon cancer cells: An in vitro cellular mechanism study**. J Cancer *13*, 373–384, doi:10.7150/jca.65511.

Penna, M., Hompes, R., Arnold, S., Wynn, G., Austin, R., Warusavitarne, J., Moran, B., Hanna, G. B., Mortensen, N. J., Tekkis, P. P., and International TaTME Registry Collaborative (2019). **Incidence and Risk Factors for Anastomotic Failure in 1594 Patients Treated by Transanal Total Mesorectal Excision**. Surg Endosc *269*, 700–711, doi:10.1097/SLA.0000000000002653.

Penna, M., Hompes, R., Arnold, S., Wynn, G., Austin, R., Warusavitarne, J., Moran, B., Hanna, G. B., Mortensen, N. J., Tekkis, P. P., and TaTME Registry Collaborative (2017). **Transanal Total Mesorectal Excision**. Ann Surg *269*, 111–117, doi:10.1097/SLA.0000000000001948.

Rahbari, N. N., Aigner, M., Thorlund, K., Mollberg, N., Motschall, E., Jensen, K., Diener, M. K., Büchler, M. W., Koch, M. and Weitz, J. (2010). **Meta-analysis shows that detection of circulating tumor cells indicates poor prognosis in patients with colorectal cancer**. Gastroenterology *138*, 1714–1726, doi:10.1053/j.gastro.2010.01.008.

Ren, J., Ding, L., Zhang, D., Shi, G., Xu, Q., Shen, S., Wang, Y., Wang, T. and Hou, Y. (2018). **Carcinoma-associated fibroblasts promote the stemness and chemoresistance of colorectal cancer by transferring exosomal lncRNA H19**. Theranostics *8*, 3932–3948, doi:10.7150/thno.25541.

Sachs, N., de Ligt, J., Kopper, O., Gogola, E., Bounova, G., Weeber, F., Balgobind, A. V., Wind, K., Gracanin, A., Begthel, H., Korving, J., van Boxtel, R., Duarte, A. A., Lelieveld, D., van Hoeck, A., Ernst, R. F., Blokzijl, F., Nijman, I. J., Hoogstraat, M., van de Ven, M., Egan, D. A., Zinzalla, V., Moll, J., Boj, S. F., Voest, E. E., Wessels, L., van Diest, P. J., Rottenberg, S., Vries, R. G. J., Cuppen, E. and Clevers, H. (2018). **A Living Biobank of Breast Cancer Organoids Captures Disease Heterogeneity**. Cell *172*, 373-386.e10, doi:10.1016/j.cell.2017.11.010.

Sato, T., Vries, R. G., Snippert, H. J., van de Wetering, M., Barker, N., Stange, D. E., van Es, J. H., Abo, A., Kujala, P., Peters, P. J. and Clevers, H. (2009). **Single Lgr5 stem cells build crypt-villus structures in vitro without a mesenchymal niche**. Nature *459*, 262–265, doi:10.1038/nature07935.

Savas, S. and Skardasi, G. (2018). **The SWI/SNF complex subunit genes: Their functions, variations, and links to risk and survival outcomes in human cancers**. Critical Reviews in Oncology/Hematology *123*, 114–131, doi:10.1016/j.critrevonc.2018.01.009.

Sen, M., Wang, X., Hamdan, F. H., Rapp, J., Eggert, J., Kosinsky, R. L., Wegwitz, F., Kutschat, A. P., Younesi, F. S., Gaedcke, J., Grade, M., Hessmann, E., Papantonis, A., Ströbel, P. and Johnsen, S. A. (2019). **ARID1A facilitates KRAS signaling-regulated enhancer activity in an AP1-dependent manner in colorectal cancer cells**. Clinical Epigenetics *11*, 92, doi:10.1186/s13148-019-0690-5.

Shen, J., Ju, Z., Zhao, W., Wang, L., Peng, Y., Ge, Z., Nagel, Z. D., Zou, J., Wang, C., Kapoor, P., Ma, X., Ma, D., Liang, J., Song, S., Liu, J., Samson, L. D., Ajani, J. A., Li, G.-M., Liang, H., Shen, X., Mills, G. B. and Peng, G. (2018). **ARID1A deficiency promotes mutability and potentiates therapeutic antitumor immunity unleashed by immune checkpoint blockade**. Nat Med *24*, 556–562, doi:10.1038/s41591-018-0012-z.

Shi, J., Wang, Li, Yin, X., Wang, Lixia, Bo, L., Liu, K., Feng, K., Lin, S., Xu, Y., Ning, S. and Zhao, H. (2022). **Comprehensive characterization of clonality of driver genes revealing their clinical relevance in colorectal cancer**. J Transl Med *20*, 362, doi:10.1186/s12967-022-03529-x.

Siegel, R. L., Miller, K. D., Fuchs, H. E. and Jemal, A. (2022). **Cancer statistics, 2022**. CA: A Cancer Journal for Clinicians *72*, 7–33, doi:10.3322/caac.21708.

Siegel, R. L., Miller, K. D. and Jemal, A. (2017). **Colorectal Cancer Mortality Rates in Adults Aged 20 to 54 Years in the United States, 1970-2014**. JAMA *318*, 572–574, doi:10.1001/jama.2017.7630.

Siegel, R. L., Miller, K. D., Wagle, N. S. and Jemal, A. (2023). **Cancer statistics, 2023**. CA A Cancer J Clinicians *73*, 17–48, doi:10.3322/caac.21763.

Siegel, R. L., Torre, L. A., Soerjomataram, I., Hayes, R. B., Bray, F., Weber, T. K. and Jemal, A. (2019). **Global patterns and trends in colorectal cancer incidence in young adults**. Gut *68*, 2179–2185, doi:10.1136/gutjnl-2019-319511.

Sorich, M. J., Wiese, M. D., Rowland, A., Kichenadasse, G., McKinnon, R. A. and Karapetis, C. S. (2015). **Extended RAS mutations and anti-EGFR monoclonal antibody survival benefit in metastatic colorectal cancer: a meta-analysis of randomized, controlled trials**. Annals of Oncology *26*, 13–21, doi:10.1093/annonc/mdu378.

Stern, M., Jensen, R. and Herskowitz, I. (1984). **Five SWI genes are required for expression of the HO gene in yeast**. Journal of Molecular Biology *178*, 853–868, doi:10.1016/0022-2836(84)90315-2.

Sun, B. L. (2021). **Current Microsatellite Instability Testing in Management of Colorectal Cancer**. Clinical Colorectal Cancer *20*, e12–e20, doi:10.1016/j.clcc.2020.08.001.

Takebe, T. and Wells, J. M. (2019). **Organoids by design**. Science *364*, 956–959, doi:10.1126/science.aaw7567.

Tam, W. L. and Weinberg, R. A. (2013). **The epigenetics of epithelial-mesenchymal plasticity in cancer**. Nat Med *19*, 1438–1449, doi:10.1038/nm.3336.

TANABE, S., AOYAGI, K., YOKOZAKI, H. and SASAKI, H. (2014). **Gene expression signatures for identifying diffuse-type gastric cancer associated with epithelial-mesenchymal transition**. International Journal of Oncology *44*, 1955–1970, doi:10.3892/ijo.2014.2387.

Thiery, J. P., Acloque, H., Huang, R. Y. J. and Nieto, M. A. (2009). **Epithelial-Mesenchymal Transitions in Development and Disease**. Cell *139*, 871–890, doi:10.1016/j.cell.2009.11.007.

Tokunaga, R., Xiu, J., Goldberg, R. M., Philip, P. A., Seeber, A., Battaglin, F., Arai, H., Lo, J. H., Naseem, M., Puccini, A., Berger, M. D., Soni, S., Zhang, W., Chen, S., Hwang, J. J., Shields, A. F., Marshall, J. L., Baba, H., Korn, W. M. and Lenz, H.-J. (2020). **The impact of ARID1A mutation on molecular characteristics in colorectal cancer**. Eur J Cancer *140*, 119–129, doi:10.1016/j.ejca.2020.09.006.

Vart, G., Banzi, R. and Minozzi, S. (2012). **Comparing participation rates between immunochemical and guaiac faecal occult blood tests: A systematic review and meta-analysis**. Preventive Medicine *55*, 87–92, doi:10.1016/j.ypmed.2012.05.006.

Vieira, A. R., Abar, L., Chan, D. S. M., Vingeliene, S., Polemiti, E., Stevens, C., Greenwood, D. and Norat, T. (2017). **Foods and beverages and colorectal cancer risk: a systematic review and meta-analysis of cohort studies, an update of the evidence of the WCRF-AICR Continuous Update Project**. Annals of Oncology *28*, 1788–1802, doi:10.1093/annonc/mdx171.

Vuik, F. E., Nieuwenburg, S. A., Bardou, M., Lansdorp-Vogelaar, I., Dinis-Ribeiro, M., Bento, M. J., Zadnik, V., Pellisé, M., Esteban, L., Kaminski, M. F., Suchanek,

S., Ngo, O., Májek, O., Leja, M., Kuipers, E. J. and Spaander, M. C. (2019). **Increasing incidence of colorectal cancer in young adults in Europe over the last 25 years**. Gut *68*, 1820–1826, doi:10.1136/gutjnl-2018-317592.

Wang, B., Lu, F.-Y., Shi, R.-H., Feng, Y.-D., Zhao, X.-D., Lu, Z.-P., Xiao, L., Zhou, G.-Q., Qiu, J.-M. and Cheng, C.-E. (2018). **MiR-26b regulates 5-FU-resistance in human colorectal cancer via down-regulation of Pgp**. Am J Cancer Res *8*, 2518–2527.

Wang, K., Kan, J., Yuen, S. T., Shi, S. T., Chu, K. M., Law, S., Chan, T. L., Kan, Z., Chan, A. S. Y., Tsui, W. Y., Lee, S. P., Ho, S. L., Chan, A. K. W., Cheng, G. H. W., Roberts, P. C., Rejto, P. A., Gibson, N. W., Pocalyko, D. J., Mao, M., Xu, J. and Leung, S. Y. (2011). **Exome sequencing identifies frequent mutation of ARID1A in molecular subtypes of gastric cancer**. Nat Genet *43*, 1219–1223, doi:10.1038/ng.982.

Wang, Y., Krushel, L. A. and Edelman, G. M. (1996). **Targeted DNA recombination in vivo using an adenovirus carrying the cre recombinase gene.** Proc Natl Acad Sci U S A *93*, 3932–3936, URL: https://www.ncbi.nlm.nih.gov/pmc/articles/PMC39462/ [Accessed February 2023].

Weber, P. A., Merola, S., Wasielewski, A. and Ballantyne, G. H. (2002). **Telerobotic-Assisted Laparoscopic Right and Sigmoid Colectomies for Benign Disease**. Dis Colon Rectum *45*, 1689–1696, doi:10.1007/s10350-004-7261-2.

Wei, X.-L., Wang, D.-S., Xi, S.-Y., Wu, W.-J., Chen, D.-L., Zeng, Z.-L., Wang, R.-Y., Huang, Y.-X., Jin, Y., Wang, F., Qiu, M.-Z., Luo, H.-Y., Zhang, D.-S. and Xu, R.-H. (2014). **Clinicopathologic and prognostic relevance of ARID1A protein loss in colorectal cancer**. Nat Commun *20*, 18404, doi:10.3748/wjg.v20.i48.18404.

Williamson, C. T., Miller, R., Pemberton, H. N., Jones, S. E., Campbell, J., Konde, A., Badham, N., Rafiq, R., Brough, R., Gulati, A., Ryan, C. J., Francis, J., Vermulen, P. B., Reynolds, A. R., Reaper, P. M., Pollard, J. R., Ashworth, A. and Lord, C. J. (2016). **ATR inhibitors as a synthetic lethal therapy for tumours deficient in ARID1A**. Nat Commun *7*, 13837, doi:10.1038/ncomms13837.

Wilson, B. G. and Roberts, C. W. M. (2011). **SWI/SNF nucleosome remodellers and cancer**. Nat Rev Cancer *11*, 481–492, doi:10.1038/nrc3068.

Wu, R.-C., Wang, T.-L. and Shih, I.-M. (2014). **The emerging roles of ARID1A in tumor suppression**. Cancer Biol Ther *15*, 655–664, doi:10.4161/cbt.28411.

Xie, C., Fu, L., Han, Y., Li, Q. and Wang, E. (2014). **Decreased ARID1A expression facilitates cell proliferation and inhibits 5-fluorouracil-induced apoptosis in colorectal carcinoma**. Tumor Biol *35*, 7921–7927, doi:10.1007/s13277-014-2074-y.

Yamauchi, S., Matsuyama, T., Tokunaga, M. and Kinugasa, Y. (2021). **Minimally Invasive Surgery for Colorectal Cancer**. Journal of Thoracic Oncology *4*, 17–23, doi:10.31662/jmaj.2020-0089.

Ye, J., Zhou, Y., Weiser, M. R., Gönen, M., Zhang, L., Samdani, T., Bacares, R., DeLair, D., Ivelja, S., Vakiani, E., Klimstra, D. S., Soslow, R. A. and Shia, J. (2014). **Immunohistochemical detection of ARID1A in colorectal carcinoma: loss of staining is associated with sporadic microsatellite unstable tumors with medullary histology and high TNM stage**. Human Pathology *45*, 2430–2436, doi:10.1016/j.humpath.2014.08.007.

Yoshimoto, M., Kagawa, S., Kajioka, H., Taniguchi, A., Kuroda, S., Kikuchi, S., Kakiuchi, Y., Yagi, T., Nogi, S., Teraishi, F., Shigeyasu, K., Yoshida, R., Umeda, Y., Noma, K., Tazawa, H., Fujiwara, T., Guo, Y., Wang, M., Zou, Y., Jin, L., Zhao, Z., Liu, Q., Wang, S. and Li, J. (2023). **Mechanisms of chemotherapeutic resistance and the application of targeted nanoparticles for enhanced chemotherapy in colorectal cancer**. J Nanobiotechnol *20*, 371, doi:10.1186/s12951-022-01586-4.

Yu, C., Lei, X., Chen, F., Mao, S., Lv, L., Liu, H., Hu, X., Wang, R., Shen, L., Zhang, N., Meng, Y., Shen, Y., Chen, J., Li, P., Huang, S., Lin, C., Zhang, Z. and Yuan, K. (2014). **ARID1A loss derepresses a group of human endogenous retrovirus-H loci to modulate BRD4-dependent transcription**. Nat Commun *13*, 3501, doi:10.1038/s41467-022-31197-4.

Zhang, L., Lu, Z. and Zhao, X. (2021). **Targeting Bcl-2 for cancer therapy**. Biochimica et Biophysica Acta (BBA) - Reviews on Cancer *1876*, 188569, doi:10.1016/j.bbcan.2021.188569.

Zhang, M., Atkinson, R. L. and Rosen, J. M. (2010). **Selective targeting of radiation-resistant tumor-initiating cells**. Proc Natl Acad Sci USA *107*, 3522–3527, doi:10.1073/pnas.0910179107.

Zhu, Y., Yan, C., Wang, X., Xu, Z., Lv, J., Xu, X., Yu, W., Zhou, M. and Yue, L. (2022). **Pan-cancer analysis of ARID family members as novel biomarkers for immune checkpoint inhibitor therapy**. Cancer Biol Ther *23*, 104–111, doi:10.1080/15384047.2021.2011643.

7 CURRICULUM VITAE

PERSONAL INFORMATION

Name	FUKANG JIN
Date of birth	25/02/1990
Gender	Male
Nationality	China
University	University of Heidelberg
Email	fukangjin@hotmail.com

WORK EXPERIENCE

06/2015-05/2021 Resident doctor, Department of Thoracic Surgery, the First Bethune Hospital of Jilin University, Changchun, China

EDUCATION

06/2021-06/2024 Department of Surgery, University Hospital & Faculty of Medicine Mannheim, University of Heidelberg; Clinical Cooperation Unit Translational Surgical Oncology (A430), German Cancer Research Center (**DKFZ**)

Degree: Doctor of Medicine (Surgery)

Major: Molecular marker detection and drug screening of solid tumors

Advisor: Prof. Dr. med. Sebastian Schölch

09/2013-06/2015 Norman Bethune College of Medicine and the First Bethune Hospital of Jilin University, China

Degree: Master of Clinical Medicine (Surgery)

Major: Upper Gastrointestinal Disease and Pulmonary Disease.

Advisor: Professor Guoguang Shao

09/2008-06/2013 Norman Bethune College of Medicine, Jilin University, China

Degree: Bachelor of Clinical Medicine

Major: Clinical medicine and basic medicine

GPA:4.0, 91.2(hundred-mark system)

09/2008-06/2013 The First High School of Shangqiu City, Shangqiu, China.

High School Diploma

CLINICAL TRAINEESHIPS AND SKILLS

06/2015-04/2021 Proficient in the general treatment of lung cancer, esophageal cancer, and other common diseases in thoracic surgery, and able to independently complete thoracic closed drainage surgery. Department of Thoracic Surgery, The First Bethune Hospital of Jilin University, Changchun, China

07/2013-08/2013 Student Exchange at the Department of Surgery and Endoscopy Center, the Prince of Wales Hospital of the Chinese University of Hong Kong, Hong Kong, China

RESEARCH EXPERIENCE AND PUBLICATIONS

Jin F, Zhu L, Shao J, Yakoub M, Schmitt L, Reißfelder C, Loges S, Benner A, Schölch S. Circulating tumor cells in patients with lung cancer universally indicate poor prognosis. Eur Respir Rev. 2022 Dec 14;31(166):220151. doi: 10.1183/16000617.0151-2022 IF: 9.5, Q1. PMID: 36517047; PMCID: PMC9879327.

Jin F, Yang Z, Shao J, Tao J, Reißfelder C, Loges S, Zhu L, Schölch S. ARID1A mutations in lung cancer: biology, prognostic role, and therapeutic implications. Trends Mol Med. 2023 Aug;29(8):646-658. doi: 10.1016/j.molmed.2023.04.005 IF: 15.3 Q1. Epub 2023 May 11. PMID: 37179132.

06/2012-10/2012
Skills training in the research: "**Inhibition of CLC-3 expression promotes apoptosis of human ovarian cancer SKOV3/DDP cells induced by cisplatin**" Laboratory of Pathophysiology, Bethune Medical College, Jilin University, Changchun, China

SCHOLARSHIPS AND AWARDS

2022-2024 Chinese Scholarship Council

2014 Obtained the certificate of the medical practitioner

2011-2012 Second-class Scholarship, Jilin University
Selected "Outstanding Student Leader "

2010-2011 First-class Scholarship, Jilin University
Selected "Outstanding Student "

2009-2010 First-class Scholarship, Jilin University
Selected "Outstanding Student "

2008-2009 First-class Scholarship, Jilin University
Selected "Outstanding Student "

2010 Award nomination for Top 10 College Students, Jilin University

EXTRACURRICULAR ACTIVITIES

06/2013–06/2015 Summer volunteer teacher, Qinghai Province and Inner Mongolia

LANGUAGE

English: IELTS Test Results: Listening 6.5, Reading 8.5, Writing 6.5, Speaking 7.0,
Overall Band Score: **7.0**, CEFR Level: **C1**

8 ACKNOWLEDGEMENTS

Here, I sincerely want to express my gratitude to those who have supported, encouraged and assisted me throughout my doctoral research journey. It is with your support that I have been able to complete this challenging and growth-filled academic endeavor.

First and foremost, I want to extend my heartfelt appreciation to Professor Sebastian Schölch. Your guidance and support throughout the entire research process have been invaluable. The high standards you set have driven me to continuously pursue excellence, enabling me to meticulously refine each paper and achieve unimaginable results. Your mentorship has not only provided me with valuable academic guidance but also imparted numerous insights into life and career planning. I've learned a great deal from you, including maintaining a work-life balance, effective personnel management, and efficient laboratory operations. Your example has profoundly influenced me.

I would like to offer special thanks to the members of the laboratory and all my colleagues. First, I am grateful to Lei. Your recommendation provided me with the opportunity to work alongside all of you. Your planning skills, generosity, and diligence have left a lasting impression on me. Your ambition and grounded work ethic serve as models for my learning. Thank you for your assistance in crafting my articles and designing research topics; you are the "MVP" of our laboratory.

As one of our exceptional technical staff members, Lukas, you have always been adept in laboratory operations. Your strong research training makes you one of our most reliable colleagues, and you are always the first person we turn to when faced with challenges. Your friendly disposition and willingness to help everyone are truly commendable. I vividly remember your meticulous care and assistance when I first arrived in Germany, helping me smoothly navigate university registration and complex visa procedures.

A special thank you goes to Mina, who taught me how to create figures in presentations and introduced me to the Grammarly software. Although you later moved to work in Göttingen, I still appreciate your guidance in my academic and writing pursuits.

As time has passed, our laboratory team has continued to grow with the addition of members like Ting, Jianxin, Alessandro, Ana, Yugeng, and others. This has allowed us to share techniques, discuss topics, and provide mutual support, creating an atmosphere much like a big family. I would also like to extend my gratitude to Ting and Wanning for helping take care of my child in the office during weekends when I needed to conduct experiments. Among the other Chinese students in the lab, Qianwen, in particular, has not only taught me many experimental skills but also brought a lot of joy and laughter to the lab. You're like Doraemon; we often come to you for things, and you always seem to have everything.

Next, I want to give special thanks to my wife, He. It's been 11 years since we met, and we've experienced numerous ups and downs together. Whether during peaks or valleys in life and regardless of our journeys across different places, you have consistently accompanied and encouraged me. During our successes, you remain humble and ready to help those in need. When facing setbacks, you remain strong and steadfast, silently providing support. You've shown understanding for the decisions I've made and sacrificed your bright prospects for my dreams. Especially during my over two years in Germany, you held our small family together in China. To be with our daughter, Yingyun, you even gave up a high-paying job. Your sacrifices go far beyond that – you've endured my lesser-known side and shared the burdens of my pressures. You are not only my rock but also the harbor I yearn for during my voyages. Even when I couldn't be at home, you bought gifts for Yingyun in my name, showing my love for her. I am thankful for your sacrifices; you are the dearest person to me. I also want to thank my daughter, Yingyun. Your birth has shown me how joyful being a father can be. As I accompany your growth, I continuously improve myself and relish the happiness you bring. In the two-plus years since Dad left, I've consistently video-called you and written you a letter every day. I hope this becomes an example for you – persistence and dedication in everything you do. These hundreds of letters not only record the details of life but also serve as invaluable spiritual treasures.

I must also express gratitude to my parents and my brother, as well as friends and family. Your support has enabled me to complete this journey successfully. Thank you, Mom and Dad, for nurturing and guiding me, and teaching me the path of

righteousness. I've witnessed your hospitality towards those without shelter in cold storms, teaching me the concept of "it is more blessed to give than to receive." To act justly, love mercy walk humbly with God – these teachings are your greatest legacy to me. I also appreciate my brother's family; your example has given me the courage to face challenges, and I hope I can be a role model for Jiayin and Junjun. To all friends and family, though I can't name each one, I hold your help and encouragement dear in my heart. I also remember my grandmother, uncle, and my wife's grandfather, and every thought of you fills me with a mix of emotions – your care during your lifetimes warms my heart, and losing you brings tears to my eyes. Your love for me will never fade. With confidence, love, and hope, I will continue moving forward.

I want to thank Professor Shao, Professor Yang and Dr.Lin. Thank you for your support in both professional knowledge and life guidance. Your encouragement and teachings will benefit me for a lifetime, and your examples guide my efforts. I am grateful for the financial support from the China Scholarship Council.

Lastly, I want to express gratitude to all the authors whose works I've cited. Every person I've encountered on my doctoral journey has left an indelible impact on my life. To everyone I've met and every experience I've had, thank you deeply for your presence.

Thank you all!